Dynamic Control of DNA Nanotube Self-Assembly Processes

by
Ruoyu Jiang

A thesis submitted to Johns Hopkins University in conformity with the requirements for the degree of Master of Science in Engineering

Baltimore, Maryland

May 2018

Abstract

DNA and RNA have become emerging biomaterials used to construct molecular self-assembly devices that mimic cellular networks and cascades composed primarily of nucleic acids. The introduction of DNA origami, a technique requiring the folding of one long scaffold DNA strand into a desired nanoscale pattern, has demonstrated novel ways to construct self-assembled nanoscale structures and circuits that aid our understanding of cellular behavior and responsiveness. A vital design for constructing complex DNA self-assembly networks is to precisely regulate nanostructure assembly and to intelligently diversify self-assembly processes. Although many studies on self-assembling desired nanostructures have been developed, few have been able to program multicomponent DNA devices. In this thesis, we explore ways to construct various DNA nanotube pathways, and to control DNA self-assembly processes.

We describe the design principles of how to build connections between DNA nanotubes with different sticky end sequences and unknown molecular landmarks. Specific DNA nanotubes nucleate, grow on these landmarks, diffuse and then form stable connections. We first construct two separate DNA point to point assembly systems with "R tiles and S tiles" and "UEd tiles and VEd tiles" to demonstrate that DNA point to point assembly is extensible. We discover additional processes to self-assemble multiple DNA wiring programs that can occur in tandem. By designing multicomponent point-to-point assembly processes, we show precise control over self-assembling complex DNA wiring processes and filament architectures, and these features serve as a starting point for programmatically directing nanotube fiber network assembly processes.

Next, we demonstrate technique to show that a designed nanostructure can selectively stop DNA nanotube growth. We designed nanostructures termed "Cap" and

these structures bind to free nanotube ends and prevent free tiles from attaching to the facet. We use previously mentioned DAE-E DNA tiles termed "R tiles and S tiles" and "UEd tiles and VEd tiles" to examine selectively controlled DNA nucleation and termination mechanisms. We then develop a model to quantitatively measure the kinetics of the capping processes to predict the behavior of DNA termination mechanism.

Acknowledgements

I am grateful for my advisor Rebecca Schulman. Her wisdom and patience have guided me to understand problems and taught me to appreciate the journey of learning. Her insights on science and technology have unraveled some of my doubts and offered me confidence to believe that knowledge and research have the power to give to the society. I would also like to thank Deepak Agrawal who has supported, motivated and challenged me to be better. I thank Abdul Mohammed for mentoring and teaching me how to use fluorescence microscopy and PCR, and for being a solid foundation for my research project. I also express my gratitude to Samuel Schaeffer for giving me feedbacks on my experiments and analysis, and to all Schulman lab members for facilitating a joyful learning platform. I am always grateful for my mother and father and I'm very fortunate to encounter friends who love and trust me.

"*If I rise on the wings of the dawn, if I settle on the far side of the sea, even there your hand will guide me, your right hand will hold me fast.*"

Psalm 139: 9-10

Table of Contents

List of Figures

Introduction

Bottom up fabrication has become increasingly important to construct nanostructures with controlled feature. Various self-assembly techniques and processes have been introduced to fabricate molecular devices, and many self-assembled materials have potential applications in medicine, biology, sensing and electronics.[1-10] DNA hybridization and unique Watson- Crick complementary sequences have enabled DNA materials such as DNA nanotubes as a building block to self-assemble complex nanostructures.[11-14]

Although DNA nanotechnology has been emphasizing on constructing product with a desired feature, it has great promises on creating self-assembled devices in which reaction can be triggered by the present environment. This type of structure and processes requires precise control over material nucleation and organization, thus making it essential to develop controlled reactions whose processes can be changed by the present environment. Previous study has reported the significance of DNA sticky ends and how they can hybridize and interact to form tile assembly. It has shown that DNA can be self-assembled into a seed structure on which DNA nanotube can nucleate, assemble and grow with the presence of DNA tile mix.[15] DNA tile and sticky end sequences can direct the pathway of the assembly rules and point to point assembly system has been developed to form DNA nanotube connections within single image plane between fixed A and B seeds known as molecular landmarks. This assembly system is analogous to the components of cytoskeleton that can be organized and constructed by cellular assembly rules and the environment. Components usually contain proteins and tissues that govern cellular interactions and cell behavior, so investigating such processes illuminates better understanding on cellular function and behavior. However, cellular environment contains diverse cytoskeletal structures that

govern cellular function and these functions are achieved through multiple cytoskeletal interactions which make it necessary to gain more understanding on multicomponent assembly processes and to diversify point to point assembly systems that can be potentially connected to various cellular components.

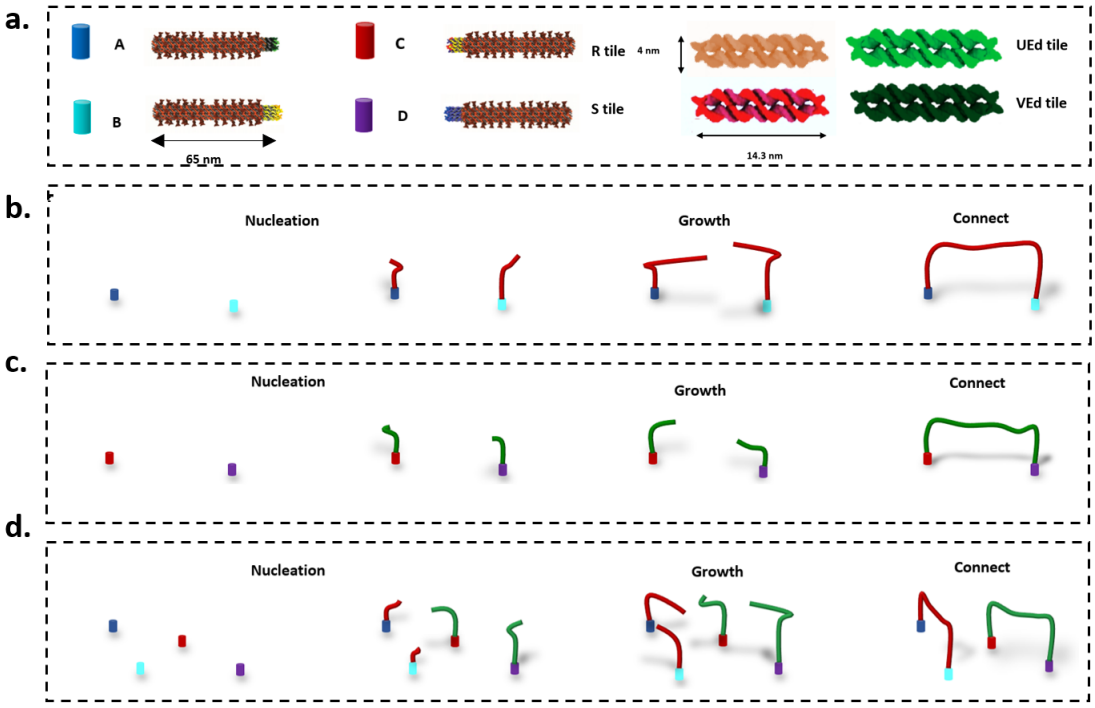

Figure 1. Multicomponent DNA Nanotube Connections Scheme. (A) DNA tile structure and DNA seed structure. ATTO647 tiles are termed RS tile (R tile and S tile), and Cy3 tiles are termed UV tile (UEd and VEd tile). A seed is labeled ATTO488, B seed is labeled ATTO488 and Cy3, C seed is labeled ATTO647, and D seed is labeled ATTO647N and ATTO488. (B) Schematic of AB DNA Nanotube Point to Point Assembly. RS nanotubes nucleate at the A and B molecular landmarks, grow, and then join to form a stable connection. (C) Schematic of CD DNA Nanotube Point to Point Assembly. CD nanotube point to point connection is labeled as Cy3 (D) Schematic of AB & CD DNA Nanotube Connections. A, B, C, and D seeds are attached on the surface, AB and CD point to point assembly occur in tandem.

Furthermore, DNA nanostructures that have different DNA sequences can also enable selective control over mechanisms that govern complex growth and termination processes.[15-17] As a result, DNA nanostructure termed "cap" is designed to bind on the

growing ends of the DNA nanotube to prevent growth. Multiple types of DNA tile can be designed to selectively control a certain type of nanotube growth while allowing the other types of nanotube growth to continue.

Two Types of DNA DAE-E Tile System Can Form Multiple DNA Nanotube Connections.

Here we develop a technique to selectively connect different molecular landmarks and to form multiple DNA nanotube connections based on different DNA sticky end sequences (Fig. 1). We use DAE-E DNA tile nanotubes, a model system for understanding and controlling the dynamics of DNA tile self-assembly that has been used to study controlled nucleation,[15] architecture formation and triggerable growth,[13] and driven assembly and disassembly.[16] The DNA nanotubes we study are assembled from DAE-E tiles that form from 5 component DNA strands (Fig. 1a, Supp. Note. S1). These DNA tiles assemble into nanotubes through the hybridization of short, single-stranded sticky ends which contain 4 sticky ends which allow nanotubes to nucleate under room temperature. Nanotubes that nucleate homogenously can have a range of circumferences, ranging from 4 to 12 tiles, but nanotubes grown from DNA origami templates have a monodisperse circumference of 6 tiles.[15] Because seeds control where and when nanotube assemble, so we hypothesize that monomer connection could form through nanotube growth and diffusion by placing seeds on the horizontal glass surface plane. Seeds that are fixed on a surface plane can direct nanotube growth, and growth of nanotube occurs at free nanotube ends.

Previous study has shown that point-to-point assembly can be designed and formed between A and B seeds that are attached on a glass bottom surface at 32°C and 40nM. We use the same type of seeds named long seeds that contain 72 staples but with 4 sticky ends rather

than 5 sticky ends, and we demonstrate that point to point assembly is extensible and we can perform such assembly processes multiple times under room temperature. 150 nM of RS (labeled as ATTO647N) tile mix will first start to nucleate on the A, B seeds; once nucleation starts to occur, nanotubes will then diffuse and join and form connections under room temperature and connections are verified using fluorescence microscopy (Fig. 1b). We then show we can design additional point to point assembly system connecting C and D seeds using 40 nM of different DNA tiles termed as "UV" tiles (UEd and VEd tiles are labeled as Cy3) (Fig. 1c). In both cases, different combinations of fluorescence labeling are adopted to distinguish diverse connections. Furthermore, complex nanotube connections can occur in tandem and two types of tile mix can form multiple DNA nanotube connections simultaneously when all four types of seeds are present on a single image plane, and can form correct nanotube connection pairs such as RS only connects A and B seeds, UV only connects C and D seeds (Fig. 1d).

Two Types of Nanotubes Can Enable Nanostructures to Selectively Terminate DNA Nanotube Growth.

Based on abovementioned tiles, we develop a method to selectively terminate the assembly of growing structures in which a designed complex binds to a facet where growth is occurring, preventing the attachment of further monomers. We slightly adjust the seed structure in this study and allow the seeds to have 24 staples rather than 72 staples but with the same number of sticky ends. We term a nanostructure that binds to the growing end of DNA tile nanotubes and halts nanotube growth "cap". To develop an effective capping structure, we show first how nanostructures that act as templates for nanotube nucleation from specific nanotube facets can also act as caps by binding to that facet on existing

nanotubes. Caps are modified based on existing seed structure that can halt the growth of existing DNA nanotubes by binding to their ends, but do not themselves nucleate new nanotubes. We also show that these caps selectively bind to nanotubes with complementary tile types and that multiple types of caps can selectively act on their respective nanotube tile ends. Together, seeds and caps allow control over both the initiation and termination of nanotube growth. This control could allow precise control over the assembly and disassembly of DNA nanotubes and nanotube architectures. This design serves as a guide to construct a variety of nucleation and termination mechanisms.

Results and Discussion

Seeded Nanotube Growth Can Occur at Room Temperature.

To study point to point assembly and nanotube capping, we characterized how assembly yield changes with time, and how caps interacted with nanotubes grown from DNA origami seeds. DNA origami seeds consisting of 12 parallel DNA helices connected by crossover points arranged into a cylinder.[15] Attached to this structure are *adapter strands* whose crossover structure matches that of the DNA nanotubes. These adapter strands are designed to minimize structural dissimilarity between the origami and present sticky ends for tile binding.

It was previously shown that seeds can template nucleation of DNA tile nanotubes at 32 ºC where spontaneous nucleation of nanotubes is very rare.[15] At room temperature, however, the tiles used in that study can rapidly nucleate new nanotubes even in the absence of seeds, which limits how control over nucleation can be applied in practice. Here we modified the tiles and seeds so that the nucleation and growth of nanotubes is controlled by seeds at room temperature so that the self-assembly processes considered here and the characterization of the resulting structures both took place under ambient conditions (Supp. Notes S1, S3). Because these modified seeds were designed to allow nanotubes to nucleate and grow at room temperature from the A facet of the nanotubes (Fig. 1a), we called them RT (room temperature) A seeds. These seeds have 24 staples, and dish experiment uses long seed structure that have 72 staples.

To test that RT A seeds can direct nanotube nucleation, we annealed and purified RT A seeds labeled with Atto 647N dye and purified them using membrane filters and centrifugation (See Methods, Supp. Note S9). Separately, we annealed aliquots of RS tile strands and after the solutions reached room temperature, added either 2 pM of RT A seeds

or an equivalent volume of buffer (for a control) such that the final tile concentration in each mixture was 45 nM (Supp. Note S11). We measured the number of nanotubes that grew and their lengths using two-color fluorescence microscopy images of the reaction mixtures that were pipetted onto a glass surface. RT A seeds were visible at most nanotube ends in the seeded sample, consistent with their roles as templates for growth. To construct point to point assembly experiment, A, B, C and D seeds were modified to have 72 staples because long seed structure is suitable to conduct dish experiment.

Seed Labeling Fluorescence Verification.

The first step to construct multiple DNA nanotube connections is the determination of multiple types of seeds in the assembly process. Because we have 4 types of seeds (A, B, C and D seeds) and two types of nanotubes but limited fluorescence (ATTO647N, ATTO488, and Cy3), so it is essential to distinguish diverse molecular landmarks. Previous studies have shown that seeds can nucleate and direct nanotube nucleation under room temperature. Seeds along with their adapters can be extended and modified with different DNA sequences to nucleate different nanotubes. We annealed four types of seeds (A, B, C and D seeds), and then added either 4 pM of A and B seeds or 4 pM of C and D seeds on a treated glass surface (Supp. Notes S19, S20, S21).

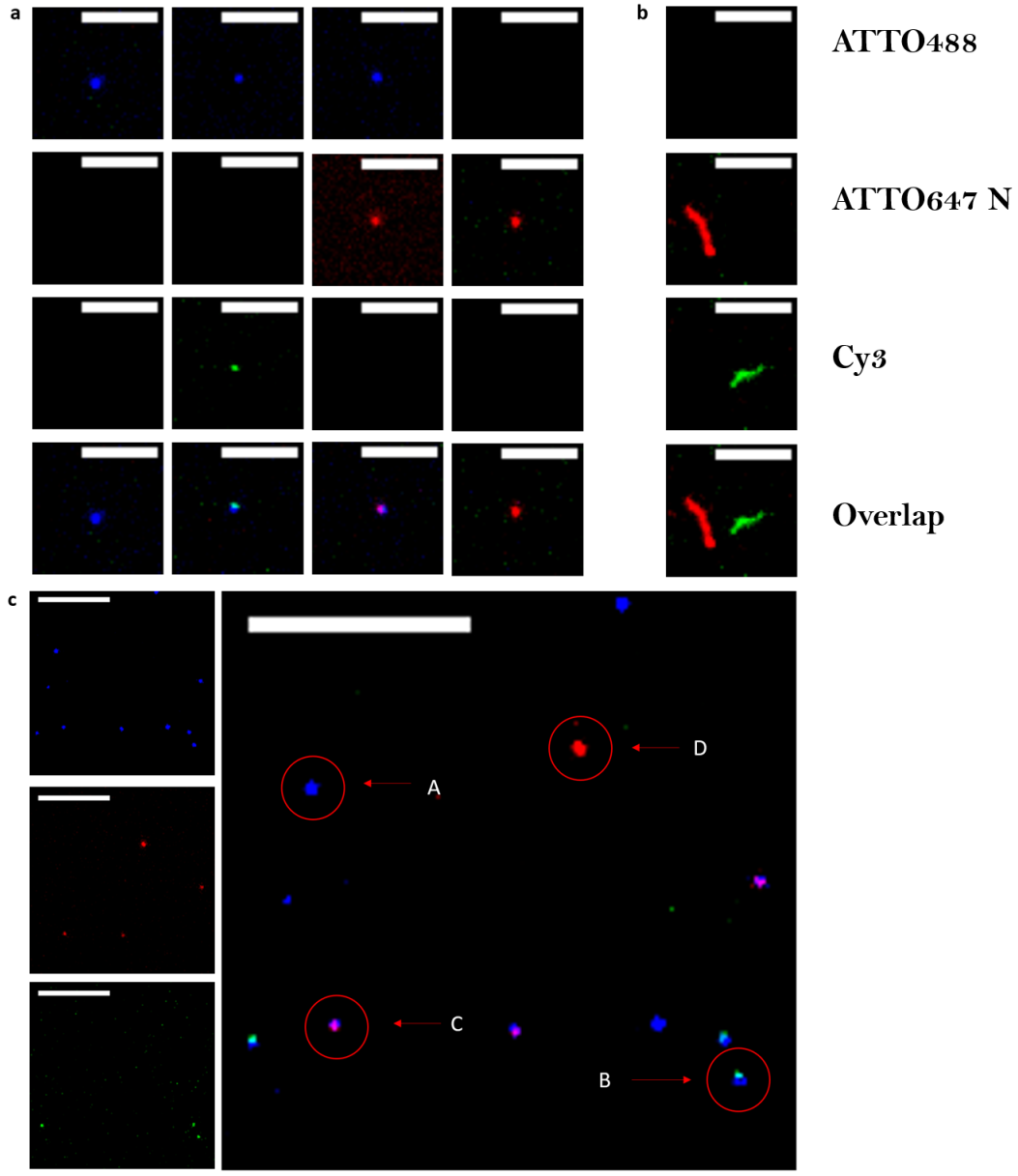

Figure 2. Multicolor fluorophore labeling of different types of seeds and nanotubes. (A) Example fluorescent origami assembly species, both in individual channels and overlays, for objects in three channels. Size of each fluorescent image: 5.95 × 5.95 μm. Scale bar: 3 μm. (B) Example fluorescent nanotubes, both in individual channels and overlays. Size of each fluorescent image: 9.35 × 9.35 μm. Scale bar: 5 μm. (C) The four types of seeds are labeled with three different fluorophore types Pixel locations of seed structures are visualized in individual fluorescence channels (red, green and blue). Image sizes: 21.25 × 21.25 μm. Scale bar: 10 μm.

Each of the seeds was labeled with different fluorophores or different combinations of fluorophores so that static fluorescent micrographs of surface-linked seeds provided a 2D

representation of seed composites (Fig. 2c). We captured the images of seeds under three microscopic channels and then confirmed the four types of seeds using standard MATLAB detection algorithm and measured their corresponding pixel positions. The presence of the seeds was verified if pixel positions of threshold fluorescent images were returned the same (Supp. Fig. S22). The seeds types were then manually checked for precision.

Point to Point Assembly Is Extensible and Multiple Nanotube Connections Can Form Separately.

We then explore design principles to build multicomponent assembly devices that respond to environment by forming multicomponent DNA nanotube connections. It was previously shown that point to point assembly can be directed by DNA origami A and B seeds that were passivated on a glass surface via biotin linker strand at 32 ºC with nanotubes that have 5 sticky ends. At room temperature, however, the tiles used in that study can no longer effectively nucleate on seed structure and are restricted to form only one type of connection, which limits how point to point assembly at various temperature can be applied in practice. Here we adopted seeds and tiles that can nucleate efficiently at room temperature with 4 sticky ends so that the self-assembly processes considered here can take place under ambient conditions (Supp. Notes S1, S2, S3, S4).

We performed point to point assembly in two separate reaction processes: RS connections labeled as ATTO647N were formed between A and B seeds; UV connections labeled as Cy3 were formed between C and D seeds (Supp. Notes S19, S20). A, B, C, D seeds were attached on glass surface at random locations. We grew these two different types of nanotubes at different concentrations, RS (ATTO647N) tile at 150nM and UV (Cy3) tile at

60nM with AB seeds concentration at 4pM and CD seeds concentration at 4pM. We first studied how nanotubes grew and formed connections when seeds were present on the surface. Nanotubes grew from all seed types and increased in length gradually. Two types of nanotube connections formed between A and B seeds, C and D seeds. Connections have no kinks upon joining.

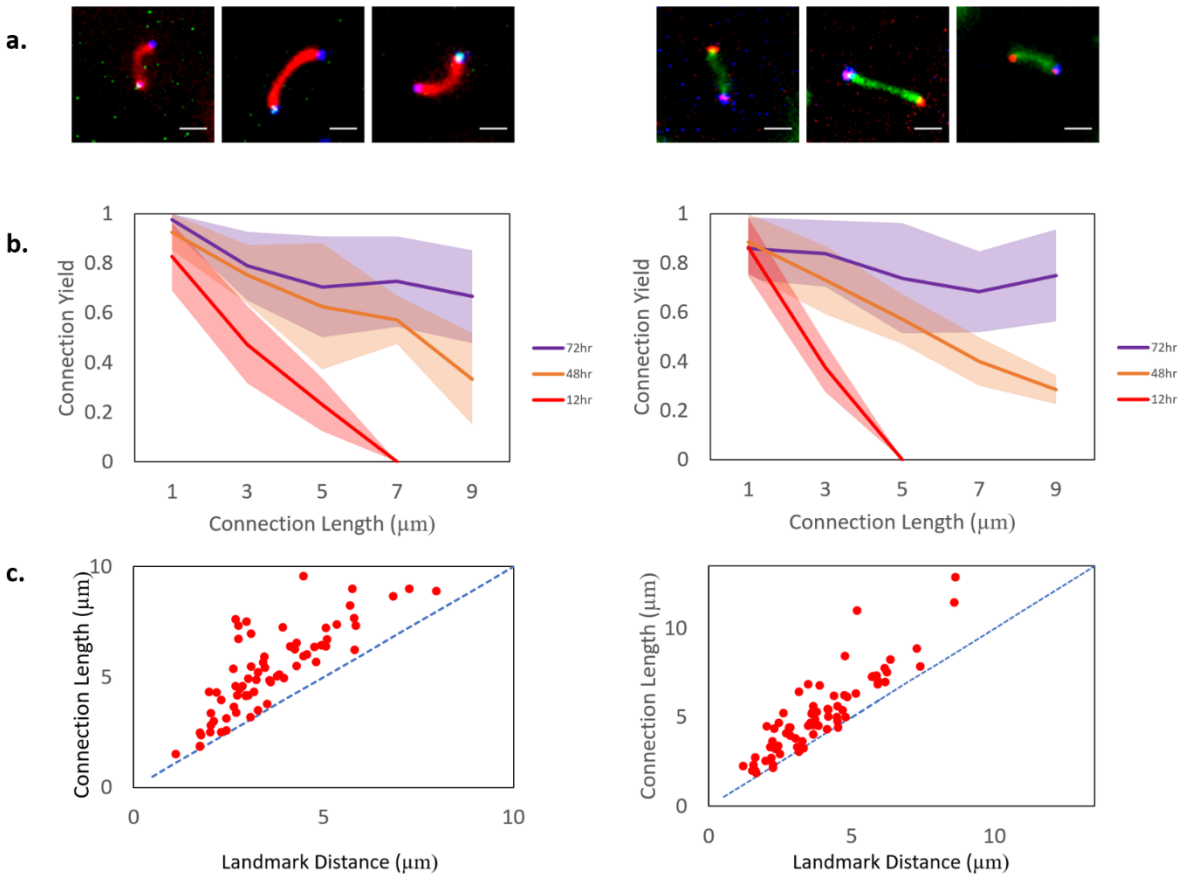

Figure 3. Interconnecting AB and CD DNA nanotube connections in isolation. (a) fluorescence micrograph showing RS nanotube connections connecting A and B seeds and UV nanotube connections connecting C and D seeds. RS nanotubes are labelled with ATTO647N (red) and UV nanotubes are labelled with Cy3 dye (green). A seeds are labeled with ATTO488 and Cy3 so they appear as Cyan, B seeds are labeled with ATTO488 and appear as blue, C seeds are labeled with ATTO647 and ATTO488 and appear as purple and D seeds are labeled with ATTO647 and appear as red. Scale bars, 2μm. (b) Connection yield as a function of inter-seeds distance for different assembly times. N = 177, 106 and 202 for AB nanotube connections. N = 121, 216 and 152 for CD nanotube connections. (c) Scatter plot of landmark distance and the length of nanotube connection after 48hr of reaction time. Left is AB nanotube connections scatter plot and right is CD nanotube connections scatter plot.

One potential source of error to skew the observation of connections is that ends of nanotubes join and appear to be connected. To verify that nanotube connections formed, we captured ten continuous dynamic fluorescence microscopy images of nanotube connections, nanotube connections were confirmed if connections continued to exist throughout additional images.

To understand point to point assembly, we used fluorescence microscope to characterize connection yield at 12hr, 48hr and 72hr by counting the isolated pairs of seeds such as A and B, C and D seeds. An isolated pair was determined when AB nanotube connection was separated by distance d between A seed and B seed, and no other A or B seeded nanotubes were found within 1.5×d distance of the connection distance (Supp. Note S23). AB and CD DNA nanotube point to point assemblies were performed under separate reaction schemes (Fig. 2a). After 12 hr, AB and CD DNA nanotube connections both showed high yield (>80%) at interlandmark distance 1 μm but with a decreased trend in yield as landmark distance increased. After 48 hr, connection yield increased as a function of molecular landmark distance for both AB and CD DNA nanotube connections: AB DNA nanotube connection yield increased from 47% and 23% at interlandmark distance 3 μm and 5 μm at 12hr to 75.5%, 62.5%, 57.1%, and 33.3% at interlandmark distance 3 μm, 5 μm, 7 μm and 9 μm. CD DNA nanotube connection yield increased from 37.5% and 0% at interlandmark distance 3 μm and 5 μm at 12hr to 73.1%, 57.1%, 40.0%, and 28.6% at interlandmark distance 3 μm, 5 μm, 7 μm and 9 μm. After 72h, longer point to point assemblies formed for both types of connections: AB DNA nanotube connections had above 66.7% yield for all distances and CD DNA nanotube connections had above 68.4% yield for all distances (Fig. 3b). Scatter plots showed connected nanotube lengths had approximately the same length as the landmark

distance (Fig. 3c). AB and CD DNA nanotube connections scatter plots indicated nanotube connections length was approximately the length of interlandmark distance. Over the 72-hour reaction process, nanotube tiles were replenished every 24 hours to ensure the depletion of tile mix did not affect nanotube growth rate.

Multicomponent DNA Connections Can Form Simultaneously.

Because seeds and sticky end sequences direct what connections to form, we hypothesized that specific connections can form when these two types of nanotubes are presented simultaneously along with all types of seeds. To test this hypothesis, we characterized connection yield for these two types of connections to determine how assembly can be affected.

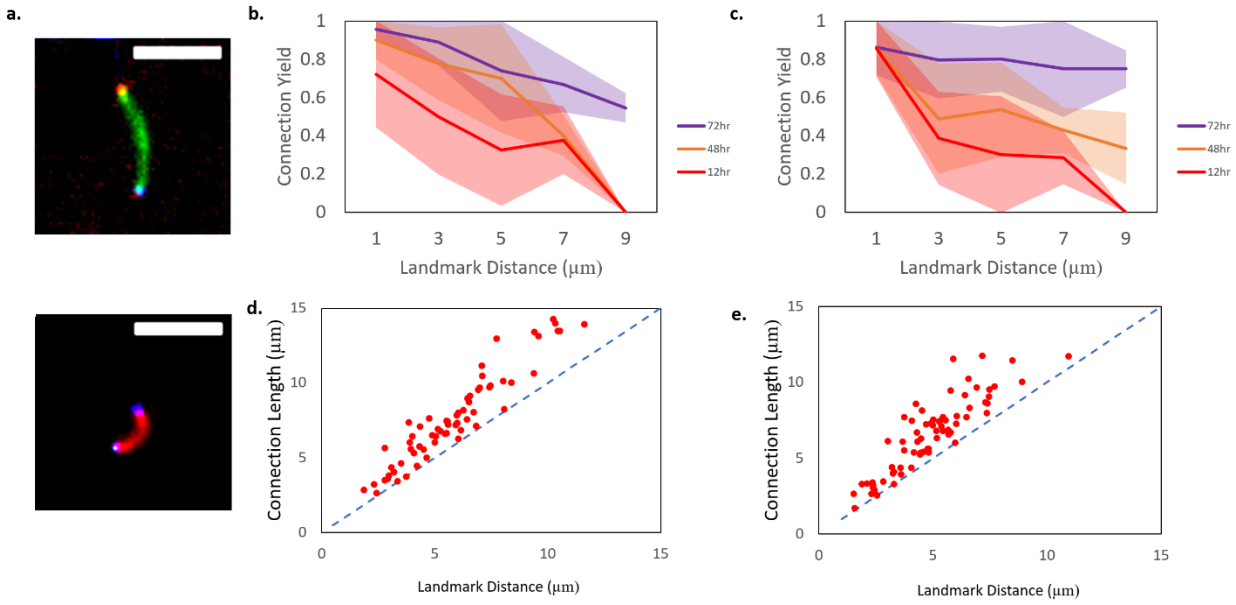

Figure 4. Forming AB and CD DNA nanotube connections simultaneously. (a) fluorescence micrograph showing two types of nanotube connections connecting four nanotube seeds (A, B, C and D). Labeling scheme is the same as described before. Scale bars, 5μm. 11.05×11.05 μm. (b-c) Connection yield as a function of inter-seeds distance for different assembly times. N = 95, 63, 87 for AB nanotube connections. N = 79, 138 and 124 for CD nanotube connections. (d-e) Scatter plot of landmark distance and the length of nanotube connection after 48hr of reaction time. Left is AB nanotube connections scatter plot and right is CD nanotube connections scatter plot.

We adopted the same methodology to grow nanotubes directly on dish surface from 4 pM of A, B, C and D seeds with RS (ATTO647N) tile at 150nM and UV (Cy3) tile at 60nM (Supp. Note S21). Seeds were later detected and confirmed with overlapping pixel positions and then manually checked for presence (Supp. Note S22).

We measured connection yield at 12hr, 48hr and 72hr and characterized them by counting the isolate pair for both A and B seeds, C and D seeds (Supp. Note S23). The connection yield increased as a function of connection distances for different assembly times and the yield of both A and B, C and D connections were comparable. After 12 hr, AB and CD DNA nanotube connections both showed high yield (>70%) at interlandmark distance 1 μm but with a decreased trend in yield as landmark distance increased. After 48 hr, connection yield increased as a function of molecular landmark distance for both AB and CD DNA nanotube connections: AB nanotube connection yield increased from 50% and 32.5% at interlandmark distance 3 μm and 5 μm at 12hr to 77.8%, 70.0%, 40.0% at interlandmark distance 3 μm, 5 μm, 7 μm. CD nanotube connection yield increased from 38.7%, 30.0% and 28.6% at interlandmark distance 3 μm, 5 μm, 7 μm at 12hr to 48.9%, 53.6%, 42.9%, and 33.3% at interlandmark distance 3 μm, 5 μm, 7 μm and 9 μm. After 72h, longer point to point assemblies formed for both types of connections: AB nanotube connections had above 55.6% yield for all distances and CD nanotube connections had above 75.0% yield for all distances (Fig. 4b. and 4c.). When growing AB and CD DNA connections together, scatter plots showed connected nanotube lengths had approximately the same length as the landmark distance (Fig. 4d. and 4e.).

The Connection Ratio Distribution of Interconnected Connections.

We discovered that when AB or CD DNA nanotube connections formed, C or D seeded nanotubes, A or B seeded nanotubes also could appear within 1.5d of the interlandmark

distance. It is possible that C or D seeded nanotube will interfere with the formation of AB DNA nanotube connections, and A or B seeded nanotubes will interfere with the formation of CD DNA nanotube connections. We intended to study the interaction of these cases and to determine the ratio of connection nanotube length to the landmark distance for isolated pairs and unisolated pairs to compare and study the effect of the interaction. If the interactions between different interconnected nanotubes were significant, they should produce a different distribution of the ratio compared to the ratio of that of the isolated pairs because connections would take longer to form due to the spatial occupation of other molecules. We plotted the histogram of the ratio distribution for isolated AB and CD DNA nanotube connections and compared it with unisolated AB and CD DNA nanotube connections and observed a similar peak distribution in the ratio of connection nanotube length to the landmark distance (Fig. 5 d-e). If the peak distribution showed differences, that meant the other seeded nanotube affected AB or CD DNA nanotube connections and suggested the presence of other seeded nanotube forced longer or shorter connection to form. We observed a similar peak distribution which indicated that these two cases allowed connections to have roughly the same average nanotube length to landmark distance ratio (Fig. 5 d-e). Thus, we interpreted that a particular type of nanotube connection was not significantly affected by the presence of other types of seeded nanotubes.

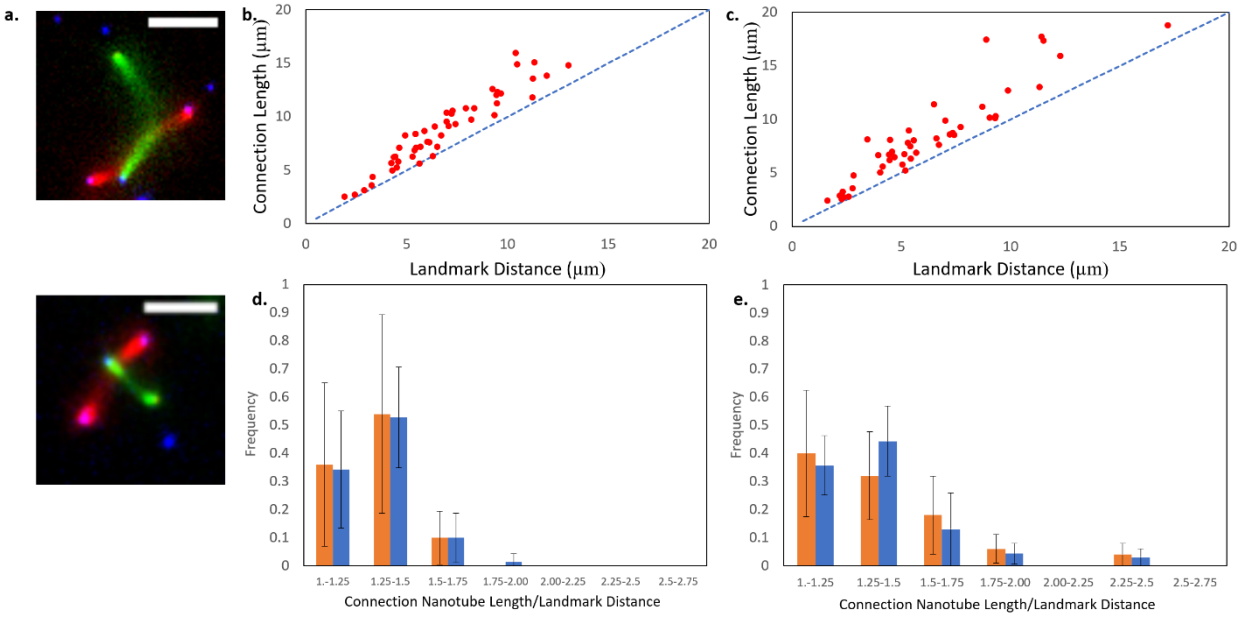

Figure 5. Proximity of nanotube connections to determine interactions. (a) fluorescence micrograph showing two types of nanotube connections forming interconnecting structures. Scale bars, 5µm. (b-c) Scatter plot of landmark distance and the length of nanotube connection after 48hr of reaction time. Scatter plot on the left is AB connections with at least a C or D seeded nanotubes, on the right is CD connections with at least a A or B seeded nanotubes. (d) Frequency distribution of AB DNA nanotube connection length to landmark distance. Blue histogram shows ratio of AB DNA connections to landmark distance. Orange histogram shows ratio of AB DNA connections to landmark distance with the presence of the other C or D seeded nanotube. (e) Frequency distribution of CD DNA nanotube connection length to landmark distance. Blue histogram shows ratio of CD DNA connections to landmark distance. Orange histogram shows ratio of CD DNA connections to landmark distance with the presence of the other A or B seeded nanotube.

Flexible caps that present tile binding sites on a single-stranded scaffold bind to nanotube ends and stop nanotube growth but cannot nucleate new nanotubes.

A flexible cap is a seed structure without the staples so that seed will not be formed to nucleate nanotubes but can still bind on nanotube ends. Flexible caps were effective at stopping the growth of seeded nanotubes, and the flexible cap functioned reliably as a nanotube cap but did not otherwise observably affect the self-assembly process.

Because these seeds remained attached to nanotubes at one facet throughout the growth process, growth of seeded nanotubes occurred at only one facet. The binding of caps to that facet would therefore stop all growth of nanotubes, making it possible to determine whether caps are functional by determining whether nanotubes stop increasing in length after caps bind to nanotube ends. To understand how to use caps within controlled, dynamic assembly processes, we also measured the rate of nanotube growth and the rate at which flexible caps bind to growing nanotube ends. We attached nanotube seeds to a passivated glass surface using biotin-streptavidin linkers (Supp. Note S12) and used time-lapse fluorescence microscopy to track the state of each of a set of nanotubes throughout a growth or capping process (Supp. Notes S13-14).

Under these conditions, slightly different concentrations of tiles were needed to achieve reliable growth and capping, perhaps because of a difference in reagents used to minimize nonspecific adsorption of reaction components and differences that arise because of presence of the dish, rather than Eppendorf tube, surface (Supp. Note S13). At 75 nM of tile monomers, we observed that nanotubes grew at an average rate of 0.165 ± 0.0052 μm/hr (Supp. Figs. S9), similar to earlier measurements made in other systems. We measured capping by tracking the rate at which caps attached to seeded nanotubes on the surface (Fig. 5, Supp. Figs. S10) and fitting the fraction of capped nanotubes to find a reaction rate of $k_f = 1.85 \times 10^6$ $M^{-1}s^{-1}$ (Supp. Note S18). This rate is similar to the measured forward rate of tile attachment and of origami hybridization, suggesting that the kinetics of capping are controlled by multivalent hybridization of sticky ends in similar fashion.[23] Capping takes a long time to complete because the concentrations of both nanotube ends and caps are both low.

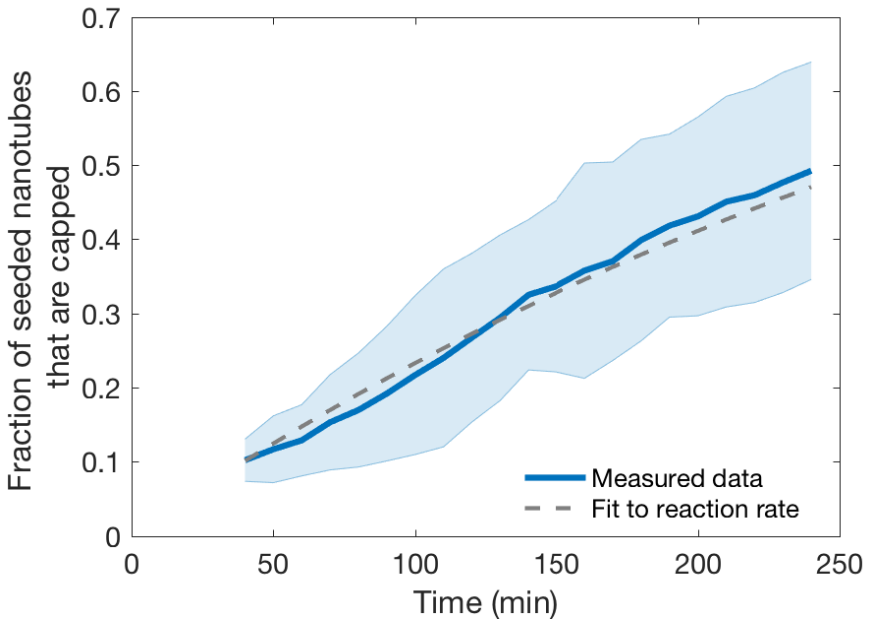

Figure 6: The fraction of nanotubes that were capped over time characterized using time-lapse microscopy following individual seeded nanotubes. Individual A seeded, RS tile nanotubes were attached to a passivated glass dish in a solution of 24 pM caps and 75 nM tiles (Supp. Note S15). The measured fraction of capped nanotubes was used to fit a binding constant between tubes and caps. A 95% confidence interval, determined by bootstrapping, is shown in the shaded light blue region. N=301.

Flexible caps selectively bind to and stop the growth only of nanotubes presenting complementary sticky ends.

Caps are designed to present nanotube sticky end sites and therefore should bind selectively only to nanotube sticky ends. Sets of caps that each bind only their specific nanotube type could be instrumental in constructing complex networks and structures containing multiple types of nanotube filaments. To ask whether caps selectively bind nanotubes with complementary sticky ends, we designed a new seed (termed RT C) for tiles with different sequences, termed UV tiles (Supp. Notes S2 and S4).[14] Sequence-specific

binding of RS and UV tiles ensure that RT A nucleate only RS tile nanotubes and RT C nucleate only UV tile nanotubes.[18]

We next designed a set of adapters for a flexible cap designed to attach to the growing end of UV tile nanotubes (Supp. Note S7). The flexible caps with these adapters were termed D caps. To test that the binding of B and D caps was selective for nanotube type, we grew RS and UV nanotubes from 2 pM RT A and RT C seeds in four tubes. To the four tubes, we added either no caps, 10 pM B caps, 10 pM D caps or 10 pM of both B and D caps after 8 hours of growth (Supp. Notes S15 and S16). We used fluorescence images to determine where binding occurred. UV tiles were labeled so that their fluorescence intensity would be only 25% of the RS tubes, making it possible to distinguish the two types of tubes, and B and D caps were labeled with different combinations of fluorescent dyes so that they could also be distinguished visually. We measured the lengths of the resulting nanotubes and determined whether each nanotube had a seed and/or which cap using 3-color fluorescence micrographs of reaction aliquots adhered to a microscope slide taken after 8.5, 25 and 50 hours of growth (Fig. 6a-d, Supp. Note S12).

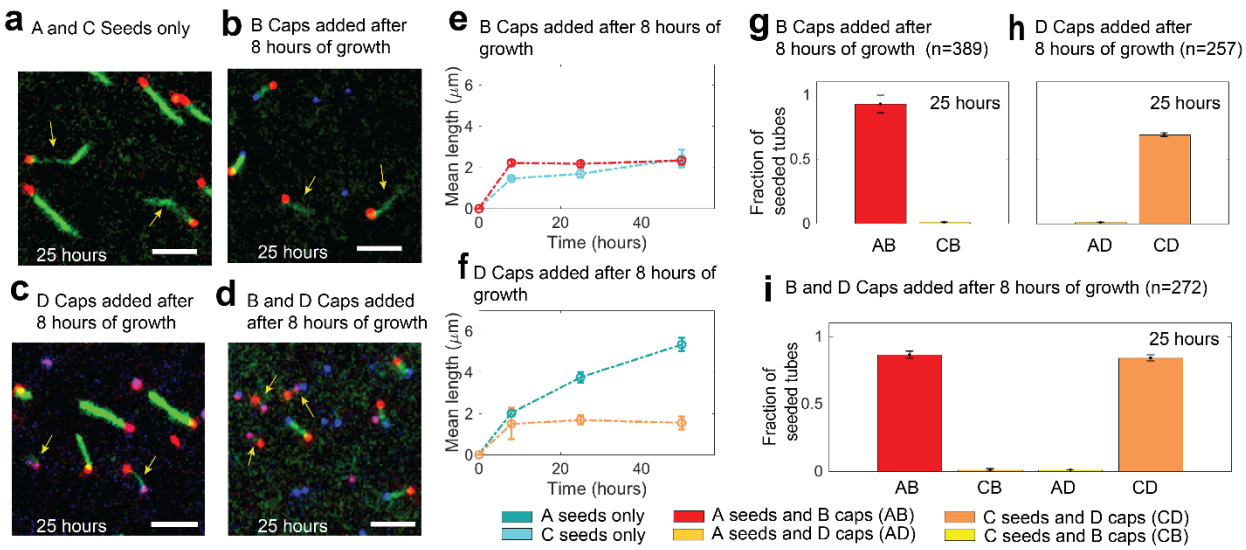

Figure 7: Flexible caps bind selectively to nanotubes end with complementary sticky ends. RS tile nanotubes (Cy3 bright green) grew from RT A seeds labeled with Atto 647N (red) and UV tile nanotubes (Cy3 dim green at 25% incorporation) grew from RT C seeds labeled with Atto 647N (red). Flexible cap B was labeled with Atto 488 (blue) and flexible cap D was labeled with 50% Atto 647N and 50% Atto 488 dyes (purple). Example fluorescence micrographs of nanotubes grown in the presence of RT A and C seeds to which (a) buffer was added, (b) flexible B caps and (c) flexible D caps and (d) flexible B and D caps were added at 8 hours. Yellow arrows identify RT C seeded UV nanotubes. e) RS tile nanotubes stopped growing after B caps are added at 8 hours but UV tile nanotubes did not. (f) UV tile nanotubes stopped growing after D caps were added at 8 hours but RS tile nanotubes did not. (g) Fractions of seeded RS and UV tile nanotubes that were capped by B seeds (AB vs CB) after 25 hours. Caps were added at 8 hours. (h) Fractions of seeded RS and UV tile nanotubes capped by D seeds (AD vs CD) after 25 hours. Caps are added at 8 hours. (i) Fractions of seeded RS and UV tile nanotubes capped by the two types of caps when both B and D caps are added at 8 hours. Scale bars are 4 μm.

The average lengths of RT A and C seeded nanotubes plateaued only when their respective flexible caps were present, suggesting that each cap bound only to nanotubes with the complementary growing end to prevent further nanotube growth (Fig. 6e-f, Supp. Fig. S12). When both B and C caps were added, 86 ± 3.6% of RT A seeded nanotubes and 83 ± 3% of RT C seeded nanotubes had B and D caps bound respectively at their growing ends. We observed almost no RT C seeded nanotube with B caps at their ends or RT A seeded

nanotube with D caps at their ends (Fig. 4g-i). Thus, the flexible caps selectively terminate the growth of seeded nanotubes.

CONCLUSION

In this thesis we demonstrate how multicomponent point-to-point assembly system can be designed to form complex patterns. These DNA nanotube connections can occur in tandem and are formed between molecular landmarks where the orientations are unknown. Spatial control of self-assembly could be achieved by placing seeds at specific locations and we demonstrated temporal control of growth by varying nanotube connection length and molecular landmark distance. This multicomponent DNA origami technique illuminated new ways to expand the usage of DNA sequences, and thus makes it possible to construct multiple channels to interconnect different cellular components and to produce a wide variety of functional nanotube networks. More generally, multicomponent point to point assembly demonstrates that self-assembly processes can be selectively formed to achieve complicated nanostructure pattern that could potentially govern cellular interactions. Engineered structures shines light on understanding complicated biological assembly materials such as the cytoskeleton in which filaments are precisely controlled and manipulated.

We further demonstrate that nanostructures can bind to the facets of DNA nanotubes and terminate their growth selectively. Such structures could be used to arrest assembly reactions far from equilibrium such that growth rates and the time over which growth occurs can be independently controlled.

The systematic approach taken to understanding multicomponent point to point assembly and capping process in this work illuminate the design principles for assembling nanotube network and the termination mechanism. The use of DNA nanostructures in our study suggests ways to demonstrate the motif of multicomponent devices over the spatial arrangement of such nanostructures. These nucleation and crystal growth design rules can be

extended to design functional structures and systems that guide the crystallization of proteins,[19, 20] metals and the assembly of carbon nanotubes.[21,22]

Materials and Methods

DNA nanotube, seed and cap components: The sequences of RT tiles, adapter, seeds and caps used in this study are listed in the supporting information. DNA tile, adapter, staple, dye strands, dye attachment strands, biotin attachment and biotin attachment linker strands were synthesized by Integrated DNA Technologies, Inc. M13mp18 was purchased from Bayou Biolabs. Glass marker dishes (μ-Dish 35mm, high Grid-50 Glass Bottom) and glass bottom dishes (D29-20-1-N, In Vitro Scientific) were purchased from Ibidi. Biotin-PEG-Silane (Biotin-PEG-SIL-3400-500mg) was purchased from Layson Bio, and Neutravidin (31000), Streptavidin (21122) and BSA (Bovine Serum Albumin) were purchased from Thermo Fisher Scientific. Adapter strands with sticky ends and tile strands without fluorescent labels were PAGE purified. Tile and origami strands with fluorescent labels were HPLC purified. All other strands were used directly after desalting. Sequences for seeds and tiles are given in Supp. Notes S1-S4. Sequences for caps are in Supp. Notes S5 and S7 and Fig. S7.
For capping project, RT RS tiles were labeled with Cy3 fluorescent dye to allow fluorescence imaging of nanotubes while RT UV tiles were labeled with 25% Cy3 fluorescent dye, making it possible to distinguish RS tile nanotubes from UV tile nanotubes in the same image (Fig. 6a-d, Supp. Note S16). RT A seeds and RT B seeds (or caps) in experiments characterizing their yields when used were labeled with Atto 647N dye and Atto 488 dye respectively (Supp. Note S6). RT C seeds and flexible D caps in experiments characterizing their yields when used were labeled with Atto 647N dye, and a mixture of 50% Atto 647N 50% Atto 488 dyes respectively (Supp. Notes S6). All seed and cap structures used a common set of strands for labeling that attach to unfolded regions of the scaffold strand and present binding sites for a fluorescent strand (Supp. Note S6). All samples were prepared in TAE

Mg^{2+} buffer (40 mM Tris-Acetate, 1 mM EDTA to which 12.5 mM magnesium acetate was added). In experiments with RS tiles performed in Eppendorf tubes, the strands for each tile were present at 45 nM except for the strands presenting sticky ends, which were present at 90 nM to minimize the concentration of malformed tiles (Supp. Note S10). In experiments with RS tiles performed in glass-bottom dishes, the strands for each tile were present at 75 nM except for the strands presenting sticky ends, which were present at 150 nM to minimize the concentration of malformed tiles (Supp. Notes S13). In experiments with UV tiles, the strands for each tile were present at 30 nM except for the strands presenting sticky ends, which were present at 60 nM. Adapter strands presenting sticky end sequences were analogously included at a 2-fold excess over other adapters (Supp. Notes S15).

For point to point assembly project, RS tiles were labeled with ATTO647N fluorescent dye to allow fluorescence imaging of nanotubes while UV tiles were labeled with Cy3 fluorescent dye, making it possible to distinguish RS tile nanotubes connections from UV tile nanotubes connections. A seeds and B seeds in experiments characterizing their yields when used were labeled with Atto 488 dye while B seeds were labeled with a mixture of 50% Atto488 and Cy3 dye respectively. C seeds in experiments characterizing their yields when used were labeled with Atto 488 dye, and D seeds were labeled with a mixture of 50% Atto 647N and 50% Atto 488 dyes respectively. All seed structures used a common set of strands for labeling that attach to unfolded regions of the scaffold strand and present binding sites for a fluorescent strand (Supp. Note S6). In experiments with RS tiles performed in glass-bottom dishes, the strands for each tile were present at 150 nM except for the strands presenting sticky ends, which were present at 300 nM to minimize the concentration of malformed tiles (Supp. Notes S19). In experiments with UV tiles, the strands for each tile were present at 60 nM except for the strands presenting sticky ends, which were present at 120 nM (Supp.

Notes S20). Concentrations of tile and adapter strands were determined using 260 nm absorbance spectroscopy while the concentrations of staple, attachment and labeling strands concentration were assumed to be those provided by IDT.

Sample preparation: To grow RT A or C seeded nanotubes, 19.7 μL of a tile solution was annealed from 90 ºC to 20 ºC and then 0.3 μL of a solution of purified seeds was added after the solution reached 20 ºC (Supp. Note S10) so that either the RS tile concentration was 45 nM or the UV tile concentration was 30 nM after addition. To grow RT A seeded B capped nanotubes, 19.4 μL of a tile solution was annealed from 90 ºC to 20 ºC and then 0.3 μL of a solution of purified seeds was added after the solution reached 20 ºC (Supp. Note S11). To measure the growth rate of seeded nanotubes, purified RT A seeds with linker and attachment strands in 1 × TAE Mg^{2+} buffer were added to glass bottomed dishes where the surface prepared as described in Supp. Note S12. This was followed by 3 washes of 1 × TAE Mg^{2+} buffer to remove the unattached seeds and then 1000 μL of 75 nM of the RS tile mixture were placed into the dish (Supp. Note S13). At each time point (0, 6, 12 and 24 hours) before imaging, the tile mixture in the dish was replaced by 1000 μL of 1 × TAE Mg^{2+} buffer and once the imaging was over, the same tile mixture was placed back into the dish. Upon each transfer, the dish was sealed with Parafilm to prevent solution evaporation. To measure the capping rate, 19.7 μL of RS tile solution was annealed from 90 ºC to 20 ºC and then 0.3 μL of a solution of purified full RT A seeds with linker and attachment strands was added into the tile mixture so that the final tile and seed concentration will be 75 nM and 2 pM respectively after the addition (Supp. Note S18). Solutions were incubated at 20 ºC in an Eppendorf Mastercycler for 6 hours before transferring into the glass surface made using Supp. Note S12.

This was followed by 3 washes of 1 × TAE Mg^{2+} buffer to remove the unattached seeded nanotubes and then 985 μL of 1 × TAE Mg^{2+} buffer and 15 μL of the purified flexible B caps (Supp. Notes S14) were added so that the cap concentration will be 24 pM after the addition. The dish was then sealed with Parafilm to prevent solution evaporation (Supp. Note S12). Experiments with glass-bottomed dishes where the seed is anchored used the staples for the seed from Mohammed *et al.*[16] (see Supp. Note S12). To grow RT A seeded B capped and RT C seeded D capped nanotubes in a single pot reaction, 19.4 μL of RS and UV tile solution was annealed from 90 ºC to 20 ºC and then 0.3 μL of a solution of purified A and C seeds was added after the solution reached 20 ºC. Flexible B and/or D caps were added at the times described in the text by adding 0.3 μL of a purified cap solution to the resulting mixture (Supp. Note S16) so that the RS and UV tile concentration was 45 nM and 30 nM respectively after addition of seeds and caps. Solutions were incubated at 20 ºC in an Eppendorf Mastercycler. To grow AB or CD nanotubes connections, 7.5 μL of a solution of purified seeds was added after the solution reached 20 ºC and 500 μL of a tile solution was added. To measure the connection yield at each time point, purified seeds with linker and attachment strands in 1 × TAE Mg^{2+} buffer were added to glass bottomed dishes where the surface prepared as described in Supp. Note S12. This was followed by 3 washes of 1 × TAE Mg^{2+} buffer to remove the unattached seeds and then 500 μL of 150 nM of the RS tile mixture or 40 nM of UV tile mixture were placed into the dish (Supp. Note S19, S20). At each time point (12, 48 and 72 hours) before imaging, the tile mixture in the dish was replaced by 500 μL of 1 × TAE Mg^{2+} buffer and once the imaging was over, the same tile mixture was placed back into the dish. Upon each transfer, the dish was sealed with Parafilm to prevent solution evaporation.

Seed and cap preparation: Seeds and caps were prepared by annealing a solution of 5 nM M13mp18 scaffold, 500 nM of each staple strand, 100 nM adapter strand mix (See Supp. Note 8), 25 nM of each attachment strand and 5000 nM of each labeling strand in TAE Mg^{2+} buffer and 0.05 mg/ml BSA biotin (A8549, Sigma-Aldrich Co.) to prevent surface absorption in PCR tubes from 90 ºC to 20 ºC using an Eppendorf Mastercycler (Supp. Note S9). After annealing, 50 μL of the seed or cap solution and 350 μL of 1 × TAE Mg^{2+} buffer was added to a 100 kDA Amicon Ultra-0.5 mL Centrifugal Filter (UFC510096) and centrifuged at 2,000 RCF for 4 min in a fixed angle centrifuge to remove excess staple and adapter strands. The samples were washed three more times by adding 200 μL of 1 × TAE Mg^{2+} buffer in remaining solution and repeating centrifugation. The remaining solution was recovered by spinning the filter inverted in a fresh tube and the purified mixture was stored at 4 ºC until use. The concentration of seeds or caps in the resulting solution was determined using a calibration method based on fluorescence imaging of different concentrations of structures before and after purification .

Fluorescence microscopy: For every time point at which fluorescence microscopy images of nanotubes were analyzed, 2 slides were prepared by adding 6 μL of reaction solution to 2 cover slips and inverting them onto glass slides. We then captured 2-3 images of nanotubes on each slide at randomly chosen locations. Background caused by adsorption of free tiles was reduced by adding 0.3 μL of a solution of 1 μM of 54 bp DNA strand (*D01)* with a sequence that did not interact with tiles, staples or adapters to each 20 μL sample (Supp. Note S10). This strand acted as a competitor for DNA tile-glass binding. During the experiments performed in glass-bottomed dishes, custom time-lapse image acquisition software was used to collect images at four specific locations, which were selected randomly, over the reaction

period. For measurements of nanotube growth rates, 10 200 ms exposure images of both the Cy3 (RS tile nanotubes) and Atto 647N (RT A seed) channels were collected (Supp. Note S13).

For the capping rate measurement, once the caps were added into the dish, one image of Atto 647N, three images Atto 488 (flexible B cap) and three images of Cy3 were collected. every ten minutes over 4 hours (Supp. Note S18).

For the point to point assembly project, for every time point at which fluorescence microscopy images of nanotubes were analyzed, glass surface of a dish was prepared. We then captured 10 images of nanotube connections at randomly chosen locations. During the experiments performed in glass-bottomed dishes, custom time-lapse image acquisition software was used to collect images. For measurements of connection yield, 10 200 ms exposure images of all the fluorescence channels were collected (Supp. Note S19). Samples were imaged on an inverted microscope (Olympus IX71) using a 60X/1.45 NA oil immersion objective with a cooled CCD camera (iXon3, Andor).

Measurement of nanotube length, capping yield, nanotube connection length and landmark distance: Multicolor images of nanotubes, seeds and caps were prepared by overlaying images of Atto 647, Atto 488 and Cy3 fluorescence that were flattened beforehand using histogram equalization. To measure nanotube lengths and seed locations, fluorescent channel images were first converted into binary form at a manually determined brightness threshold. The structures were then thinned using the bwmorph Matlab function that reduced the binary objects (nanotubes) into single pixel-thick curves. The locations were then measured using Matlab and converted into pixel locations. The length of these curves was then measured using

Matlab and converted into microns using the pixel to micron relation (1 pixel = 0.17 μm). The small number of nanotubes that overlapped one another or were at the edges of images were not included in analysis. To measure the lengths of RT A seeded nanotubes that grew in the dishes as well as DNA nanotube connections, nanotube contour length was calculated by assessing 2D projection of DNA nanotube length via ImageJ JFilament 2D (http://athena.physics.lehigh.edu/jfilament/). The measured pixel length was converted into microns using the pixel to micron relation. A nanotube was considered capped when a cap and seed were detected in the same pixel location over multiple consecutive time points. The small number of nanotubes that overlapped one another or were at the edges of images were not included in analysis. A nanotube connection was considered connected when seeds were detected at both ends of the connection in the same pixel location over multiple consecutive time points.

References

1. Barone, P. W.; Baik, S.; Heller, D. A.; Strano, M. S., Near-Infrared Optical Sensors Based on Single-Walled Carbon Nanotubes. *Nat. Mater.* **2005,** *4*, 86-92.

2. Kreno, L. E.; Leong, K.; Farha, O. K.; Allendorf, M.; Van Duyne, R. P.; Hupp, J. T., Metal–Organic Framework Materials as Chemical Sensors. *Chem. Rev.* **2011,** *112*, 1105-1125.

3. Ge, Z.; Lin, M.; Wang, P.; Pei, H.; Yan, J.; Shi, J.; Huang, Q.; He, D.; Fan, C.; Zuo, X., Hybridization Chain Reaction Amplification of MicroRNA Detection with a Tetrahedral DNA Nanostructure-Based Electrochemical Biosensor. *Anal. Chem.* **2014,** *86*, 2124-2130.

4. Zhang, P.; Cheetham, A. G.; Lin, Y.-a.; Cui, H., Self-Assembled Tat Nanofibers as Effective Drug Carrier and Transporter. *ACS Nano* **2013,** *7*, 5965-5977.

5. Joshi, R. K.; Schneider, J. J., Assembly of One Dimensional Inorganic Nanostructures into Functional 2D and 3D Architectures. Synthesis, Arrangement and Functionality. *Chem. Soc. Rev.* **2012,** *41*, 5285-5312.

6. Veneziano, R.; Ratanalert, S.; Zhang, K.; Zhang, F.; Yan, H.; Chiu, W.; Bathe, M., Designer Nanoscale DNA Assemblies Programmed from the Top Down. *Science* **2016,** *352*, 1534-1534.

7. Benson, E.; Mohammed, A.; Gardell, J.; Masich, S.; Czeizler, E.; Orponen, P.; Högberg, B., DNA Rendering of Polyhedral Meshes at the Nanoscale. *Nature* **2015,** *523*, 441-444.

8. Douglas, S. M.; Dietz, H.; Liedl, T.; Högberg, B.; Graf, F.; Shih, W. M., Self-Assembly of DNA into Nanoscale Three-Dimensional Shapes. *Nature* **2009,** *459*, 414-418.

9. Huang, P.-S.; Boyken, S. E.; Baker, D., The Coming of Age of De Novo Protein Design. *Nature* **2016,** *537*, 320-327.

10. Lin, Y.-R.; Koga, N.; Tatsumi-Koga, R.; Liu, G.; Clouser, A. F.; Montelione, G. T.; Baker, D., Control over Overall Shape and Size in De Novo Designed Proteins. *Proc. Natl. Acad. Sci.* **2015,** *112*, E5478-E5485.

11. Douglas, S. M.; Bachelet, I.; Church, G. M., A Logic-Gated Nanorobot for Targeted Transport of Molecular Payloads. *Science* **2012,** *335*, 831-834.

12. Tian, Y.; Wang, T.; Liu, W.; Xin, H. L.; Li, H.; Ke, Y.; Shih, W. M.; Gang, O., Prescribed Nanoparticle Cluster Architectures and Low-Dimensional Arrays Built Using Octahedral DNA Origami Frames. *Nat. Nanotechnol.* **2015,** *10*, 637-644.

13. Marras, A. E.; Zhou, L.; Su, H.-J.; Castro, C. E., Programmable Motion of DNA Origami Mechanisms. *Proc. Natl. Acad. Sci.* **2015,** *112*, 713-718.

14. Li, Y.; Liu, Z.; Yu, G.; Jiang, W.; Mao, C., Self-Assembly of Molecule-Like Nanoparticle Clusters Directed by DNA Nanocages. *J. Am. Chem. Soc.* **2015,** *137*, 4320-4323.

15. Mohammed, A. M.; Schulman, R., Directing Self-Assembly of DNA Nanotubes Using Programmable Seeds. *Nano Lett.* **2013,** *13*, 4006-4013.

16. Mohammed, A. M.; Šulc, P.; Zenk, J.; Schulman, R., Self-Assembling DNA Nanotubes to Connect Molecular Landmarks. *Nat. Nanotechnol.* **2017,** *12*, 312-316.

17. Wei, B.; Ong, L. L.; Chen, J.; Jaffe, A. S.; Yin, P., Complex Reconfiguration of DNA Nanostructures. *Angew. Chem.* **2014,** *126*, 7605-7609.

18. Chen, H.-L.; Schulman, R.; Goel, A.; Winfree, E., Reducing Facet Nucleation During Algorithmic Self-Assembly. *Nano Lett.* **2007,** *7*, 2913-2919.

19. Askarieh, G.; Nordling, K.; Saenz, A.; Casals, C.; Rising, A.; Johansson, J.; Knight, S. D., Self-Assembly of Spider Silk Proteins Is Controlled by a pH-Sensitive Relay. *Nature* **2010,** *465*, 236-238.

20. Li, P.; Banjade, S.; Cheng, H.-C.; Kim, S.; Chen, B.; Guo, L.; Llaguno, M.; Hollingsworth, J. V.; King, D. S.; Banani, S. F., Phase Transitions in the Assembly of Multivalent Signalling Proteins. *Nature* **2012,** *483*, 336-340.

21. Weiner, S.; Dove, P. M., An Overview of Biomineralization Processes and the Problem of the Vital Effect. *Rev. Mineral. Geochem.* **2003,** *54*, 1-29.

22. Stadermann, M.; Sherlock, S. P.; In, J.-B.; Fornasiero, F.; Park, H. G.; Artyukhin, A. B.; Wang, Y.; De Yoreo, J. J.; Grigoropoulos, C. P.; Bakajin, O., Mechanism and Kinetics of Growth Termination in Controlled Chemical Vapor Deposition Growth of Multiwall Carbon Nanotube Arrays. *Nano Lett.* **2009,** *9*, 738-744.

23. Hariadi, R. F.; Yurke, B.; Winfree, E., Thermodynamics and Kinetics of DNA Nanotube Polymerization from Single-Filament Measurements. *Chem. Sci.* **2015,** *6*, 2252-2267.

Supplementary Information

Supplementary Note S1: RS Nanotube tile sequences

We modified the design of previously studied DAE-E nanotube tiles [1] by reducing the length of sticky ends from 5 base pairs to 4 in order to enable seeds to control whether nanotubes nucleate at room temperature (*i.e.* 20 ºC) when tiles are present at concentrations around 40-50 nM. An additional base pair was added to the double stranded region of the tiles to maintain the proper distance between crossovers.

R tile sequences:

RE-4bp-1: CGTATTGGACATTTCCGTAGACCGACTGGACATCTTCG
RE-4bp-2EE01: TGGTCCTTCACACCAATACGGCAT
RE-4bp-3Cy3:
/Cy3/TCTACGGAAATGTGGCAGAATCAATCATAAGACACCAGTCGG
RE-4bp-4: CAGACGAAGATGTGGTAGTGGAATGC
RE-4bp-5: TCCACTACCTGTCTTATGATTGATTCTGCCTGTGAAGG

S tile sequences:

SE-4bp-1: CTCAGTGGACAGCCGTTCTGGAGCGTTGGACGAAACTC
SE-4bp-2DIAG: TCTGGTAGAGCACCACTGAGAGGT
SE-4bp-3Cy3:
/Cy3/CCAGAACGGCTGTGGCTAAACAGTAACCGAAGCACCAACGCT
SE-4bp-4DIAG: ACCAGAGTTTCGTGGTCATCGTACCT
SE-4bp-5: ACGATGACCTGCTTCGGTTACTGTTTAGCCTGCTCTAC

Here /Cy3/ denotes a covalently attached Cy3 fluorophore.

For point to point assembly:
R tile sequences:

RE-4bp-1: CGTATTGGACATTTCCGTAGACCGACTGGACATCTTCG
RE-4bp-2EE01: TGGTCCTTCACACCAATACGGCAT
RE-4bp-3ATTO647:
/ATTO647N/TCTACGGAAATGTGGCAGAATCAATCATAAGACACCAGTCGG
RE-4bp-4: CAGACGAAGATGTGGTAGTGGAATGC
RE-4bp-5: TCCACTACCTGTCTTATGATTGATTCTGCCTGTGAAGG

S tile sequences:

SE-4bp-1: CTCAGTGGACAGCCGTTCTGGAGCGTTGGACGAAACTC
SE-4bp-2DIAG: TCTGGTAGAGCACCACTGAGAGGT
SE-4bp-3ATTO647:
/ATTO647/CCAGAACGGCTGTGGCTAAACAGTAACCGAAGCACCAACGCT
SE-4bp-4DIAG: ACCAGAGTTTCGTGGTCATCGTACCT
SE-4bp-5: ACGATGACCTGCTTCGGTTACTGTTTAGCCTGCTCTAC

Here /ATTO647N/ denotes a covalently attached ATTO647N fluorophore.

Supplementary Note S2: UV Nanotube tile sequences

In order to grow two different types of nanotubes in a single pot reaction, we used UV RT tiles. UV RT tiles were modified from those developed previously [1] by shortening their sticky ends so to enable them to grow from seeds at room temperatures at concentrations similar to those used for RT tiles.

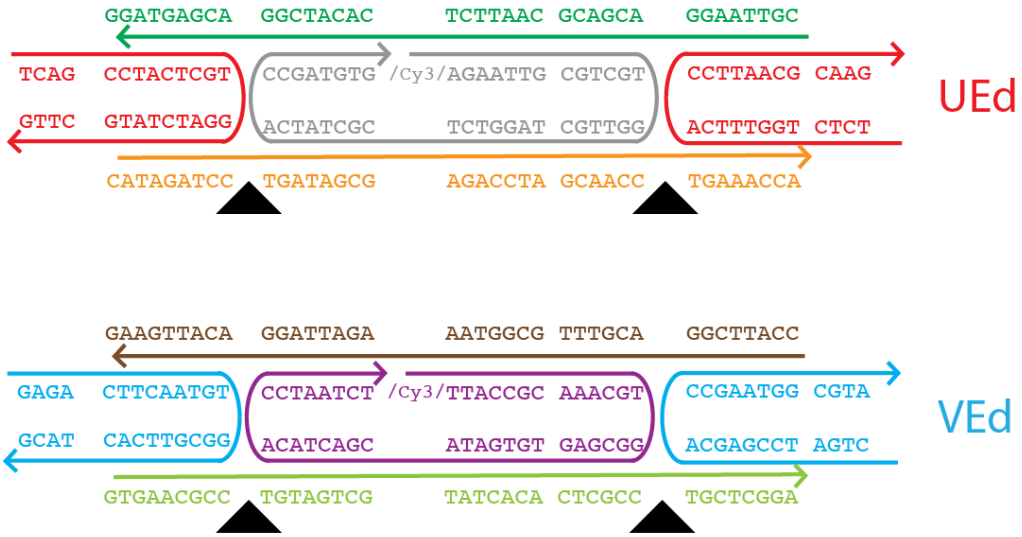

Supplementary Figure S1: Schematic showing the architecture of the U and V tiles. Cy3 represents a covalently attached /Cy3/ fluorophore.

U tile sequences:

UE1_4bp-1: CGT TAA GGA CGA CGC AAT TCT CAC ATC GGA CGA GTA GG
UE2DIAG _4bp-1: TCT CTG GTT TCA CCT TAA CGC AAG
UE3_Cy3_4bp-1: /5Cy3/AGA ATT GCG TCG TGG TTG CTA GGT CTC GCT ATC ACC GAT GTG
UE3_4bp-1: AGA ATT GCG TCG TGG TTG CTA GGT CTC GCT ATC ACC GAT GTG
UE4DIAG _4bp-1: TCA GCC TAC TCG TGG ATC TAT GCT TG
UE5_4bp-1: CAT AGA TCC TGA TAG CGA GAC CTA GCA ACC TGA AAC CA

V tile sequences:

VE1_4bp-1: CCA TTC GGA CGT TTG CGG TAA AGA TTA GGA CAT TGA AG
VE2DIAG_4bp-1: CTG ATC CGA GCA CCG AAT GGC GTA

VE3_Cy3_4bp-1: /5Cy3/TTA CCG CAA ACG TGG CGA GTG TGA TAC GAC TAC ACC TAA TCT
VE3_4bp-1: TTA CCG CAA ACG TGG CGA GTG TGA TAC GAC TAC ACC TAA TCT
VE4DIAG_4bp-1: GAG ACT TCA ATG TGG CGT TCA CTA CG
VE5_4bp-1: GTG AAC GCC TGT AGT CGT ATC ACA CTC GCC TGC TCG GA

Supplementary Note S3: RT A seed design and sequences

RT A seeds were designed by modifying the nanotube nucleation structures from Mohammed *et al* [2] to present sticky ends corresponding to the tiles in Fig. 1a / Supp. Note S1 and by reducing the number of staples used to fold the assembled structure.

RT A seed architecture

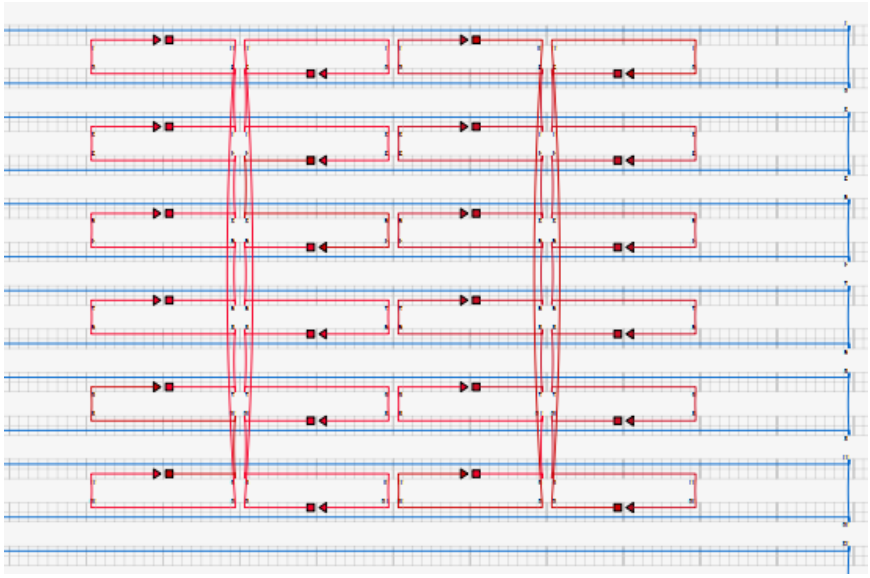

T3R2F_HP	T3R2E_HP	T5R2F_HP	T5R2E_HP
T3R4F_HP	T3R4E_HP	T5R4F_HP	T5R4E_HP
T3R6F_HP	T3R6E_HP	T5R6F_HP	T5R6E_HP
T3R8F_HP	T3R8E_HP	T5R8F_HP	T5R8E_HP
T3R10F_HP	T3R10E_HP	T5R10F_HP	T5R10E_HP
T3R12F_CYC_HP	T3R12E_CYC_HP	T5R12F_CYC_HP	T5R12E_CYC_HP

Supplementary Figure S2: **RT A seed architecture.** Crossover diagram (top) and a strand map (bottom) showing the names of the staple strands at different positions (sequences for each strand are given below) in the RT A seed. The scaffold regions shown as unbound on the right end side of the diagram were used as binding sites for adapter strands, while the remainder of the scaffold structure (including the regions shown as unbound on the left side of the crossover diagram) remained unfolded (See Supp. Note S18).

RT A seed staple sequences:

T3R2F_HP:
TGCCTTGACAGTCTCTGTCGGTGCTTTTGCACCGACTTGAATTTACCCCTCAGA
T3R4F_HP:

GCCACCACTCTTTTCACGGTCGGCTTTTGCCGACCGTTTAATCAAATAGCAAG
G
T3R6F_HP:
CCGGAAACTAAAGGTGGACCTGGCTTTTGCCAGGTCTTAATTATCATAAAAGA
A
T3R8F_HP:
ACGCAAAGAAGAACTGTCGGCTCGTTTTCGAGCCGATTGCATGATTTGAGTTA
A
T3R10F_HP:
GCCCAATAGACGGGAGCACAGGCGTTTTCGCCTGTGTTAATTAACTTTCCAGA
G
T3R12F_CYC_HP:
CCTAATTTACCAGGCGTCGGAGCGTTTTCGCTCCGATTGATAAGTGGGGGTC
AG

T3R2E_HP:
GGAAAGCGGTAACAGTGTGGCAGCTTTTGCTGCCACTTGCCCGTATCGGGGT
TT
T3R4E_HP:
GTTTGCCACCTCAGAGACCAGGCGTTTTCGCCTGGTTTCCGCCACCGCCAGAA
T
T3R6E_HP:
TTATTCATGTCACCAAGCTCGCTGTTTTCAGCGAGCTTTGAAACCATTATTAGC
T3R8E_HP:
ATACCCAAACACCACGCCTACCGCTTTTGCGGTAGGTTGAATAAGTGACGGAA
A
T3R10E_HP:
GCGCATTAATAAGAGCCTGGACGCTTTTGCGTCCAGTTAAGAAACAATAACGG
A
T3R12E_CYC_HP:
TGCTCAGTGCCAGTTAGGTGGTCGTTTTCGACCACCTTCAAAATAAACAGGGA
A

T5R2F_HP:
AATGCCCCATAAATCCGCTCGGACTTTTGTCCGAGCTTTCATTAAAAGAACCAC
T5R4F_HP:
CACCAGAGTTCGGTCAGCCGAGCGTTTTCGCTCGGCTTTAGCCCCCTCGATAG
C
T5R6F_HP:
AGCACCGTAGGGAAGGTCGGAGGCTTTTGCCTCCGATTTAAATATTTTATTTTT
G
T5R8F_HP:
TCACAATCCCGAGGAACTGGTGGCTTTTGCCACCAGTTACGCAATAATGAAAT
A

T5R10F_HP:
GCAATAGCAGAGAATACCGCAGGCTTTTGCCTGCGGTTACATAAAAACAGCCA
T
T5R12F_CYC_HP:
ATTATTTAGAAGGATTGCCATCGCTTTTGCGATGGCTTAGGATTAGAAACAGT
T

T5R2E_HP:
ACAAACAACTGCCTATCACGACGCTTTTGCGTCGTGTTTTCGGAACCTGAGAC
T
T5R4E_HP:
TCGGCATTCCGCCGCCGTCGCTGCTTTTGCAGCGACTTAGCATTGATGATATT
C
T5R6E_HP:
ATTGAGGGAATCAGTACGGAGCACTTTTGTGCTCCGTTGCGACAGACGTTTTC
A
T5R8E_HP:
GAAGGAAAAATAGAAAGCCTAGCGTTTTCGCTAGGCTTATTCATATTTCAACC
G
T5R10E_HP:
CTTTACAGTATCTTACCGCTCGTGTTTTCACGAGCGTTCGAAGCCCAGTTACCA
T5R12E_CYC_HP:
CCTCAAGATCCCAATCCGTGGAGCTTTTGCTCCACGTTCAAATAAGATAGCAG
C

Hairpins (highlighted in red) were incorporated into staples to induce a preference in the direction of cyclization.

Long seed A seed staple sequences

T_5R12F_CYC_HP:
GGAATTACCACCACCCGTGAGGCGTTTTCGCCTCACTTTCATTTTCCGTAACAC
T_5R12E_CYC_HP:
CTCAGAGCGAGGCATAGGCTCCGCTTTTGCGGAGCCTTGTAAGAGCACAGGT
AG T_3R12F_CYC_HP:
CATAACCCACCGCCACCTGGCTCGTTTTCGAGCCAGTTCCTCAGAAACAACGCC
T_3R12E_CYC_HP:
CCCTCAGATCGTTTACCGCTTGCGTTTTCGCAAGCGTTCAGACGACTTAATAAA
T_1R12F_CYC_HP:
CCAAAATATACTCAGGTGCGGTCGTTTTCGACCGCATTAGGTTTAGATAGTTA
G T_1R12E_CYC_HP:
TATCACCGGCGAGAGGCTGCGTCGTTTTCGACGCAGTTCTTTTGCAATCCTGA
A
T1R12F_CYC_HP:
TCTTACCATATAAGTACCGAGGCGTTTTCGCCTCGGTTTAGCCCGGAATAGGT
G
T1R12E_CYC_HP:
AGGGTTGAACGCTAACGCCAGGACTTTTGTCCTGGCTTGAGCGTCTGAACACC
C
T3R12F_CYC_HP:
CCTAATTTACCAGGCGTCGGAGCGTTTTCGCTCCGATTGATAAGTGGGGGTC
AG
T3R12E_CYC_HP:
TGCTCAGTGCCAGTTAGGTGGTCGTTTTCGACCACCTTCAAAATAAACAGGGA
A
T5R12F_CYC_HP:
ATTATTTAGAAGGATTGCCATCGCTTTTGCGATGGCTTAGGATTAGAAACAGT
T
T5R12E_CYC_HP:
CCTCAAGATCCCAATCCGTGGAGCTTTTGCTCCACGTTCAAATAAGATAGCAG
C
T_5R2F_HP:
TGAGTTTCAAAGGAACGTCCACCGTTTTCGGTGGACTTAACTAAAGATCTCCA
A
T_5R4F_HP:
AAAAAAGGCTTTTGCGGTGGTCCGTTTTCGGACCACTTGGATCGTCGGGTAG
CA
T_5R6F_HP:
ACGGCTACAAGTACAACTCGGCACTTTTGTGCCGAGTTCGGAGATTCGCGACC
T
T_5R8F_HP:
GCTCCATGACGTAACACGGATCGCTTTTGCGATCCGTTAAGCTGCTACACCAG
A

T_5R10F_HP:
ACGAGTAGATCAGTTGCACCGCTGTTTTCAGCGGTGTTAGATTTAGCGCCAAA
A
T_5R2E_HP:
GAGAATAGGTCACCAGCGGAACCGTTTTCGGTTCCGTTTACAAACTCCGCCAC
C
T_5R4E_HP:
AAAGGCCGCTCCAAAACCGTGGCGTTTTCGCCACGGTTGGAGCCTTAGCGGA
GT
T_5R6E_HP:
GCGAAACAAGAGGCTTGTGCTGCGTTTTCGCAGCACTTTGAGGACTAGGGAG
TTT
T_5R8E_HP:
CCAAATCATTACTTAGACGCTGGCTTTTGCCAGCGTTTCCGGAACGTACCAAG
C
T_5R10E_HP:
AAAGATTCTAAATTGGCGACGGACTTTTGTCCGTCGTTGCTTGAGATTCATTA
C
T_3R2F_HP:
TGTAGCATAACTTTCAGGCATCCGTTTTCGGATGCCTTACAGTTTCTAATTGTA
T_3R4F_HP:
TCGGTTTAGGTCGCTGGCTGACGCTTTTGCGTCAGCTTAGGCTTGCAAAGACT
T
T_3R6F_HP:
TTTCATGATGACCCCCACCAGCCGTTTTCGGCTGGTTTAGCGATTAAGGCGCA
G
T_3R8F_HP:
ACGGTCAATGACAAGACGGAGGCGTTTTCGCCTCCGTTACCGGATATGGTTTA
A
T_3R10F_HP:
TTTCAACTACGGAACACTCGCTGCTTTTTGCAGCGAGTTACATTATTAACACTAT
T_3R2E_HP:
TGCTAAACTCCACAGAGCCAGTGCTTTTTGCACTGGCTTCAGCCCTCTACCGCCA
T_3R4E_HP:
ATATATTCTCAGCTTGCCGTCCGCTTTTTGCGGACGGTTCTTTCGAGTGGGATT
T
T_3R6E_HP:
CTCATCTTGGAAGTTTCGGATGGCTTTTTGCCATCCGTTCCATTAAACATAACCG
T_3R8E_HP:
AGTAATCTTCATAAGGTCTGGTCGTTTTTCGACCAGATTGAACCGAACTAAAAC
A
T_3R10E_HP:
ACGAACTATTAATCATGGCACCTGTTTTTCAGGTGCCTTTGTGAATTTCATCAAG

T_1R2F_HP:
CGTAACGAAAATGAATCCTGCCTGTTTTCAGGCAGGTTTTTCTGTAGTGAATTT
T_1R4F_HP:
CTTAAACAACAACCATCGGTGCCGTTTTCGGCACCGTTCGCCCACGCGGGTAAA
T_1R6F_HP:
ATACGTAAGAGGCAAACTCGGTCGTTTTCGACCGAGTTAGAATACACTGACCAA
T_1R8F_HP:
CTTTGAAAATAGGCTGCCGAGGACTTTTGTCCTCGGTTGCTGACCTACCTTATG
T_1R10F_HP:
CGATTTTAGGAAGAAACGGCAGGCTTTTGCCTGCCGTTAATCTACGGATAAAAA
T_1R2E_HP:
ACGTTAGTTCTAAAGTCGCTTGGCTTTTGCCAAGCGTTTTTTGTCGTGATACAGG
T_1R4E_HP:
CAATGACAGCTTGATATGGCGAGCTTTTTGCTCGCCATTCCGATAGTCTCCCTCA
T_1R6E_HP:
AAACGAAATGCCACTACCACCTCGTTTTTCGAGGTGGTTCGAAGGCAGCCAGCAA
T_1R8E_HP:
CCAGGCGCGAGGACAGCTCTGGACTTTTTGTCCAGAGTTATGAACGGGTAGAAAA
T_1R10E_HP:
GGACGTTGAGAACTGGCGAGGCACTTTTTGTGCCTCGTTCTCATTATGCGCTAAT
T1R2F_HP:
AGTGTACTATACATGGCTCCTGCGTTTTTCGCAGGAGTTCTTTTTGATCTTTCCAG
T1R4F_HP:
GAGCCGCCCCACCACCGTCAGGCGTTTTTCGCCTGACTTGGAACCGCTGCGCCGA
T1R6F_HP:
AATCACCACCATTTTGGCGTCCTGCTTTTTGCAGGACGTTGAATTAGACCAACCTA
T1R8F_HP:
TACATACACAGTATGTCGGACCTGTTTTTCAGGTCCGTTTAGCAAACTGTACAGA
T1R10F_HP:
ATCAGAGAGTCAGAGGCGAGGTCGTTTTTCGACCTCGTTGTAATTGAACCAGTCA

T1R2E_HP:
TAAGCGTCGGTAATAACAGGAGCGTTTTCGCTCCTGTTGTTTTAACCCGTCGA
G
T1R4E_HP:
AACCAGAGACCCTCAGGCAGTCGCTTTTGCGACTGCTTAACCGCCACGTTCCA
G
T1R6E_HP:
GACTTGAGGTAGCACCGTCTGGCGTTTTCGCCAGACTTATTACCATATCACCG
G
T1R8E_HP:
TTATTACGTAAAGGTGTGGCTGCGTTTTCGCAGCCATTGCAACATACCGTCAC
C
T1R10E_HP:
TGAACAAAGATAACCCAGTGCCTGTTTTCAGGCACTTTACAAGAATAAGACTC
C
T3R2F_HP:
TGCCTTGACAGTCTCTGTCGGTGCTTTTGCACCGACTTGAATTTACCCCTCAGA
T3R4F_HP:
GCCACCACTCTTTTCACGGTCGGCTTTTGCCGACCGTTTAATCAAATAGCAAG
G
T3R6F_HP:
CCGGAAACTAAAGGTGGACCTGGCTTTTGCCAGGTCTTAATTATCATAAAAGA
A
T3R8F_HP:
ACGCAAAGAAGAACTGTCGGCTCGTTTTCGAGCCGATTGCATGATTTGAGTTA
A
T3R10F_HP:
GCCCAATAGACGGGAGCACAGGCGTTTTCGCCTGTGTTAATTAACTTTCCAGA
G
T3R2E_HP:
GGAAAGCGGTAACAGTGTGGCAGCTTTTTGCTGCCACTTGCCCGTATCGGGGT
TT
T3R4E_HP:
GTTTGCCACCTCAGAGACCAGGCGTTTTCGCCTGGTTTCCGCCACCGCCAGAA
T
T3R6E_HP:
TTATTCATGTCACCAAGCTCGCTGTTTTCAGCGAGCTTTGAAACCATTATTAGC
T3R8E_HP:
ATACCCAAACACCACGCCTACCGCTTTTGCGGTAGGTTGAATAAGTGACGGAA
A
T3R10E_HP:
GCGCATTAATAAGAGCCTGGACGCTTTTGCGTCCAGTTAAGAAACAATAACGG
A
T5R2F_HP:
AATGCCCCATAAATCCGCTCGGACTTTTGTCCGAGCTTTCATTAAAAGAACCAC

T5R4F_HP:
CACCAGAGTTCGGTCAGCCGAGCGTTTTCGCTCGGCTTTAGCCCCCTCGATAG
C
T5R6F_HP:
AGCACCGTAGGGAAGGTCGGAGGCTTTTGCCTCCGATTTAAATATTTTATTTTT
G
T5R8F_HP:
TCACAATCCCGAGGAACTGGTGGCTTTTGCCACCAGTTACGCAATAATGAAAT
A
T5R10F_HP:
GCAATAGCAGAGAATACCGCAGGCTTTTGCCTGCGGTTACATAAAAACAGCCA
T
T5R2E_HP:
ACAAACAACTGCCTATCACGACGCTTTTGCGTCGTGTTTTCGGAACCTGAGAC
T
T5R4E_HP:
TCGGCATTCCGCCGCCGTCGCTGCTTTTGCAGCGACTTAGCATTGATGATATTC
C
T5R6E_HP:
ATTGAGGGAATCAGTACGGAGCACTTTTGTGCTCCGTTGCGACAGACGTTTTCA
T5R8E_HP:
GAAGGAAAAATAGAAAGCCTAGCGTTTTCGCTAGGCTTATTCATATTTCAACC
G
T5R10E_HP:
CTTTACAGTATCTTACCGCTCGTGTTTTCACGAGCGTTCGAAGCCCAGTTACCA

Hairpins (highlighted in red) were incorporated into staples.
Long seed contains 72 staples and is used for dish experiment.

RT A seed adapters:

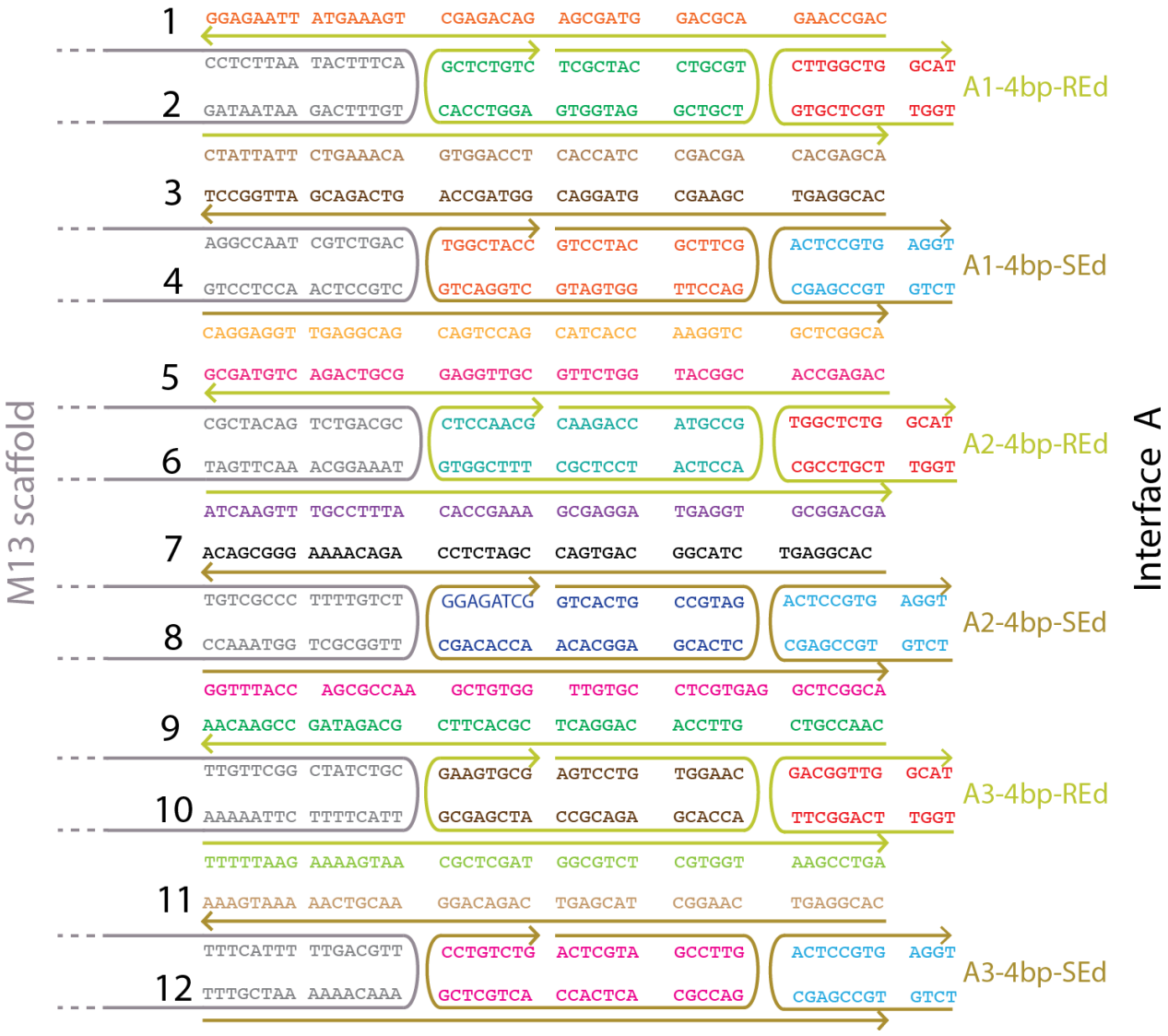

Supplementary Figure S3: **RT A seed adapters.** Structure of assembled adapters for RT A seed. The gray lines and associated sequences are portions of the M13mp18 scaffold.

RT A seed adapter strand sequences:

A-4bp-1REd_1:
CAGCCAAGACGCAGGTAGCGAGACAGAGCTGAAAGTATTAAGAGG
A-4bp-1_2REd_3:
TCGCTACCTGCGTTCGTCGGATGGTGAGGTCCACGCTCTGTC
A-4bp-1_2REd_5:
CTATTATTCTGAAACAGTGGACCTCACCATCCGACGACACGAGCA
A-4bp-2REd_2:
TGGTTGCTCGTGCTTGGCTGGCAT
A-4bp-3SEd_1:
CACGGAGTCGAAGCGTAGGACGGTAGCCAGTCAGACGATTGGCCT
A-4bp-3_4SEd_3:
GTCCTACGCTTCGGACCTTGGTGATGCTGGACTGTGGCTACC
A-4bp-4SEd_5:
CAGGAGGTTGAGGCAGCAGTCCAGCATCACCAAGGTCGCTCGGCA
A-4bp-3_4SEd_2:
TCTGTGCCGAGCACTCCGTGAGGT
A-4bp-5REd_1:
CAGAGCCACGGCATGGTCTTGCGTTGGAGGCGTCAGACTGTAGCG
A-4bp-5_6REd_3:
CAAGACCATGCCGACCTCATCCTCGCTTTCGGTGCTCCAACG
A-4bp-6REd_5:
ATCAAGTTTGCCTTTACACCGAAAGCGAGGATGAGGTGCGGACGA
A-4bp-5_6REd_2:
TGGTTCGTCCGCTGGCTCTGGCAT
A-4bp-7SEd_1:
CACGGAGTCTACGGCAGTGACCGATCTCCAGACAAAAGGGCGACA
A-4bp-7_8SEd_3:
GTCACTGCCGTAGCTCACGAGGCACAACCACAGCGGAGATCG
A-4bp-8SEd_5:
GGTTTACCAGCGCCAAGCTGTGGTTGTGCCTCGTGAGGCTCGGCA
A-4bp-7_8SEd_2:
TCTGTGCCGAGCACTCCGTGAGGT
A-4bp-9REd_1:
CAACCGTCGTTCCACAGGACTCGCACTTCGCAGATAGCCGAACAA
A-4bp-9_10REd_3:
AGTCCTGTGGAACACCACGAGACGCCATCGAGCGGAAGTGCG
A-4bp-10SEd_5:
TTTTTAAGAAAAGTAACGCTCGATGGCGTCTCGTGGTAAGCCTGA
A-4bp-9_10SEd_2:
TGGTTCAGGCTTGACGGTTGGCAT
A-4bp-11SEd_1:
CACGGAGTCAAGGCTACGAGTCAGACAGGAACGTCAAAAATGAAA

A-4bp-11_12SEd_3:
ACTCGTAGCCTTGGACCGCACTCACCACTGCTCGCCTGTCTG
A-4bp-12SEd_5:
AAACGATTTTTTGTTTCGAGCAGTGGTGAGTGCGGTCGCTCGGCA
A-4bp-11_12SEd_2:
TCTGTGCCGAGCACTCCGTGAGGT

In the dish experiments, RT A seeds were attached to Biotin attachment linker strands and Biotin attachment strand, their sequences are:

Biotin attachment linker strand sequences for A and C Seeds

Biotin_positive_01	AGGGATAGCAAGCCCATTTTCACATCGTCACTCCT
Biotin_positive_02	GAATTGCGAATAATAATTTTCACATCGTCACTCCT
Biotin_positive_03	ACCCTCAGCAGCGAAATTTTCACATCGTCACTCCT
Biotin_positive_04	TGTATCATCGCCTGATTTTTCACATCGTCACTCCT
Biotin_positive_05	CATTCAGTGAATAAGGTTTTCACATCGTCACTCCT
Biotin_positive_06	GAATACCACATTCAACTTTTCACATCGTCACTCCT

Biotin attachment linker strand sequences for B and D Seeds

Biotin_negative_01	CTATTATTCTGAAACATTTTCACATCGTCACTCCT
Biotin_negative_02	CAGGAGGTTGAGGCAGTTTTCACATCGTCACTCCT
Biotin_negative_03	ATCAAGTTTGCCTTTATTTTCACATCGTCACTCCT
Biotin_negative_04	GGTTTACCAGCGCCAATTTTCACATCGTCACTCCT
Biotin_negative_05	TTTTTAAGAAAAGTAATTTTCACATCGTCACTCCT
Biotin_negative_06	AAACGATTTTTTGTTTTTTTCACATCGTCACTCCT

Biotin attachment strand sequence

Biotin_attachment_strand	/5BiosG/AGGAGTGACGATGTG

Supplementary Note S4: RT C seed design and sequences

RT C seeds use the same set of staples as the RT A seeds but a different set of adapters to provide complementary binding sites to UV tiles.

RT C seed adapters:

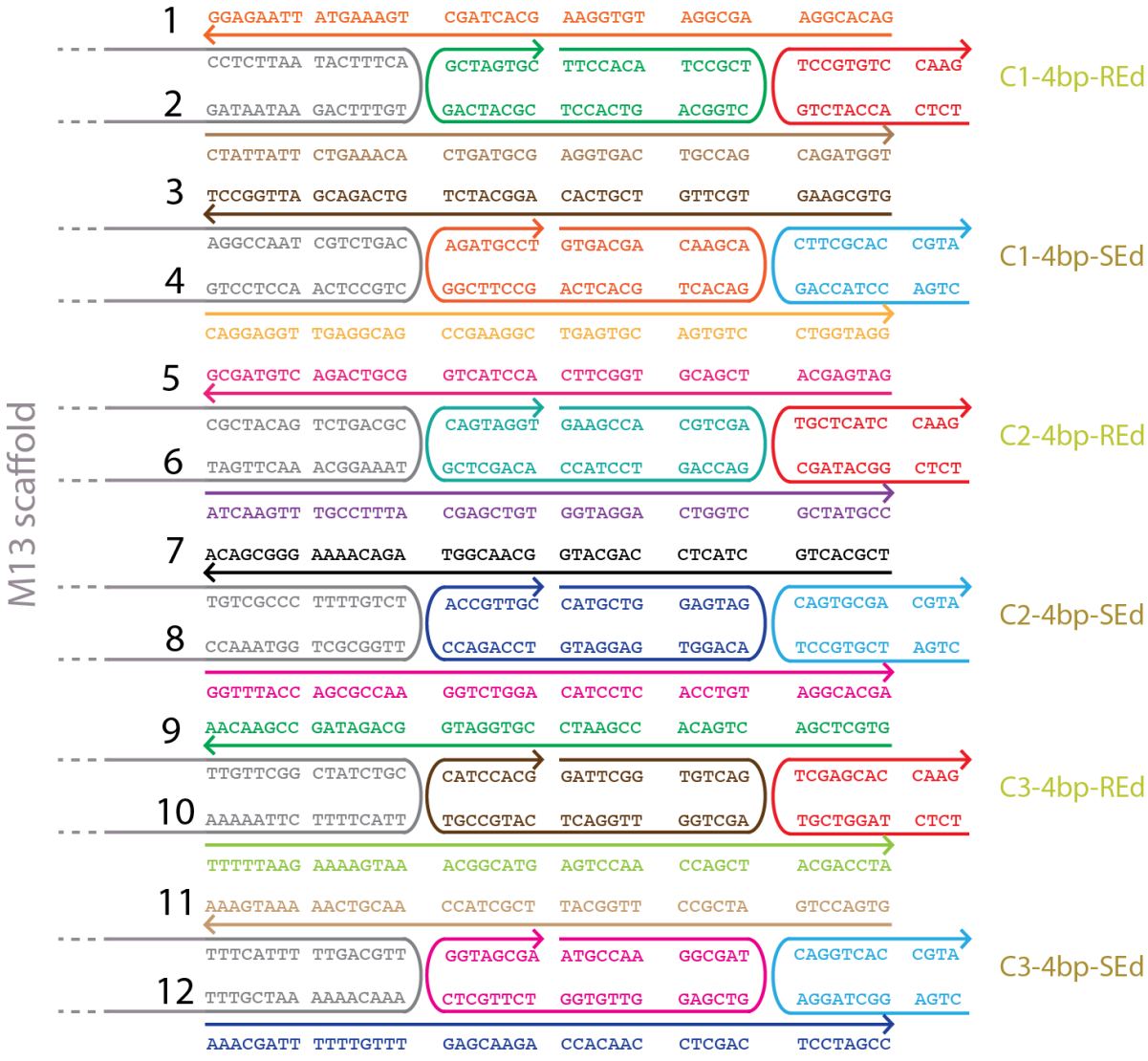

Supplementary Figure S4: **RT C seed adapters.** Structure of assembled adapters for RT C seed. The gray lines and associated sequences are portions of the M13mp18 scaffold.

RT C seed adapter strand sequences:

AD1UEd_1: GAC ACG GAA GCG GAT GTG GAA GCA CTA GCT GAA AGT ATT AAG AGG
AD1_2UEd_3:TTC CAC ATC CGC TCT GGC AGT CAC CTC GCA TCA GGC TAG TGC
AD2UEd_5: CTATTATTCTGAAACACTGATGCGAGGTGACTGCCAGCAGAT GGT
AD1_2UEd_2:TCT CAC CAT CTG TCC GTG TCC AAG

AD3VEd_1: GTGCGAAGTGCTTGTCGTCACAGGCATCTGTCAGACGATTGG CCT
AD3_4VEd_3:GTGACGACAAGCAGACACTGCACTCAGCCTTCGGAGATGCCT
AD4VEd_5: CAGGAGGTTGAGGCAGCCGAAGGCTGAGTGCAGTGTCCTGGT AGG
AD3_4VEd_2:CTGACCTACCAGCTTCGCACCGTA

AD5UEd_1: GATGAGCATCGACGTGGCTTCACCTACTGGCGTCAGACTGTA GCG
AD5_6UEd_3:GAAGCCACGTCGAGACCAGTCCTACCACAGCTCGCAGTAGGT
AD6UEd_5: ATCAAGTTTGCCTTTACGAGCTGTGGTAGGACTGGTCGCTAT GCC
AD5_6UEd_2:TCTCGGCATAGCTGCTCATCCAAG

AD7VEd_1: TCGCACTGCTACTCCAGCATGGCAACGGTAGACAAAAGGGCG ACA
AD7_8VEd_3:CATGCTGGAGTAGACAGGTGAGGATGTCCAGACCACCGT TGC
AD8VEd_5: GGTTTACCAGCGCCAAGGTCTGGACATCCTCACCTGTAGGCA CGA
AD7_8VEd_2:CTGATCGTGCCTCAGTGCGACGTA

AD9UEd_1: GTGCTCGACTGACACCGAATCCGTGGATGGCAGATAGCCGAA CAA
AD9_10UEd_3: GATTCGGTGTCAGAGCTGGTTGGACTCATGCCG TCA TCC ACG
AD10UEd_5: TTTTTAAGAAAAGTAAACGGCATGAGTCCAACCAGCTACGAC CTA
AD9_10UEd_2: TCTCTAGGTCGTTCGAGCACCAAG

AD11VEd_1: GTGACCTGATCGCCTTGGCATTCGCTACCAACGTCAAAAATG AAA
AD11_12VEd_3: ATGCCAAGGCGATGTCGAGGTTGTGGTCTTGCTCGG TAG CGA
AD12VEd_5: AAACGATTTTTTGTTTGAGCAAGACCACAACCTCGACTCCTA GCC

AD11_12VEd_2: CTGAGGCTAGGACAGGTCACCGTA

Supplementary Note S5: Design and sequences of the RT B seed (rigid cap)

The RT B seed, which serves a nucleation site for RS nanotube tiles from their B interface, was designed by following the same design principles used in designed RT A seed.

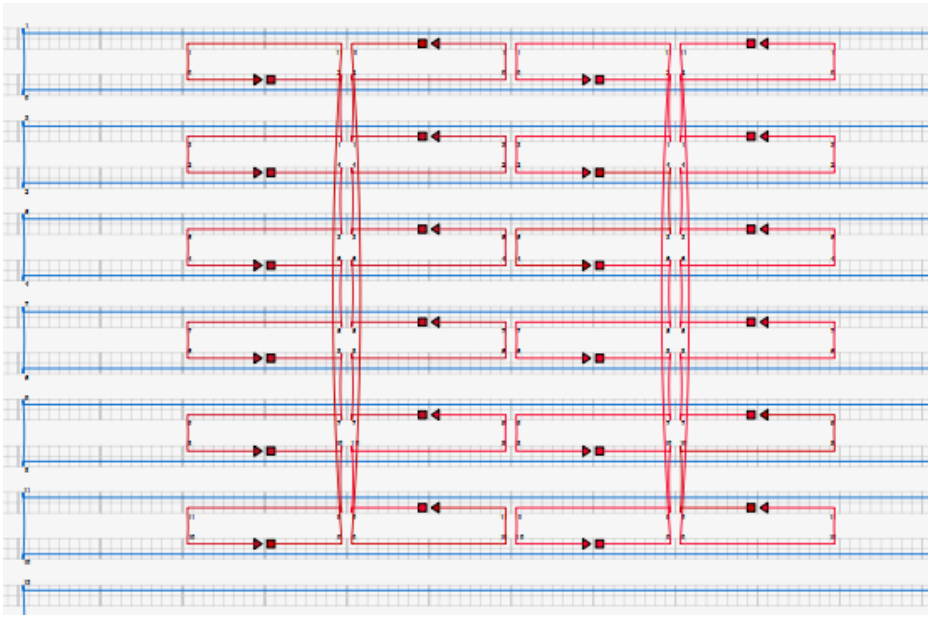

T_5R2F_HP	T_5R2E_HP	T_3R2F_HP	T_3R2E_HP
T_5R4F_HP	T_5R4E_HP	T_3R4F_HP	T_3R4E_HP
T_5R6F_HP	T_5R6E_HP	T_3R6F_HP	T_3R6E_HP
T_5R8F_HP	T_5R8E_HP	T_3R8F_HP	T_3R8E_HP
T_5R10F_HP	T_5R10E_HP	T_3R10F_HP	T_3R10E_HP
T_5R12F_CYC_HP	T_5R12E_CYC_HP	T_3R12F_CYC_HP	T_3R12E_CYC_HP

Supplementary Figure S5: **RT B seed architecture.** Crossover diagram (top) and a strand map (bottom) showing the names of the staple strands at different positions (sequences below) in the RT B seed. The scaffold regions shown as unbound on the left side of the diagram were used as binding sites for adapter strands.

RT B Seed Staple sequences:

T_5R2F_HP:
TGAGTTTCAAAGGAACGTCCACCGTTTTCGGTGGACTTAACTAAAGATCTCCAA
T_5R4F_HP:
AAAAAAGGCTTTTGCGGTGGTCCGTTTTCGGACCACTTGGATCGTCGGGTAGCA
T_5R6F_HP:
ACGGCTACAAGTACAACTCGGCACTTTTGTGCCGAGTTCGGAGATTCGCGACCT
T_5R8F_HP:
GCTCCATGACGTAACACGGATCGCTTTTGCGATCCGTTAAGCTGCTACACCAGA
T_5R10F_HP:
ACGAGTAGATCAGTTGCACCGCTGTTTTCAGCGGTGTTAGATTTAGCGCCAAAA
T_5R12F_CYC_HP:
GGAATTACCACCACCCGTGAGGCGTTTTCGCCTCACTTTCATTTTCCGTAACAC

T_5R2E_HP:
GAGAATAGGTCACCAGCGGAACCGTTTTCGGTTCCGTTTACAAACTCCGCCACC
T_5R4E_HP:
AAAGGCCGCTCCAAAACCGTGGCGTTTTCGCCACGGTTGGAGCCTTAGCGGAGT
T_5R6E_HP:
GCGAAACAAGAGGCTTGTGCTGCGTTTTCGCAGCACTTTGAGGACTAGGGAGTT
T_5R8E_HP:
CCAAATCATTACTTAGACGCTGGCTTTTGCCAGCGTTTCCGGAACGTACCAAGC
T_5R10E_HP:
AAAGATTCTAAATTGGCGACGGACTTTTGTCCGTCGTTGCTTGAGATTCATTAC
T_5R12E_CYC_HP:
CTCAGAGCGAGGCATAGGCTCCGCTTTTGCGGAGCCTTGTAAGAGCACAGGTAG

T_3R2F_HP:
TGTAGCATAACTTTCAGGCATCCGTTTTCGGATGCCTTACAGTTTCTAATTGTA
T_3R4F_HP:
TCGGTTTAGGTCGCTGGCTGACGCTTTTGCGTCAGCTTAGGCTTGCAAAGACTT

T_3R6F_HP:
TTTCATGATGACCCCCACCAGCCGTTTTCGGCTGGTTTAGCGATTAAGGCGCA
G
T_3R8F_HP:
ACGGTCAATGACAAGACGGAGGCGTTTTCGCCTCCGTTACCGGATATGGTTTA
A
T_3R10F_HP:
TTTCAACTACGGAACACTCGCTGCTTTTGCAGCGAGTTACATTATTAACACTAT
T_3R12F_CYC_HP:
CATAACCCACCGCCACCTGGCTCGTTTTCGAGCCAGTTCCTCAGAAACAACGCC

T_3R2E_HP:
TGCTAAACTCCACAGAGCCAGTGCTTTTGCACTGGCTTCAGCCCTCTACCGCCA
T_3R4E_HP:
ATATATTCTCAGCTTGCCGTCCGCTTTTGCGGACGGTTCTTTCGAGTGGGATT
T
T_3R6E_HP:
CTCATCTTGGAAGTTTCGGATGGCTTTTGCCATCCGTTCCATTAAACATAACCG
T_3R8E_HP:
AGTAATCTTCATAAGGTCTGGTCGTTTTCGACCAGATTGAACCGAACTAAAAC
A
T_3R10E_HP:
ACGAACTATTAATCATGGCACCTGTTTTCAGGTGCCTTTGTGAATTTCATCAAG

Hairpins (highlighted in red) were incorporated to induce a preference in the direction of cyclization.

RT B seed adapters design:

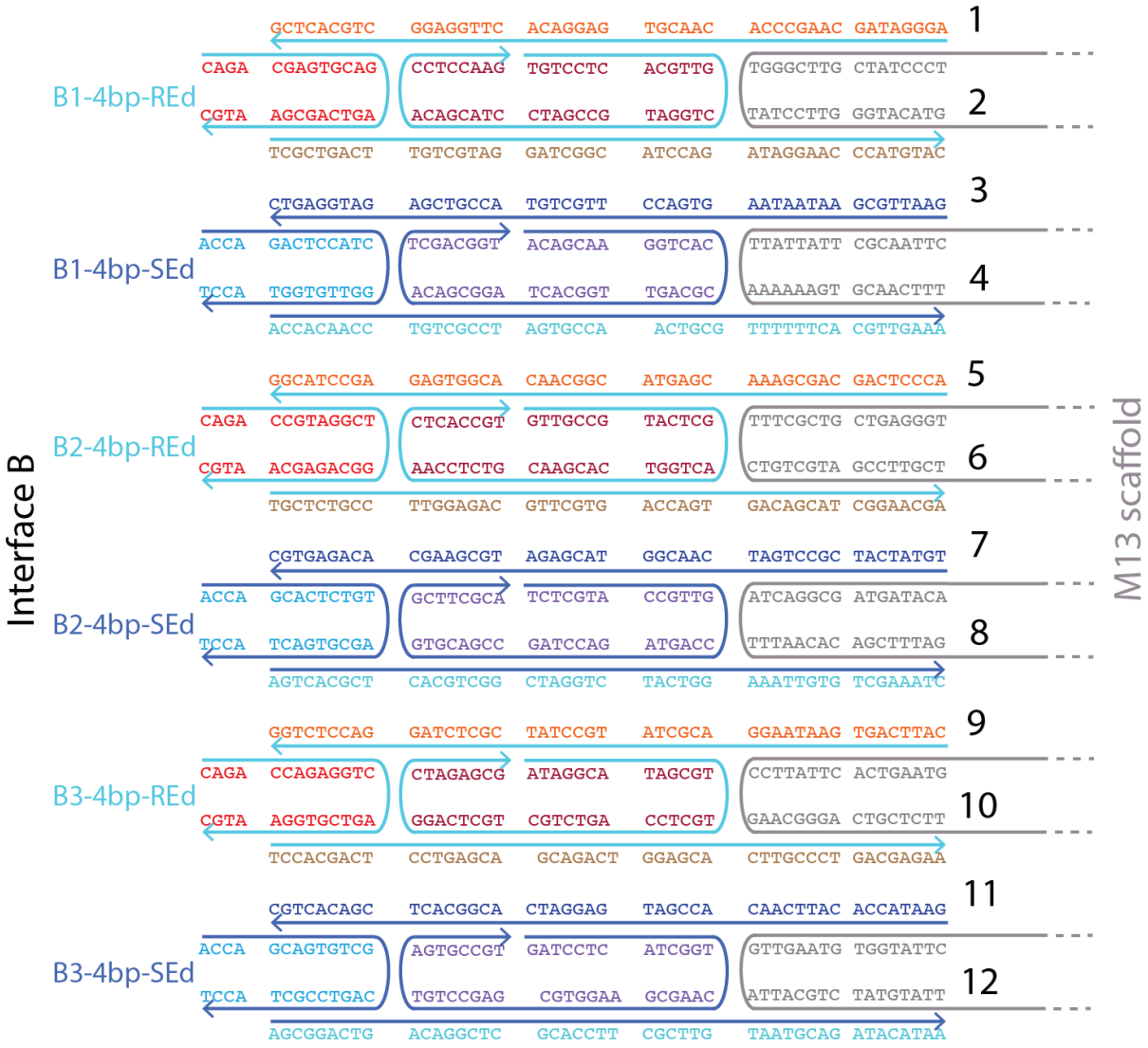

Supplementary Figure S6: **RT B seed adapter architecture.** Structure of assembled adapters for RT B seeds. The gray lines and associated sequences are portions of the M13mp18 scaffold.

RT B seed adapter strand sequences:

B-4bp-1REd_1:
AGGGATAGCAAGCCCACAACGTGAGGACACTTGGAGGCTGCACTCG
B-4bp-1_2REd_3:
TGTCCTCACGTTGCTGGATGCCGATCCTACGACACCTCCAAG
B-4bp-2REd_5:
TCGCTGACTTGTCGTAGGATCGGCATCCAGATAGGAACCCATGTAC
B-4bp-1_2REd_4:
CAGACGAGTGCAGAGTCAGCGAATGC
B-4bp-3SEd_1:
GAATTGCGAATAATAAGTGACCTTGCTGTACCGTCGAGATGGAGTC
B-4bp-3_4SEd_3:
ACAGCAAGGTCACCGCAGTTGGCACTAGGCGACATCGACGGT
B-4bp-4SEd_5:
ACCACAACCTGTCGCCTAGTGCCAACTGCGTTTTTTCACGTTGAAA
B-4bp-3_4SEd_4:
ACCAGACTCCATCGGTTGTGGTACCT
B-4bp-5REd_1:
ACCCTCAGCAGCGAAACGAGTACGGCAACACGGTGAGAGCCTACGG
B-4bp-5_6REd_3:
GTTGCCGTACTCGACTGGTCACGAACGTCTCCAACTCACCGT
B-4bp-6REd_5:
TGCTCTGCCTTGGAGACGTTCGTGACCAGTGACAGCATCGGAACGA
B-4bp-5_6REd_4:
CAGACCGTAGGCTGGCAGAGCAATGC
B-4bp-7SEd_1:
TGTATCATCGCCTGATCAACGGTACGAGATGCGAAGCACAGAGTGC
B-4bp-7_8SEd_3:
TCTCGTACCGTTGCCAGTAGACCTAGCCGACGTGGCTTCGCA
B-4bp-8SEd_5:
AGTCACGCTCACGTCGGCTAGGTCTACTGGAAATTGTGTCGAAATC
B-4bp-7_8SEd_4:
ACCAGCACTCTGTAGCGTGACTACCT
B-4bp-9REd_1:
CATTCAGTGAATAAGGACGCTATGCCTATCGCTCTAGGACCTCTGG
B-4bp-9_10REd_3:
ATAGGCATAGCGTTGCTCCAGTCTGCTGCTCAGGCTAGAGCG
B-4bp-10REd_5:
TCCACGACTCCTGAGCAGCAGACTGGAGCACTTGCCCTGACGAGAA
B-4bp-9_10REd_4:
CAGACCAGAGGTCAGTCGTGGAATGC
B-4bp-11SEd_1:
GAATACCACATTCAACACCGATGAGGATCACGGCACTCGACACTGC

B-4bp-11_12SEd_3:
GATCCTCATCGGTCAAGCGAAGGTGCGAGCCTGTAGTGCCGT
B-4bp-12SEd_5:
AGCGGACTGACAGGCTCGCACCTTCGCTTGTAATGCAGATACATAA
B-4bp-11_12SEd_4:
ACCAGCAGTGTCGCAGTCCGCTACCT

Supplementary Note S6: Labeling seeds and caps with fluorophores

For capping project:
To label seeds with fluorescent dyes for visualization *via* fluorescence microscopy, we included 100 *attachment strands* as part of each assembled seed or cap. One domain of each adapter strand bound to a specific respective section of the M13mp18 scaffold that was not folded by staples for any of the seeds or caps. The other domain of each attachment strand was bound to a *labeling strand* with an Atto fluorophore dye on one of its ends. The labeling scheme was changed by varying which labeling strand was included during seed or cap annealing. Unless otherwise noted, RT A and C seeds were labeled with Atto 647N dye and RT B seeds or caps were labeled with Atto 488 dye. D caps were labeled with a dye mixture containing equimolar concentrations of Atto 647N and Atto 488 dye strands (see Supp. Note S8).
For point to point assembly project:
We bind fluorescent dyes on the 100 *attachment strands* of unfolded m13 of each assembled seed to conduct visualization *via* fluorescence microscopy. One part of the attachment strands bound to a part of the unfolded M13mp18 scaffold. The other part of the attachment strand ends bound to an Atto fluorophore dye. Different combinations of fluorophores are used to distinguish four different types of seeds. Unless otherwise noted, A seeds were labeled with Atto 488 dye, B seeds were labeled with Atto 488 and Cy3 dye, C seeds were labeled with Atto 647N and Atto 488 dye and D seeds were labeled with Atto 647N dye. B were labeled with a dye mixture containing equimolar concentrations of Atto488 and Cy3 and D seeds were labeled with Atto 647N and Atto 488 dye strands (see Supp. Note S8).

Dye labeling strand sequences

Labeling_strand_ATTO647N_seed
/5ATTO647NN/AAGCGTAGTCGGATCTC
Labeling_strand_ATTO488_cap and seeds
/5ATTO488N/AAGCGTAGTCGGATCTC
Labeling_strand_Cy3_seed /5Cy3/AAGCGTAGTCGGATCTC

Dye attachment strand sequences

Unused_m13mp18_01
AAATTCTTACCAGTATAAAGCCAACTTTTGAGATCCGACTACGC
Unused_m13mp18_02
GCCTGTTTAGTATCATATGCGTTATTTTTGAGATCCGACTACGC
Unused_m13mp18_03
ACACCGGAATCATAATTACTAGAAATTTTGAGATCCGACTACGC
Unused_m13mp18_04
GATAAATAAGGCGTTAAATAAGAATTTTTGAGATCCGACTACGC
Unused_m13mp18_05
TTTAATGGTTTGAAATACCGACCGTTTTTGAGATCCGACTACGC
Unused_m13mp18_06
TTAGTTAATTTCATCTTCTGACCTATTTTGAGATCCGACTACGC
Unused_m13mp18_07
ACGCGAGAAAACTTTTTCAAATATATTTTGAGATCCGACTACGC
Unused_m13mp18_08
GATGCAAATCCAATCGCAAGACAAATTTTGAGATCCGACTACGC
Unused_m13mp18_09
TGGGTTATATAACTATATGTAAATGTTTTGAGATCCGACTACGC
Unused_m13mp18_10
ACTACCTTTTTAACCTCCGGCTTAGTTTTGAGATCCGACTACGC
Unused_m13mp18_11
AATTTATCAAAATCATAGGTCTGAGTTTTGAGATCCGACTACGC
Unused_m13mp18_12
TTAAGACGCTGAGAAGAGTCAATAGTTTTGAGATCCGACTACGC
Unused_m13mp18_13
TCCTTGAAAACATAGCGATAGCTTATTTTGAGATCCGACTACGC
Unused_m13mp18_14
TCGCTATTAATTAATTTTCCCTTAGTTTTGAGATCCGACTACGC
Unused_m13mp18_15
AGTGAATAACCTTGCTTCTGTAAATTTTTGAGATCCGACTACGC
Unused_m13mp18_16
GAAACAGTACATAAATCAATATATGTTTTGAGATCCGACTACGC
Unused_m13mp18_17
ATTTCATTTGAATTACCTTTTTTAATTTTGAGATCCGACTACGC
Unused_m13mp18_18
AGAAAACAAAATTAATTACATTTAATTTTGAGATCCGACTACGC
Unused_m13mp18_19
CAAAAGAAGATGATGAAACAAACATTTTTGAGATCCGACTACGC
Unused_m13mp18_20
GCGAATTATTCATTTCAATTACCTGTTTTGAGATCCGACTACGC
Unused_m13mp18_21
AATACCAAGTTACAAAATCGCGCAGTTTTGAGATCCGACTACGC

Unused_m13mp18_22
CAATAACGGATTCGCCTGATTGCTTTTTTGAGATCCGACTACGC
Unused_m13mp18_23
TAACAGTACCTTTTACATCGGGAGATTTTGAGATCCGACTACGC
Unused_m13mp18_24
CAGGTTTAACGTCAGATGAATATACTTTTGAGATCCGACTACGC
Unused_m13mp18_25
CAGAAATAAAGAAATTGCGTAGATTTTTTGAGATCCGACTACGC
Unused_m13mp18_26
CCATATCAAAATTATTTGCACGTAATTTTGAGATCCGACTACGC
Unused_m13mp18_27
TCTGAATAATGGAAGGGTTAGAACCTTTTGAGATCCGACTACGC
Unused_m13mp18_28
TATAATCCTGATTGTTTGGATTATATTTTGAGATCCGACTACGC
Unused_m13mp18_29
GATTATCAGATGATGGCAATTCATCTTTTGAGATCCGACTACGC
Unused_m13mp18_30
AAGGAGCGGAATTATCATCATATTCTTTTGAGATCCGACTACGC
Unused_m13mp18_31
CATTTTGCGGAACAAAGAAACCACCTTTTGAGATCCGACTACGC
Unused_m13mp18_32
TAATTTTAAAAGTTTGAGTAACATTTTTTGAGATCCGACTACGC
Unused_m13mp18_33
GTATTAAATCCTTTGCCCGAACGTTTTTTGAGATCCGACTACGC
Unused_m13mp18_34
TAGACTTTACAAACAATTCGACAACTTTTGAGATCCGACTACGC
Unused_m13mp18_35
ATAATACATTTGAGGATTTAGAAGTTTTTGAGATCCGACTACGC
Unused_m13mp18_36
CAACTAATAGATTAGAGCCGTCAATTTTTGAGATCCGACTACGC
Unused_m13mp18_37
TATCTAAAATATCTTTAGGAGCACTTTTTGAGATCCGACTACGC
Unused_m13mp18_38
ACTGATAGCCCTAAAACATCGCCATTTTTGAGATCCGACTACGC
Unused_m13mp18_39
GAATGGCTATTAGTCTTTAATGCGCTTTTGAGATCCGACTACGC
Unused_m13mp18_40
AGAATACGTGGCACAGACAATATTTTTTTGAGATCCGACTACGC
Unused_m13mp18_41
ATAGAACCCTTCTGACCTGAAAGCGTTTTGAGATCCGACTACGC
Unused_m13mp18_42
ATAAAAGGGACATTCTGGCCAACAGTTTTGAGATCCGACTACGC
Unused_m13mp18_43
GCAGATTCACCAGTCACACGACCAGTTTTGAGATCCGACTACGC

Unused_m13mp18_44
ATCGTCTGAAATGGATTATTTACATTTTTGAGATCCGACTACGC
Unused_m13mp18_45
ATGGAAATACCTACATTTTGACGCTTTTTGAGATCCGACTACGC
Unused_m13mp18_46
CCAGCCATTGCAACAGGAAAAACGCTTTTGAGATCCGACTACGC
Unused_m13mp18_47
CTGGTAATATCCAGAACAATATTACTTTTGAGATCCGACTACGC
Unused_m13mp18_48
GTAGAAGAACTCAAACTATCGGCCTTTTTGAGATCCGACTACGC
Unused_m13mp18_49
TGATTAGTAATAACATCACTTGCCTTTTTGAGATCCGACTACGC
Unused_m13mp18_50
AAATTAACCGTTGTAGCAATACTTCTTTTGAGATCCGACTACGC
Unused_m13mp18_51
CCGAGTAAAAGAGTCTGTCCATCACTTTTGAGATCCGACTACGC
Unused_m13mp18_52
GAAGTGTTTTTATAATCAGTGAGGCTTTTGAGATCCGACTACGC
Unused_m13mp18_53
GACAGGAACGGTACGCCAGAATCCTTTTTGAGATCCGACTACGC
Unused_m13mp18_54
AACAGGAGGCCGATTAAAGGGATTTTTTTGAGATCCGACTACGC
Unused_m13mp18_55
TCCTCGTTAGAATCAGAGCGGGAGCTTTTGAGATCCGACTACGC
Unused_m13mp18_56
GCTTTGACGAGCACGTATAACGTGCTTTTGAGATCCGACTACGC
Unused_m13mp18_57
CGCCGCTACAGGGCGCGTACTATGGTTTTGAGATCCGACTACGC
Unused_m13mp18_58
TAACCACCACACCCGCCGCGCTTAATTTTGAGATCCGACTACGC
Unused_m13mp18_59
TGGCAAGTGTAGCGGTCACGCTGCGTTTTGAGATCCGACTACGC
Unused_m13mp18_60
AAGCGAAAGGAGCGGGCGCTAGGGCTTTTGAGATCCGACTACGC
Unused_m13mp18_61
CGAACGTGGCGAGAAAGGAAGGGAATTTTGAGATCCGACTACGC
Unused_m13mp18_62
GATTTAGAGCTTGACGGGGAAAGCCTTTTGAGATCCGACTACGC
Unused_m13mp18_63
TAAATCGGAACCCTAAAGGGAGCCCTTTTGAGATCCGACTACGC
Unused_m13mp18_64
TTTTGGGGTCGAGGTGCCGTAAAGCTTTTGAGATCCGACTACGC
Unused_m13mp18_65
TACGTGAACCATCACCCAAATCAAGTTTTGAGATCCGACTACGC

Unused_m13mp18_66
AAACCGTCTATCAGGGCGATGGCCCTTTTGAGATCCGACTACGC
Unused_m13mp18_67
ACGTGGACTCCAACGTCAAAGGGCGTTTTGAGATCCGACTACGC
Unused_m13mp18_68
TTTGGAACAAGAGTCCACTATTAAATTTTGAGATCCGACTACGC
Unused_m13mp18_69
CCGAGATAGGGTTGAGTGTTGTTCCTTTTGAGATCCGACTACGC
Unused_m13mp18_70
AAATCCCTTATAAATCAAAAGAATATTTTGAGATCCGACTACGC
Unused_m13mp18_71
TGTTTGATGGTGGTTCCGAAATCGGTTTTGAGATCCGACTACGC
Unused_m13mp18_72
CTGGTTTGCCCCAGCAGGCGAAAATTTTTGAGATCCGACTACGC
Unused_m13mp18_73
TGAGAGAGTTGCAGCAAGCGGTCCATTTTGAGATCCGACTACGC
Unused_m13mp18_74
AGCTGATTGCCCTTCACCGCCTGGCTTTTGAGATCCGACTACGC
Unused_m13mp18_75
TTTCTTTTCACCAGTGAGACGGGCATTTTGAGATCCGACTACGC
Unused_m13mp18_76
GTTTGCGTATTGGGCGCCAGGGTGGTTTTGAGATCCGACTACGC
Unused_m13mp18_77
GAATCGGCCAACGCGCGGGGAGAGGTTTTGAGATCCGACTACGC
Unused_m13mp18_78
GAAACCTGTCGTGCCAGCTGCATTATTTTGAGATCCGACTACGC
Unused_m13mp18_79
TGCGCTCACTGCCCGCTTTCCAGTCTTTTGAGATCCGACTACGC
Unused_m13mp18_80
GAGTGAGCTAACTCACATTAATTGCTTTTGAGATCCGACTACGC
Unused_m13mp18_81
TAAAGTGTAAAGCCTGGGGTGCCTATTTTGAGATCCGACTACGC
Unused_m13mp18_82
TTCCACACAACATACGAGCCGGAAGTTTTGAGATCCGACTACGC
Unused_m13mp18_83
CTGTGTGAAATTGTTATCCGCTCACTTTTGAGATCCGACTACGC
Unused_m13mp18_84
ATTCGTAATCATGGTCATAGCTGTTTTTTGAGATCCGACTACGC
Unused_m13mp18_85
TAGAGGATCCCCGGGTACCGAGCTCTTTTGAGATCCGACTACGC
Unused_m13mp18_86
CAAGCTTGCATGCCTGCAGGTCGACTTTTGAGATCCGACTACGC
Unused_m13mp18_87
ACGACGTTGTAAAACGACGGCCAGTTTTTGAGATCCGACTACGC

Unused_m13mp18_88
TTGGGTAACGCCAGGGTTTTCCCAGTTTTGAGATCCGACTACGC
Unused_m13mp18_89
AGGGGGATGTGCTGCAAGGCGATTATTTTGAGATCCGACTACGC
Unused_m13mp18_90
CTCTTCGCTATTACGCCAGCTGGCGTTTTGAGATCCGACTACGC
Unused_m13mp18_91
CTGTTGGGAAGGGCGATCGGTGCGGTTTTGAGATCCGACTACGC
Unused_m13mp18_92
GCGCCATTCGCCATTCAGGCTGCGCTTTTGAGATCCGACTACGC
Unused_m13mp18_93
CGCTTCTGGTGCCGGAAACCAGGCATTTTGAGATCCGACTACGC
Unused_m13mp18_94
ATCGCACTCCAGCCAGCTTTCCGGCTTTTGAGATCCGACTACGC
Unused_m13mp18_95
GACGACGACAGTATCGGCCTCAGGATTTTGAGATCCGACTACGC
Unused_m13mp18_96
GTAACCGTGCATCTGCCAGTTTGAGTTTTGAGATCCGACTACGC
Unused_m13mp18_97
GGTCACGTTGGTGTAGATGGGCGCATTTTGAGATCCGACTACGC
Unused_m13mp18_98
AAACGGCGGATTGACCGTAATGGGATTTTGAGATCCGACTACGC
Unused_m13mp18_99
ACAACCCGTCGGATTCTCCGTGGGATTTTGAGATCCGACTACGC
Unused_m13mp18_100
TTCATCAACATTAAATGTGAGCGAGTTTTGAGATCCGACTACGC

Supplementary Note S7: Adapters for flexible D caps

Flexible D caps have the same DNA origami structure as the flexible B caps do (see Supp. Fig. S7) but use a different set of adapters so that flexible D caps sticky ends bind the sticky ends of UV tiles.

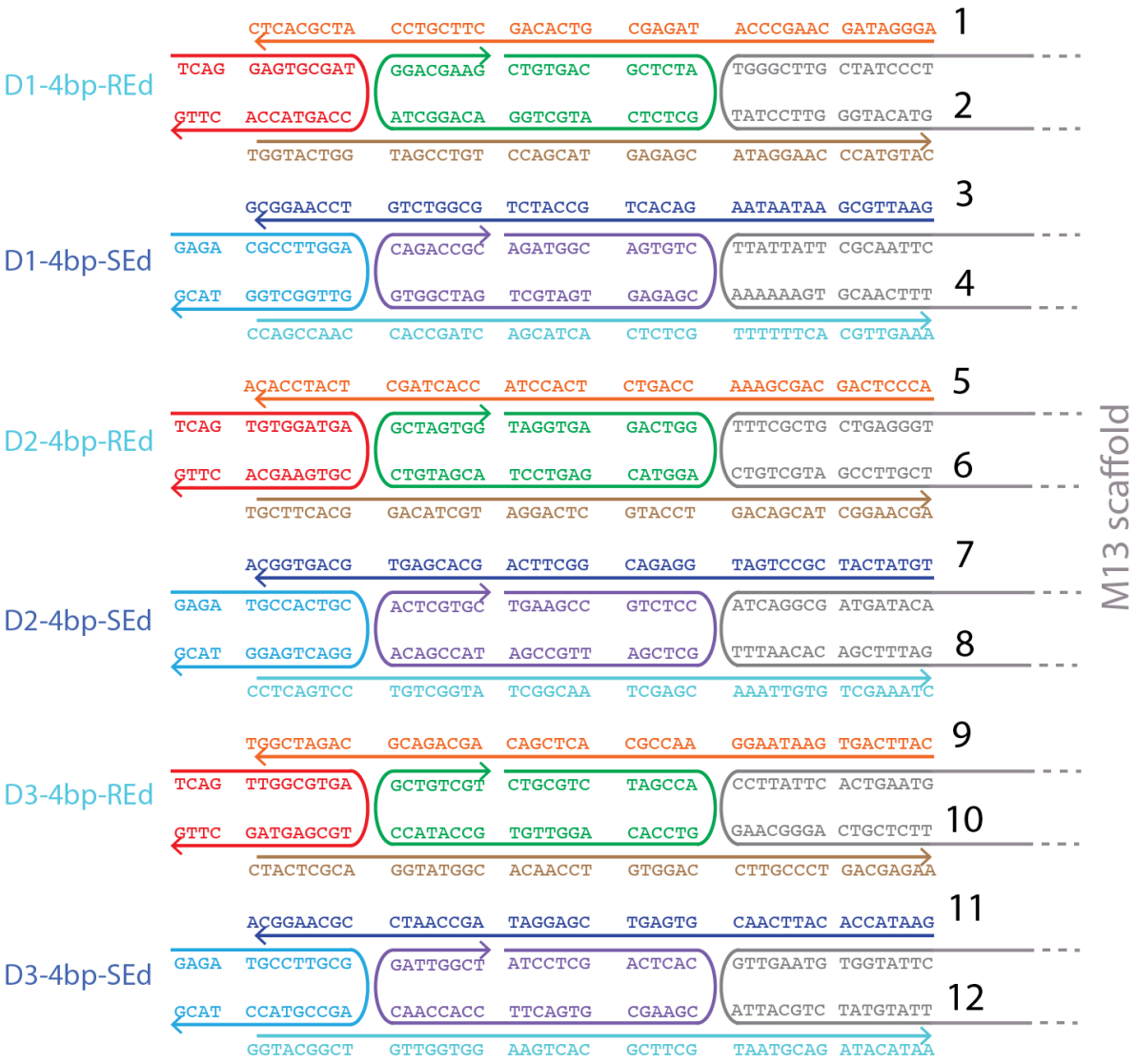

Supplementary Figure S7: Structure of the assembled adapters for D caps. The gray lines and associated sequences are portions of the M13mp18 scaffold.

RT D seed adapter strand sequences:

AD1UEd_1:
AGG GAT AGC AAG CCC ATA GAG CGT CAC AGC TTC GTC CAT CGC ACT C
AD1_2UEd_3:
CTG TGA CGC TCT AGC TCT CAT GCT GGA CAG GCT AGG ACG AAG
AD2UEd_5:
TGG TAC TGG TAG CCT GTC CAG CAT GAG AGC ATA GGA ACC CAT GTA C
AD1_2UEd_4:
TCA GGA GTG CGA TCC AGT ACC ACT TG
AD3VEd_1:
GAA TTG CGA ATA ATA AGA CAC TGC CAT CTG CGG TCT GTC CAA GGC G
AD3_4VEd_3:
AGA TGG CAG TGT CCG AGA GTG ATG CTG ATC GGT GCA GAC CGC
AD4VEd_5:
CCA GCC AAC CAC CGA TCA GCA TCA CTC TCG TTT TTT CAC GTT GAA A
AD3_4VEd_4:
GAG ACG CCT TGG AGT TGG CTG GTA CG

AD5UEd_1:
ACC CTC AGC AGC GAA ACC AGT CTC ACC TAC CAC TAG CTC ATC CAC A
AD5_6UEd_3:
TAG GTG AGA CTG GAG GTA CGA GTC CTA CGA TGT CGC TAG TGG
AD6UEd_5:
TGC TTC ACG GAC ATC GTA GGA CTC GTA CCT GAC AGC ATC GGA ACG A
AD5_6UEd_4:
TCA GTG TGG ATG ACG TGA AGC ACT TG

AD7VEd_1:
TGT ATC ATC GCC TGA TGG AGA CGG CTT CAG CAC GAG TGC AGT GGC A
AD7_8VEd_3:
TGA AGC CGT CTC CGC TCG ATT GCC GAT ACC GAC AAC TCG TGC
AD8VEd_5:
CCT CAG TCC TGT CGG TAT CGG CAA TCG AGC AAA TTG TGT CGA AAT C
AD7_8VEd_4:
GAG ATG CCA CTG CGG ACT GAG GTA CG

AD9UEd_1:
CAT TCA GTG AAT AAG GTG GCT AGA CGC AGA CGA CAG CTC ACG CCA A
AD9_10UEd_3:
CTG CGT CTA GCC AGT CCA CAG GTT GTG CCA TAC CGC TGT CGT
AD10UEd_5:
CTA CTC GCA GGT ATG GCA CAA CCT GTG GAC CTT GCC CTG ACG AGA A
AD9_10UEd_4:
TCA GTT GGC GTG ATG CGA GTA GCT TG

AD11VEd_1:
GAA TAC CAC ATT CAA CGT GAG TCG AGG ATA GCC AAT CCG CAA GGC A
AD11_12VEd_3:
ATC CTC GAC TCA CCG AAG CGT GAC TTC CAC CAA CGA TTG GCT
AD12VEd_5:
GGT ACG GCT GTT GGT GGA AGT CAC GCT TCG TAA TGC AGA TAC ATA A
AD11_12VEd_4:
GAG ATG CCT TGC GAG CCG TAC CTA CG

Supplementary Note S8: Stock preparations

Seed and cap staple mixes: Staple mixtures for all seeds and caps contained each of the staples at 4.17 μM suspended in water, except in experiments with glass-bottomed dishes, where the staple mixture contained the staples from [2] at 1388.89 nM each suspended in water.

Adapter strand mixes: Each adapter strand mix contained the respective REd and SEd adapter strands (Supp. Notes S3 and S5 respectively) that do not present sticky ends at 1 μM. The remaining adapters strands that have sticky ends were added at 2 μM (Supp. Note S4). A similar protocol was followed to prepare the UEd and VEd adapter strand mix (Supp. Notes S4 and S7).

Fluorescent labeling attachment strands mix: The attachment strand mix contained 1 μM of each of the 100 labeling attachment strands (Supp. Note S6).

Fluorescent labeling strands mix: 100 μM stocks of Labeling_strand_ATTO647N_seed and Labeling_strand_ATTO488_cap and labeling_strand_Cy3 were used to label respectively RT A or C seeds and RT B seeds or caps. The labeling strand mix for cap D contained 50 μM of each of the labeling strand (Labeling_strand_ATTO647N_seed, Labeling_strand_ATTO488_cap) suspended in water.

RT RS nanotube tiles (Cy3 labeled): The RS tile mixture contained each strand that does not present a sticky end at 600 nM and strands with sticky ends [RE-4bp-2EE01, RE-4bp-4, SE-4bp-2DIAG, SE-4bp-4DIAG] at 1200 nM.

REd-ATTO647N SEd-ATTO647N nanotube tiles: The RS tile mixture contained each strand that does not present a sticky end at 400 nM and strands with sticky ends [RE-4bp-2EE01, RE-4bp-4, SE-4bp-2DIAG, SE-4bp-4DIAG] at 800 nM.

RT UV nanotube tiles (25% Cy3 labeled): The UV tile mixture contained each 1 and 5 strands [UE1_4bp-1, UE5_4bp-1, VE1_4bp-1, VE5_4bp-1] at 400 nM and strands 2 and 4 with sticky ends [UE2DIAG-4bp-1, UE4DIAG-4bp-1,VE2DIAG-4bp-1, VE4DIAG-4bp-1] at 800 nM. To distinguish UV tiles from RS tiles, UV tiles were prepared with 100 nM each of Cy3 labeled UE3-Cy3_4bp-1 and VE3-Cy3_4bp-1 strands 300 nM each of UE3_4bp-1 and VE3_4bp-1 strands without a Cy3 label.

UV nanotube tiles (Cy3 labeled): The UV tile mixture contained each 1 and 5 strands [UE1_4bp-1, UE5_4bp-1, VE1_4bp-1, VE5_4bp-1] at 400 nM and strands 2 and 4 with sticky ends [UE2DIAG-4bp-1, UE4DIAG-4bp-1,VE2DIAG-4bp-1, VE4DIAG-4bp-1] at 800 nM.

Biotin attachment linker strands mix: The linker strand mixture for A seeds contained each of the linker strands [Biotin_positive_01 - Biotin_positive_06] listed in Supp. Note S3 at 100 nM suspended in water.

Biotin attachment negative linker strands mix: The linker strand mixture for A seeds contained each of the linker strands [Biotin_negative_01 - Biotin_negative_06] listed in Supp. Note S3 at 100 nM suspended in water.

Supplementary Note S9: Protocol for DNA origami preparation and purification

1. We made 50 µL mixtures (Supp. Table S1) containing M13mp18 scaffold, staple strands, adapter strands, fluorescent strand and attachment strands in 1 × TAE Mg^{2+} buffer (40 mM Tris-Acetate, 1 mM EDTA and 12.5 mM magnesium acetate). BSA biotin was included to reduce DNA absorption to PCR tubes [3].

   Supplementary Table S1: Seed/Cap assembly mixture.

Seed/Cap Assembly Mixture	Final desired concentration (nM or fold)	Stock concentration (nM or fold)	To add (ul)
H_2O	-	-	25.25
BSA Biotin solution	0.05 mg/ml	1 mg/ml	2.5
Staple strands mix	500 nM	4166.67 nM	6
Adapter strands mix	100 nM	1000 nM	5
M13mp18 scaffold	5 nM	100 nM	2.5
Fluorescent labeling attachment strands mix	25 nM	1000 nM	1.25
Fluorescent labeling strands mix	5000 nM	100000 nM	2.5
10 × TAE Mg++	1×	10×	5
Total volume			50

   The set of staple strands, adapter strands and dye strands included for RT A and C seeds and B and D caps were chosen as described in Supp. Notes S3-S8.

2. The seed assembly mixture was annealed using the following protocol:

   Supplementary Table S2: Annealing protocol.

Temperature range	**Rate**
90 °C	Hold for 5 min
90- 45 °C	0.1 /6 sec
45 °C	Hold for 60 min
45-20 °C	0.01 /6 sec
20 °C	Hold until sample retrieval

3. Seeds were separated from excess adapter, staple, attachment and labeling strands by following the protocol described in the Methods section of the main paper; the

concentration of seeds in the resulting solution was determined according to Supp. Note S10.

Supplementary Note S10: Protocol for growing seeded nanotubes
For capping project:

1. Solutions of seeded nanotubes were prepared by first mixing 15.23 μL of purified water, 1 μL of 1 mg/ml BSA Biotin, 1.5 μL of RT RS nanotube tile solution (Supp. Note S8) and 1.97 μL 10 × TAE Mg^{2+} buffer to a final volume of 19.7 μL per tile solution.

2. Purified seeds were prepared and their concentrations were measured as described in Supp. Notes S9 and S10. The concentration of the seed solution was adjusted by adding 1 × TAE Mg^{2+} so that the final seed concentration would be the reported concentration after adding 0.3 μL of the solution to the 19.7 μL of tile solution.

3. The tile solutions from step 1 were annealed from 90 °C to 20 °C using the protocol in Supp. Table S2. When the solution reached 20 °C, 0.3 μL of seed solution (to a final concentration of 2 pM) was added to 19.7 μL of the tile solution so that the tile concentration was 45 nM after addition of seeds, after which the mixtures were incubated for the time interval(s) described in the main text. Control experiments without seeds followed the above instructions except that 0.3 μL of 1 × TAE Mg^{2+} buffer was added in place of the seed solution.

4. To reduce imaging background due to single tile adsorption to glass, 0.3 μL of 1 μM of *D01* (sequence below) was added before imaging. This strand adsorbed more effectively than poly-T sequences but did not interact with the tiles or adapter strands.

D01 strand:
ATCAGAGAGTCAGAGGCGAGGTCGTTTTCGACCTCGTTGTAATTGAACCAGT
CA

For point to point assembly:
Dish surface treatment protocol enables seeds to bind on a glass surface via surface linker chemistry. Allowing seeds to attach on the surface can direct DNA nanotube formation and then to form a nanotube connection. A biotion-PEG-silane layer was treated and then several types of seeds are attached via neutravidin chemistry as described.

Day One Protocol:

1. Glass-bottom dishes (D29-20-1-N, In Vitro Scientific) were sonicated in 10% NaOH for 40 minutes. Dishes were left with NaOH from abovementioned step. To remove residual NaOH, dishes were washed with water three times and then by methanol three times.

2. Surface chemistry was formed by dissolving 10mg of biotin PEG silane MW 3400 with 1000 μL of a solution containing 95% methanol, 4% acetic acid, and 1% water. 500μL of the solution is used for each dish. Dishes were sealed with Parafilm overnight to prevent evaporation.

Day Two Protocol:

1. After removing the Parafilm, dishes were washed 3 times with methanol then 3 times with water. Nitrogen gas was used to blow off water from the glass surface.

2. Dishes were then placed in oven at 90 °C for 1 hour.

3. 1% BSA solution was prepared by combining 10mg of BSA with 1000 μL of 1× TNT buffer (10 mM Tris-HCl, 0.05% Tween-20, 0.1 M NaCl, pH 7.5), and then was added to dishes and incubated for 1.5 hours.

4. Washing dishes with TNT buffer to remove excessive 1% BSA solution.

5. Add 500 μl of .4 mg/mL Neutravidin (31000, Thermo Fisher Scientific) in TNT buffer or 0.4 mg/mL Streptavidin (21122, Thermo Fisher Scientific) to dishes and then dished were incubated for approximately two hours.

6. To remove excessive neutravidin or streptavidin solution, dishes were washed 3 times with TNT buffer then followed by 3 washing steps with TAE buffer. Then leave 500 μl of TAE buffer in each dish.

Supplementary Note S11: Protocol for growing RT A seeded, B capped nanotubes

1. Solutions of seeded nanotubes were prepared by first mixing 14.96 μL of purified water, 1 μL of 1 mg/ml BSA Biotin, 1.5 μL of RT RS nanotube tile solution (Supp. Note S8) and 1.94 μL 10 × TAE Mg^{2+} buffer to a final volume of 19.4 μL per tile solution.

2. Purified A seeds were prepared and their concentrations were measured as described in Supp. Notes S9 and S10. The concentration of the seed solution was adjusted by adding 1 × TAE Mg^{2+} buffer $^{+}$ so that the final seed concentration would be the reported concentration after adding 0.3 μL of the solution to the tile solution after the addition of seeds and caps.

3. Purified B caps were prepared and their concentrations were measured as described in Supp. Notes S9 and S10. The concentration of the cap solution was adjusted by adding 1 × TAE Mg^{2+} buffer so that the final seed concentration would be the reported concentration after adding 0.3 μL of the solution to the tile solution after the addition of seeds and caps.

4. The tile solutions from step 1 were annealed from 90 °C to 20 °C using the protocol in Supp. Table S2. When the solution reached 20 °C, 0.3 μL of seed solution (to a final concentration of 2 pM) was added to 19.4 μL tile solution, after which the mixture was incubated. After either 4 or 8 hours, 0.3 μL of cap solution (to a final concentration of 10 pM) was added to the mixture so that the tile concentration was 45 nM after addition of seeds and caps. Control experiments without caps followed the above instructions except that 0.3 μL of 1 × TAE Mg^{2+} buffer was added in place of the cap solution. For AFM experiments, 0.3 μL of seed solution (to a final concentration of 10 pM) was added to 19.4 μL tile solution and incubated for 2 hours and then 0.3 μL of cap solution (to a final concentration of 20 pM) was added to the mixture so that the tile concentration was 45 nM after addition of seeds and caps.

5. Slides were prepared as described in Supp. Note S11.

Supplementary Note S12: Protocol for dish glass surface treatment so that RT A seeds with linker strands can bind to the surface

The goal of this protocol is to enable seeds to bind on a monolayer formed on a glass surface *via* a specific biotin-neutravidin linker chemistry. Fixing the seeds to the surface allows individual nanotubes to be tracked during growth and capping processes. Briefly, a glass-bottomed dish with a biotin-PEG-silane monolayer and RT A seeds presented biotin are attached through biotin streptavidin chemistry. The protocol largely follows the methods in [4].

3. Glass-bottom dishes were cleaned by sonication in 10% NaOH for 40 minutes.

4. Glass-bottom dishes were then washed with water followed by methanol wash to remove residual NaOH.

5. 10 mg of biotin PEG silane MW 3400 was dissolved in 1000 μL of a solution containing 95% methanol, 4% acetic acid, and 1% water. This solution is then transferred onto glass-bottom dishes.

6. Dishes were sealed with Parafilm in an enclosed space overnight to prevent evaporation.

7. Dishes were washed with methanol followed by water to remove residual methanol.

8. The Parafilm was then removed from dishes and dishes were washed 3 times with methanol then 2 to 3 times with water. Water was then blown off the glass surface using nitrogen gas.

9. Dishes were then placed in oven at 90 °C for 1 hour.

10. 1000 μl of 1% BSA solution in TNT buffer (10 mM Tris-HCl, 0.05% Tween-20, 0.1 M NaCl, pH 7.5) was added to dishes and incubated for 1.5 hours.

11. Dishes were then washed with TNT buffer to remove excess 1% BSA solution.

12. 1000 μl of .2 mg/mL Neutravidin (31000, Thermo Fisher Scientific) in TNT buffer or 0.2 mg/mL Streptavidin (21122, Thermo Fisher Scientific) was added to dishes and incubated for approximately two hours.

13. Dishes were washed 3 times with TNT buffer followed by 3 washes with 1 × TAE Mg^{2+} buffer. 1000 μl of 1 × TAE Mg^{2+} buffer was left in each dish until use.

Supplementary Note S13: Protocol for tracking the growth of specific RT A Seeded nanotubes.

1. To measure the seeded nanotubes growth rate, we prepared dishes (μ-Dish 35mm, high Grid-50 Glass Bottom, Ibidi) using the dish preparation protocol (see Supp. Note S13) a day in advance.

2. To ensure that the facet on the seed is not too close to the surface, seeds were folded using the staples from [2] with the adapters in Supp. Fig. S3. No difference in nucleation rates has been observed between seeds using this set of staples and the seeds with the staples used here [6]. To assemble the seeds with biotin attachment and linker strands, we made a 50 μL mixture (Supp. Table S3) containing M13mp18 scaffold, staple strands, adapter strands, dye strand and dye attachment strands, biotin attachment and attachment linker strands in 1 × TAE Mg^{2+} buffer. The seed assembly mixture was annealed using the protocol mentioned in Supp. Table S2.

Supplementary Table S3: Assembly mixture of RT A seeds for dish experiments.

RT A Seed with linker strand Assembly Mixture	Final desired concentration (nM or fold)	Stock (nM or fold)	To add (μL)
H_2O			2.95
RT A Seed staples mix for long seed	500	1388.89	18
RT A Seed adapter strand mix	100	1,000	5
M13mp18 scaffold strand	5	100	2.5
Fluorescent labeling attachment strands mix	25	1000	1.25
Fluorescent labeling strands mix	5000	100000	2.5
Biotin attachment strand mix	90	850	5.3
Biotin attachment linker strands mix	15	100	7.5
10 × TAE Mg^{2+} buffer	1	10	5
Total			50

3. Purified seeds were prepared and their concentrations were measured as described in Supp. Note S10. The concentration of the seed solution was adjusted through the addition of 1 × TAE Mg^{2+} to achieve a seed density of about 100 seeds per field of view after the addition of 10 μL of the purified RT A seeds mixture into 1000 μL of the 1 × TAE Mg^{2+}solution contained in the dish. We allowed 15 minutes for seeds to attach on the dish glass surface after which time the glass surface was washed three times with 1 × TAE Mg^{2+} to remove unattached seeds.

4. After the seeds were attached to the glass surface, 1000 μL of 1 × TAE Mg^{2+} buffer was placed into the dish, and four different locations were identified using the markers embedded on the glass surface of the dish such as landmarks around which to track individual nanotubes. These locations were selected randomly. Once the locations were set, 1000 μL of 1 × TAE Mg^{2+} buffer was replaced with 1000 μL of 75 nM annealed RT RS tiles mixture that has 1 × TAE Mg^{2+}. Then the dish was sealed with Parafilm to prevent solution evaporation. In the dish experiments, we used a higher RS tile concentration (75 nM) compared to the experiments that were performed in the Eppendorf tubes (45 nM). This may be because of the absence of BSA in dish expriments. BSA prevents seeds and probably thus tiles from adhering to the walls of Eppendorf tubes [3]; more surface adsorption of tiles may have occurred in dishes

5. Images were captured at four time points- 0, 6, 12 and 24 hours. At 6 hours and all the follow-up time points, 1000 μL of the tile mixture, which was added at the earlier time points, was removed from the dish and stored in the Eppendorf tube at 20 ºC. This mixture was then transferred back into the dish after the image acquisition. After removing the tile mixture from the dish, three washing steps were performed with 1000 μL of 1 × TAE Mg^{2+} to minimize fluorescence noise. The embedded markers in the dishes were used to locate the specified dish locations. 10 images of Cy3 filter and 10 images of Atto 647N filter were collected in immediate series for all 4 locations using a time-lapse acquisition software. After the image acquisition at 6 hours and all the follow-up time points, we transferred back 1000 μL of the tile mixture in the dish to allow nanotubes to continue to grow. After transfer, dish was then sealed with Parafilm to prevent solution evaporation.

6. Nanotube lengths were estimated via ImageJ JFilament (http://athena.physics.lehigh.edu/jfilament/) [5] as the length of the 2D projection of the DNA nanotubes. 10 images of the same nanotube at each time point (6, 12 and 24 hours) were collected and the longest length determined for each time point was considered to best representation of the length of the nanotube at that time.

Supplementary Note S14: Protocol for measuring the rate of caps binding to RT A seeded nanotubes

1. To measure the rate of caps binding to RT A seeded nanotubes, we prepared glass dish surfaces (see Supp. Note S13) a day in advance and purified RT A seed mixture following the methods for these steps given in Supp. Note S14. We then followed the protocol for growing RT A seeded nanotubes mentioned in Supp. Note S11 using the following RS tile mixture.

   Supplementary Table S4: RS tile solution used for growing nanotubes in glass dishes.

	Final Desired Concentration (nM or fold)	Stock (nM or fold)	To add (μL)
H2O			15.23
RT A Seeds	0.003	0.2	0.3
RS tiles	75	600	2.5
10 × TAE Mg^{2+}	1	10	1.97
Total			20

2. After 6 hours of growth, 6 μL of the seeded nanotube mixture was transferred onto the dish in the presence of 1000 μL of 1×TAE Mg^{2+}buffer. We allowed 15 mins for the seeded nanotubes to attach to the dish glass surface by the biotin labels on the seed. After 15 minutes, the glass surface was washed three times with 1 × TAE Mg^{2+} to remove unattached seeds. Examples of seed density produced by this attachment process are shown after 0 hours in Supp. Fig. S26.

3. After washing 1000 μL of 1 × TAE Mg^{2+} solution was placed onto the dish for image acquisition. Four specific locations were chosen using the markers embedded on the glass surface of the dish as regions for tracking nanotubes over time.

4. After choosing the locations for tracking, the buffer was replaced by 985 μL of annealed RS tile mixture and 15 μL purified flexible B caps, made using Supp. Notes S9 and S10. The solutions were made so that the final concentration of tiles was 75 nM and the final concentration of the B was 24 pM. The dish was then sealed with Parafilm and kept at room temperature on a microscope stage. The presence of free tiles in solution kept the nanotubes from melting over the course of the experiment.

5. Fluorescence images of the four previous determined locations were collected every ten minutes for 4 hours and after that every 30 minutes for next 2 hours using time-lapse acquisition software. One image of the RT A seeds (Atto 647N), three images of B caps (Atto 488), and three images of the nanotubes (Cy3) were collected at each location at each time point. The high background fluorescence levels in the Cy3 channel caused by the presence of the free tiles meant that nanotube images were not used in analysis.

6. During the image acquisition process, caps entered and left the image; occasional appearance of the caps near a seed could appear to be a capping event. We thus noted that a capping event occurred when a cap appeared near a seed over multiple consecutive time points.

Supplementary Note S15: Protocol for growing RT A and C seeded nanotubes in a single pot reaction

1. Solutions of RT A and C seeded nanotubes were prepared by first mixing 13.73 μL of purified water, 1 μL of 1 mg/ml BSA Biotin, 1.5 μL of each RT RS and UV nanotube tiles (Supp. Note S8) and 1.97 μL 10 × TAE $Mg2^{+}$ buffer to a final volume of 19.7 μL per tile solution.

2. Purified seeds were prepared and their concentrations were measured as described in Supp. Notes S9 and S10. Purified A and C seeds were mixed together and the combined seed solution was adjusted through the addition of 1 × TAE Mg^{2+} so that the final concentration would be the 2 pM (each) after adding 0.3 μL of the solution containing A and C seeds to the 19.7 μL of tile solution.

3. The tile solutions from step 1 were annealed from 90 °C to 20 °C using the protocol in Supplementary Table S2. When the solution reached 20 °C, 0.3 μL of seed solution (to a final concentration of 2 pM) was added to 19.7 μL of the tile solution so that the tile concentration would be 45 nM of RS tiles and 30 nM of UV tiles after addition of seeds. After mixing, the mixtures were incubated for the time interval(s) described in the main text. Control experiments without seeds followed the above instructions except that 0.3 μL of 1 × TAE Mg^{2+} was added in place of the seed solution.

4. Slides were prepared as described in Supp. Note S11.

Supplementary Note S16: Protocol for growing RT A seeded, B capped and RT C seeded, D capped nanotubes in a single pot reaction

1. Solutions of seeded nanotubes were prepared by combining 13.46 μL of purified water, 1 μL of 1 mg/ml BSA Biotin, 1.5 μL of RT nanotube RS tile solution and 1.5 μL of RT nanotube UV tile solution (Supp. Note S8) and 1.94 μL 10 × TAE Mg^{++} buffer to a final volume of 19.4 μL per tile solution.

2. Purified A and C seeds were prepared and their concentrations were measured as described in Supp. Notes S9 and S10. Purified A and C seeds at the same concentrations were mixed together in equal volume and the combined seed solution was adjusted by adding 1 × TAE Mg^{2+} so that the final concentration of each seed would be as specified in the main text when 0.3 μL of the combined A and C seeds solution is added to the tile solution.

3. Purified flexible B and D caps were prepared and their concentrations were measured as described in Supp. Notes S9 and S10. Purified flexible B and D caps at the same concentrations so they are mixed together with equal volume and the combined seed solution was adjusted by adding of 1 × TAE Mg^{2+} so that the final concentration of each seed would be as specified in the main text when 0.3 μL of the combined B and D cap solution is added to the tile solution.

4. The tile solutions from step 1 were annealed from 90 °C to 20 °C using the protocol in Supp. Table S2. When the solution reached 20 °C, 0.3 μL of the combined A and C seed solution (to a final concentration of 2 pM) was added to 19.4 μL tile solution, after which the mixture was incubated. After either 4 or 8 hours, 0.3 μL of the combined B and D cap solution (to a final concentration of 10 pM) was added to the mixture so that the tile concentrations were set at 45 nM of RS tiles and 30 nM of UV tiles after addition of seeds and caps. Control experiments without caps followed the above instructions except that 0.3 μL of 1 × TAE Mg^{2+} was added in place of the cap solution. In this experiment with only one type of caps being added, 0.3 μL of the corresponding caps (B or D caps) was added as reported above.

5. Slides were prepared as described in Supp. Note S11.

Supplementary Note S17: M13mp18 scaffold regions

The unused sequence of M13mp18 scaffold has several complimentary sites that can bind to sticky ends at the B interface of RS tiles. These sites are highlighted in green. The sections of M13mp18 scaffold that are highlighted in red are bound by staples for the short seed or cap and the sections that are highlighted in yellow are binding sites for attachment strands.

AATGCTACTACTATTAGTAGAATTGATGCCACCTTTTCAGCTCGCGCCCCAAAT
GAAAATATAGCTAAACAGGTTATTGACCATTTGCGAAATGTATCTAATGGTCA
AACTAAATCTACTCGTTCGCAGAATTGGGAATCAACTGTTATATGGAATGAAA
CTTCCAGACACCGTACTTTAGTTGCATATTTAAAACATGTTGAGCTACAGCATT
ATATTCAGCAATTAAGCTCTAAGCCATCCGCAAAAATGACCTCTTATCAAAAGG
AGCAATTAAAGGTACTCTCTAATCCTGACCTGTTGGAGTTTGCTTCCGGTCTG
GTTCGCTTTGAAGCTCGAATTAAAACGCGATATTTGAAGTCTTTCGGGCTTCC
TCTTAATCTTTTTGATGCAATCCGCTTTGCTTCTGACTATAATAGTCAGGGTAA
AGACCTGATTTTTGATTTATGGTCATTCTCGTTTTCTGAACTGTTTAAAGCATT
TGAGGGGGATTCAATGAATATTTATGACGATTCCGCAGTATTGGACGCTATCC
AGTCTAAACATTTTACTATTACCCCCTCTGGCAAAACTTCTTTTGCAAAAGCCTC
TCGCTATTTTGGTTTTTATCGTCGTCTGGTAAACGAGGGTTATGATAGTGTTG
CTCTTACTATGCCTCGTAATTCCTTTTGGCGTTATGTATCTGCATTAGTTGAAT
GTGGTATTCCTAAATCTCAACTGATGAATCTTTCTACCTGTAATAATGTTGTTC
CGTTAGTTCGTTTTATTAACGTAGATTTTTCTTCCCAACGTCCTGACTGGTATA
ATGAGCCAGTTCTTAAAATCGCATAAGGTAATTCACAATGATTAAAGTTGAAA
TTAAACCATCTCAAGCCCAATTTACTACTCGTTCTGGTGTTTCTCGTCAGGGCA
AGCCTTATTCACTGAATGAGCAGCTTTGTTACGTTGATTTGGGTAATGAATAT
CCGGTTCTTGTCAAGATTACTCTTGATGAAGGTCAGCCAGCCTATGCGCCTGG
TCTGTACACCGTTCATCTGTCCTCTTTCAAAGTTGGTCAGTTCGGTTCCCTTAT
GATTGACCGTCTGCGCCTCGTTCCGGCTAAGTAACATGGAGCAGGTCGCGGA
TTTCGACACAATTTATCAGGCGATGATACAAATCTCCGTTGTACTTTGTTTCGC
GCTTGGTATAATCGCTGGGGGTCAAAGATGAGTGTTTTAGTGTATTCTTTTGC
CTCTTTCGTTTTAGGTTGGTGCCTTCGTAGTGGCATTACGTATTTTACCCGTTT
AATGGAAACTTCCTCATGAAAAAGTCTTTAGTCCTCAAAGCCTCTGTAGCCGTT
GCTACCCTCGTTCCGATGCTGTCTTTCGCTGCTGAGGGTGACGATCCCGCAAA
AGCGGCCTTTAACTCCCTGCAAGCCTCAGCGACCGAATATATCGGTTATGCGT
GGGCGATGGTTGTTGTCATTGTCGGCGCAACTATCGGTATCAAGCTGTTTAA
GAAATTCACCTCGAAAGCAAGCTGATAAACCGATACAATTAAAGGCTCCTTTT
GGAGCCTTTTTTTTGGAGATTTTCAACGTGAAAAAATTATTATTCGCAATTCCT
TTAGTTGTTCCTTTCTATTCTCACTCCGCTGAAACTGTTGAAAGTTGTTTAGCA
AAATCCCATACAGAAAATTCATTTACTAACGTCTGGAAAGACGACAAAACTTTA
GATCGTTACGCTAACTATGAGGGCTGTCTGTGGAATGCTACAGGCGTTGTAG
TTTGTACTGGTGACGAAACTCAGTGTTACGGTACATGGGTTCCTATTGGGCTT
GCTATCCCTGAAAATGAGGGTGGTGGCTCTGAGGGTGGCGGTTCTGAGGGT
GGCGGTTCTGAGGGTGGCGGTACTAAACCTCCTGAGTACGGTGATACACCTA
TTCCGGGCTATACTTATATCAACCCTCTCGACGGCACTTATCCGCCTGGTACTG
AGCAAAACCCCGCTAATCCTAATCCTTCTCTTGAGGAGTCTCAGCCTCTTAATA

CTTTCATGTTTCAGAATAATAGGTTCCGAAATAGGCAGGGGGCATTAACTGTT
TATACGGGCACTGTTACTCAAGGCACTGACCCCGTTAAAACTTATTACCAGTAC
ACTCCTGTATCATCAAAAGCCATGTATGACGCTTACTGGAACGGTAAATTCAG
AGACTGCGCTTTCCATTCTGGCTTTAATGAGGATTTATTTGTTTGTGAATATCA
AGGCCAATCGTCTGACCTGCCTCAACCTCCTGTCAATGCTGGCGGCGGCTCTG
GTGGTGGTTCTGGTGGCGGCTCTGAGGGTGGTGGCTCTGAGGGTGGCGGTT
CTGAGGGTGGCGGCTCTGAGGGAGGCGGTTCCGGTGGTGGCTCTGGTTCCG
GTGATTTTGATTATGAAAAGATGGCAAACGCTAATAAGGGGGCTATGACCGA
AAATGCCGATGAAAACGCGCTACAGTCTGACGCTAAAGGCAAACTTGATTCTG
TCGCTACTGATTACGGTGCTGCTATCGATGGTTTCATTGGTGACGTTTCCGGC
CTTGCTAATGGTAATGGTGCTACTGGTGATTTTGCTGGCTCTAATTCCCAAAT
GGCTCAAGTCGGTGACGGTGATAATTCACCTTTAATGAATAATTTCCGTCAAT
ATTTACCTTCCCTCCCTCAATCGGTTGAATGTCGCCCTTTTGTCTTTGGCGCTG
GTAAACCATATGAATTTTCTATTGATTGTGACAAAATAAACTTATTCCGTGGTG
TCTTTGCGTTTCTTTTATATGTTGCCACCTTTATGTATGTATTTTCTACGTTTGC
TAACATACTGCGTAATAAGGAGTCTTAATCATGCCAGTTCTTTTGGGTATTCC
GTTATTATTGCGTTTCCTCGGTTTCCTTCTGGTAACTTTGTTCGGCTATCTGCT
TACTTTTCTTAAAAAGGGCTTCGGTAAGATAGCTATTGCTATTTCATTGTTTCT
TGCTCTTATTATTGGGCTTAACTCAATTCTTGTGGGTTATCTCTCTGATATTAG
CGCTCAATTACCCTCTGACTTTGTTCAGGGTGTTCAGTTAATTCTCCCGTCTAA
TGCGCTTCCCTGTTTTTATGTTATTCTCTCTGTAAAGGCTGCTATTTTCATTTTT
GACGTTAAACAAAAAATCGTTTCTTATTTGGATTGGGATAAATAATATGGCTG
TTTATTTTGTAACTGGCAAATTAGGCTCTGGAAAGACGCTCGTTAGCGTTGGT
AAGATTCAGGATAAAATTGTAGCTGGGTGCAAAATAGCAACTAATCTTGATTT
AAGGCTTCAAAACCTCCCGCAAGTCGGGAGGTTCGCTAAAACGCCTCGCGTTC
TTAGAATACCGGATAAGCCTTCTATATCTGATTTGCTTGCTATTGGGCGCGGT
AATGATTCCTACGATGAAAATAAAAACGGCTTGCTTGTTCTCGATGAGTGCGG
TACTTGGTTTAATACCCGTTCTTGGAATGATAAGGAAAGACAGCCGATTATTG
ATTGGTTTCTACATGCTCGTAAATTAGGATGGGATATTATTTTTCTTGTTCAG
GACTTATCTATTGTTGATAAACAGGCGCGTTCTGCATTAGCTGAACATGTTGT
TTATTGTCGTCGTCTGGACAGAATTACTTTACCTTTTGTCGGTACTTTATATTC
TCTTATTACTGGCTCGAAAATGCCTCTGCCTAAATTACATGTTGGCGTTGTTAA
ATATGGCGATTCTCAATTAAGCCCTACTGTTGAGCGTTGGCTTTATACTGGTA
AGAATTTGTATAACGCATATGATACTAAACAGGCTTTTTCTAGTAATTATGATT
CCGGTGTTTATTCTTATTTAACGCCTTATTTATCACACGGTCGGTATTTCAAAC
CATTAAATTTAGGTCAGAAGATGAAATTAACTAAAATATATTTGAAAAAGTTTT
CTCGCGTTCTTTGTCTTGCGATTGGATTTGCATCAGCATTTACATATAGTTATA
TAACCCAACCTAAGCCGGAGGTTAAAAAGGTAGTCTCTCAGACCTATGATTTT
GATAAATTCACTATTGACTCTTCTCAGCGTCTTAATCTAAGCTATCGCTATGTT
TTCAAGGATTCTAAGGGAAAATTAATTAATAGCGACGATTTACAGAAGCAAG
GTTATTCACTCACATATATTGATTTATGTACTGTTTCCATTAAAAAAGGTAATT
CAAATGAAATTGTTAAATGTAATTAATTTTGTTTTCTTGATGTTTGTTTCATCA
TCTTCTTTTGCTCAGGTAATTGAAATGAATAATTCGCCTCTGCGCGATTTTGTA
ACTTGGTATTCAAAGCAATCAGGCGAATCCGTTATTGTTTCTCCCGATGTAAA
AGGTACTGTTACTGTATATTCATCTGACGTTAAACCTGAAAATCTACGCAATTT

CTTTATTTCTGTTTTACGTGCAAATAATTTTGATATGGTAGGTTCTAACCCTTC
CATTATTCAGAAGTATAATCCAAACAATCAGGATTATATTGATGAATTGCCATC
ATCTGATAATCAGGAATATGATGATAATTCCGCTCCTTCTGGTGGTTTCTTTGT
TCCGCAAAATGATAATGTTACTCAAACTTTTAAAATTAATAACGTTCGGGCAAA
GGATTTAATACGAGTTGTCGAATTGTTTGTAAAGTCTAATACTTCTAAATCCTC
AAATGTATTATCTATTGACGGCTCTAATCTATTAGTTGTTAGTGCTCCTAAAGA
TATTTTAGATAACCTTCCTCAATTCCTTTCAACTGTTGATTTGCCAACTGACCAG
ATATTGATTGAGGGTTTGATATTTGAGGTTCAGCAAGGTGATGCTTTAGATTT
TTCATTTGCTGCTGGCTCTCAGCGTGGCACTGTTGCAGGCGGTGTTAATACTG
ACCGCCTCACCTCTGTTTTATCTTCTGCTGGTGGTTCGTTCGGTATTTTTAATG
GCGATGTTTTAGGGCTATCAGTTCGCGCATTAAAGACTAATAGCCATTCAAAA
ATATTGTCTGTGCCACGTATTCTTACGCTTTCAGGTCAGAAGGGTTCTATCTCT
GTTGGCCAGAATGTCCCTTTTATTACTGGTCGTGTGACTGGTGAATCTGCCAA
TGTAAATAATCCATTTCAGACGATTGAGCGTCAAAATGTAGGTATTTCCATGA
GCGTTTTTCCTGTTGCAATGGCTGGCGGTAATATTGTTCTGGATATTACCAGC
AAGGCCGATAGTTTGAGTTCTTCTACTCAGGCAAGTGATGTTATTACTAATCA
AAGAAGTATTGCTACAACGGTTAATTTGCGTGATGGACAGACTCTTTTACTCG
GTGGCCTCACTGATTATAAAAACACTTCTCAGGATTCTGGCGTACCGTTCCTG
TCTAAAATCCCTTTAATCGGCCTCCTGTTTAGCTCCCGCTCTGATTCTAACGAG
GAAAGCACGTTATACGTGCTCGTCAAAGCAACCATAGTACGCGCCCTGTAGCG
GCGCATTAAGCGCGGCGGGTGTGGTGGTTACGCGCAGCGTGACCGCTACACT
TGCCAGCGCCCTAGCGCCCGCTCCTTTCGCTTTCTTCCCTTCCTTTCTCGCCAC
GTTCGCCGGCTTTCCCCGTCAAGCTCTAAATCGGGGGCTCCCTTTAGGGTTCC
GATTTAGTGCTTTACGGCACCTCGACCCCAAAAAACTTGATTTGGGTGATGGT
TCACGTAGTGGGCCATCGCCCTGATAGACGGTTTTTCGCCCTTTGACGTTGGA
GTCCACGTTCTTTAATAGTGGACTCTTGTTCCAAACTGGAACAACACTCAACCC
TATCTCGGGCTATTCTTTTGATTTATAAGGGATTTTGCCGATTTCGGAACCACC
ATCAAACAGGATTTTCGCCTGCTGGGGCAAACCAGCGTGGACCGCTTGCTGC
AACTCTCTCAGGGCCAGGCGGTGAAGGGCAATCAGCTGTTGCCCGTCTCACT
GGTGAAAAGAAAAACCACCCTGGCGCCCAATACGCAAACCGCCTCTCCCCGCG
CGTTGGCCGATTCATTAATGCAGCTGGCACGACAGGTTTCCCGACTGGAAAG
CGGGCAGTGAGCGCAACGCAATTAATGTGAGTTAGCTCACTCATTAGGCACC
CCAGGCTTTACACTTTATGCTTCCGGCTCGTATGTTGTGTGGAATTGTGAGCG
GATAACAATTTCACACAGGAAACAGCTATGACCATGATTACGAATTCGAGCTC
GGTACCCGGGGATCCTCTAGAGTCGACCTGCAGGCATGCAAGCTTGGCACTG
GCCGTCGTTTTACAACGTCGTGACTGGGAAAACCCTGGCGTTACCCAACTTAA
TCGCCTTGCAGCACATCCCCCTTTCGCCAGCTGGCGTAATAGCGAAGAGGCCC
GCACCGATCGCCCTTCCCAACAGTTGCGCAGCCTGAATGGCGAATGGCGCTTT
GCCTGGTTTCCGGCACCAGAAGCGGTGCCGGAAAGCTGGCTGGAGTGCGAT
CTTCCTGAGGCCGATACTGTCGTCGTCCCCTCAAACTGGCAGATGCACGGTTA
CGATGCGCCCATCTACACCAACGTGACCTATCCCATTACGGTCAATCCGCCGTT
TGTTCCCACGGAGAATCCGACGGGTTGTTACTCGCTCACATTTAATGTTGATG
AAAGCTGGCTACAGGAAGGCCAGACGCGAATTATTTTTGATGGCGTTCCTATT
GGTTAAAAAATGAGCTGATTTAACAAAAATTTAATGCGAATTTTAACAAAATA
TTAACGTTTACAATTTAAATATTTGCTTATACAATCTTCCTGTTTTTGGGGCTTT

TCTGATTATCAACCGGGGTACATATGATTGACATGCTAGTTTTACGATTACCG
TTCATCGATTCTCTTGTTTGCTCCAGACTCTCAGGCAATGACCTGATAGCCTTT
GTAGATCTCTCAAAAATAGCTACCCTCTCCGGCATTAATTTATCAGCTAGAACG
GTTGAATATCATATTGATGGTGATTTGACTGTCTCCGGCCTTTCTCACCCTTTT
GAATCTTTACCTACACATTACTCAGGCATTGCATTTAAAATATATGAGGGTTCT
AAAAATTTTTATCCTTGCGTTGAAATAAAGGCTTCTCCCGCAAAAGTATTACAG
GGTCATAATGTTTTTGGTACAACCGATTTAGCTTTATGCTCTGAGGCTTTATTG
CTTAATTTTGCTAATTCTTTGCCTTGCCTGTATGATTTATTGGATGTT

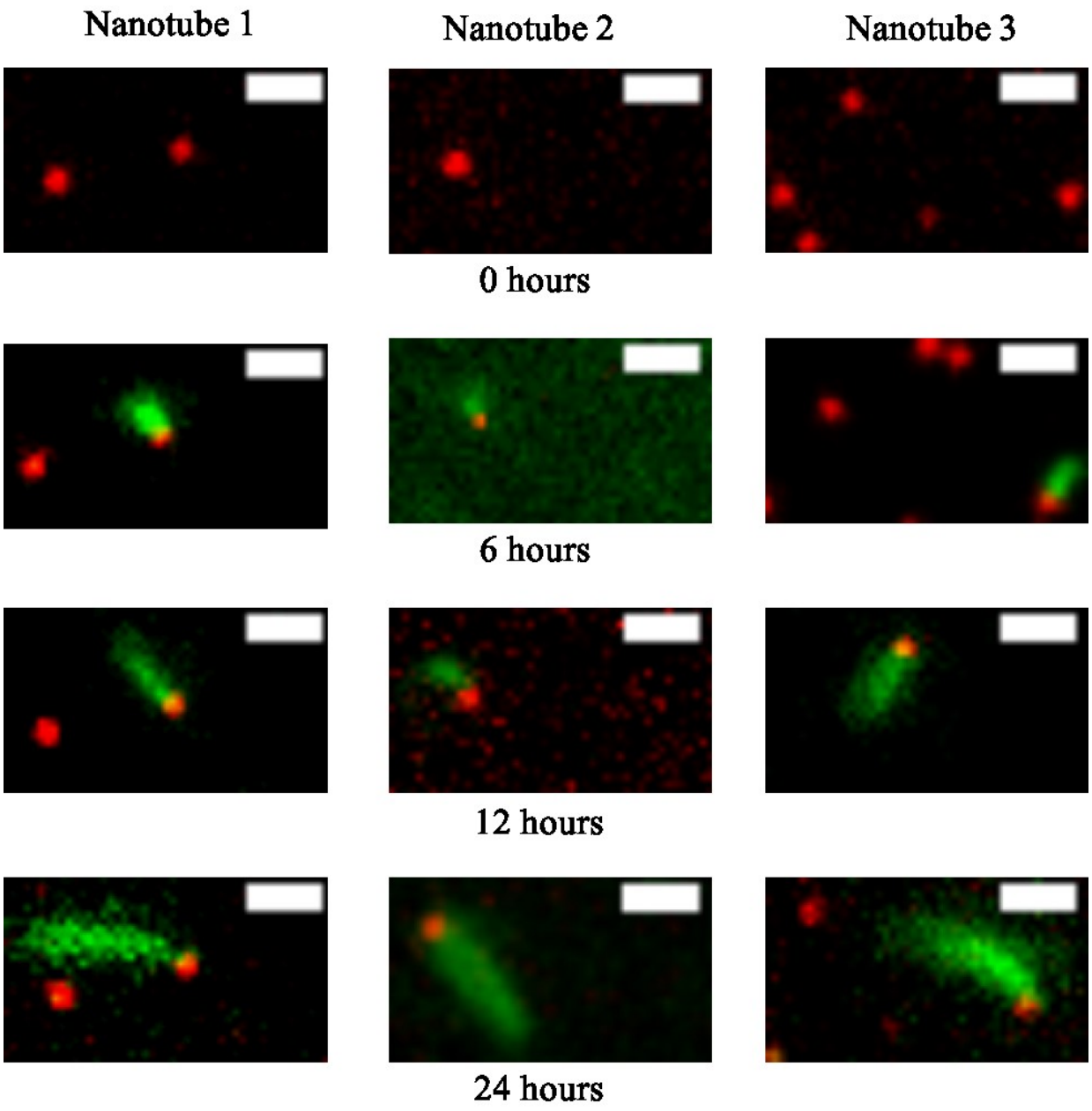

Supplementary Figure S8: **Time-lapse multicolor fluorescence micrographs showing the growth of specific RT A seeded nanotubes over 24 hours.** Individual nanotubes were grown while seeds were anchored to glass-bottomed dishes as described in Supp. Note S14. Scale bars are 2 μm.

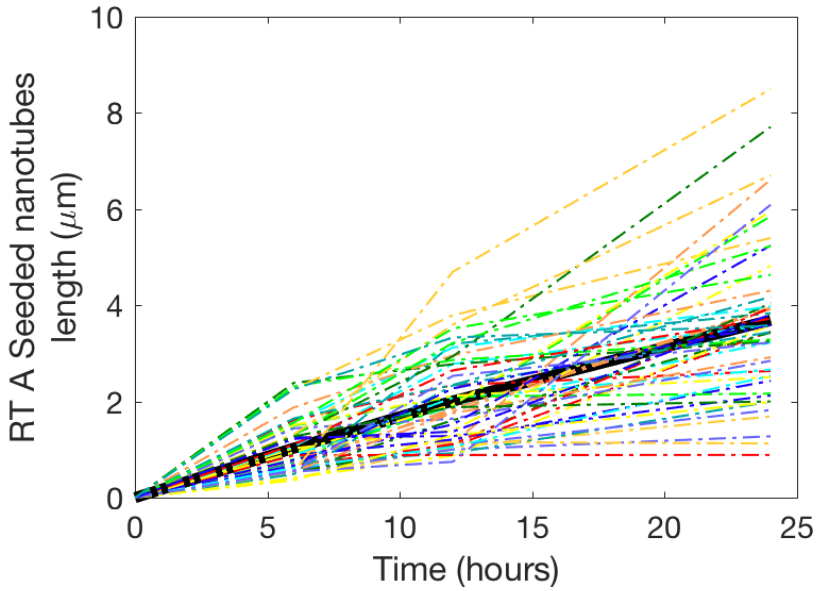

Supplementary Figure S9: **Change in the length of individual RT A seeded nanotubes over time.** 50 individual nanotubes were tracked and their lengths are reported here in dashed-dot lines. The mean of the trajectories is shown in sold black line Lengths were measured as described in Supp. Note S14. The observed growth rate, computed using the average trajectory is 0.165 ± 0.0052 μm/hr. The error reported for the growth rate was determined using the standard error of the mean of the growth rate for each time point.

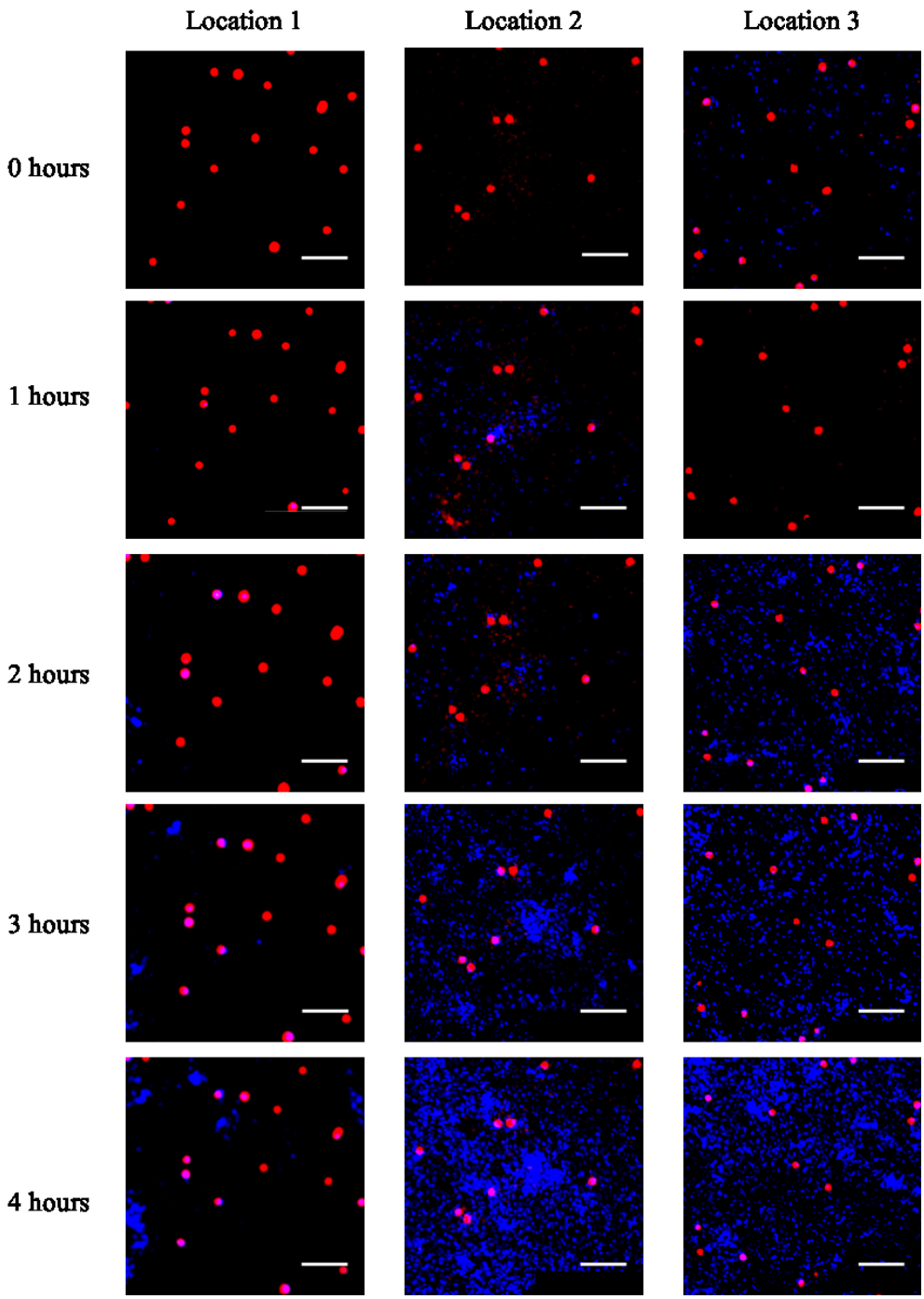

Supplementary Figure S10: **Multicolor fluorescence micrographs of the same sets of nanotubes anchored to glass bottom dishes as the capping process progresses.** RT A seeds were labeled with Atto647N (red) and flexible B caps were labeled with Atto488 (blue). Scale bars are 10 μm. Caps both bound to seeds and nonspecifically attached to the surface.

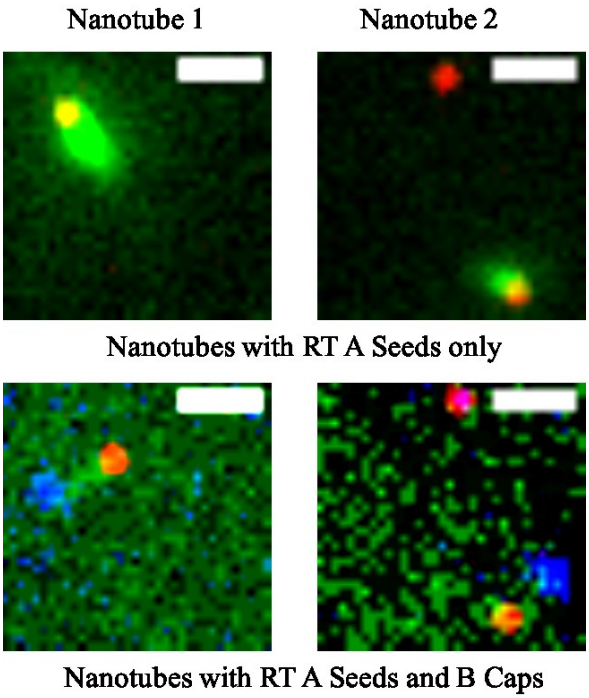

Supplementary Figure S11: **Multicolor fluorescence micrographs showing two specific seeded nanotubes before and after the caps attached to their ends**. The nanotubes were anchored to a glass bottom dish by biotin labels on their seeds (see Supp. Note S15). The top and bottom sets of images so show the same pair of nanotubes before (top) and after (bottom) caps were added. The top set of images were taken before tiles were added so there is significantly less background noise. RT A seeds were labeled with Atto 647N (red), RS nanotube were labeled with Cy3 (green) and the flexible B cap were labeled with Atto 488 (blue). RS nanotubes grew from RT A seeds for 8 hours and then flexible B caps were added and after 2 hours we found these nanotubes capped (see Supp. Note S15). Scale bars are 2 μm.

Supplementary Note S18: Measuring the rate of capping

To estimate the rate at which flexible B caps bind to RT A seeded nanotube free ends, we considered the capping reaction as a reaction of the form

$$A + B \xrightarrow{k_j} AB \qquad (2)$$

Here, A is a seeded RT nanotube, B is a free flexible B cap and AB is a nanotube with an RT A seed and B caps. k_j is the reaction rate for the capping reaction. We assumed that this capping reaction is irreversible, as we did not observed caps falling off in our study of the capping of 300 nanotubes. Using mass action kinetics, we can model the kinetics of this reaction as

$$\frac{d[AB]}{dt} = -k_j[A][B] \qquad (3)$$

where t is the reaction time and [] represents the molar concentration of the species. We define X as the fraction of RT seeded capped nanotubes out of all seeded nanotubes ($[AB]/[A]_{t=0}$). If we assume that $[B]_{t=0} >> [A]_{t=0}$, and $[AB]_{t=0}=0$ we can solve equation (1) in terms of X:

$$X = 1 - e^{-k_j t[B]_{t=0}} \qquad (4)$$

To determine the most likely value of k_j, we used the least squares fitting of the measured data (Fig. 5). In experiments, we used 2 pM of RT A seeds to grow RS nanotubes, therefore the upper bound of $[A]_{t=0}$ = 2 pM while $[B]_{t=0}$ = 24 pM (see Supp. Note S15).

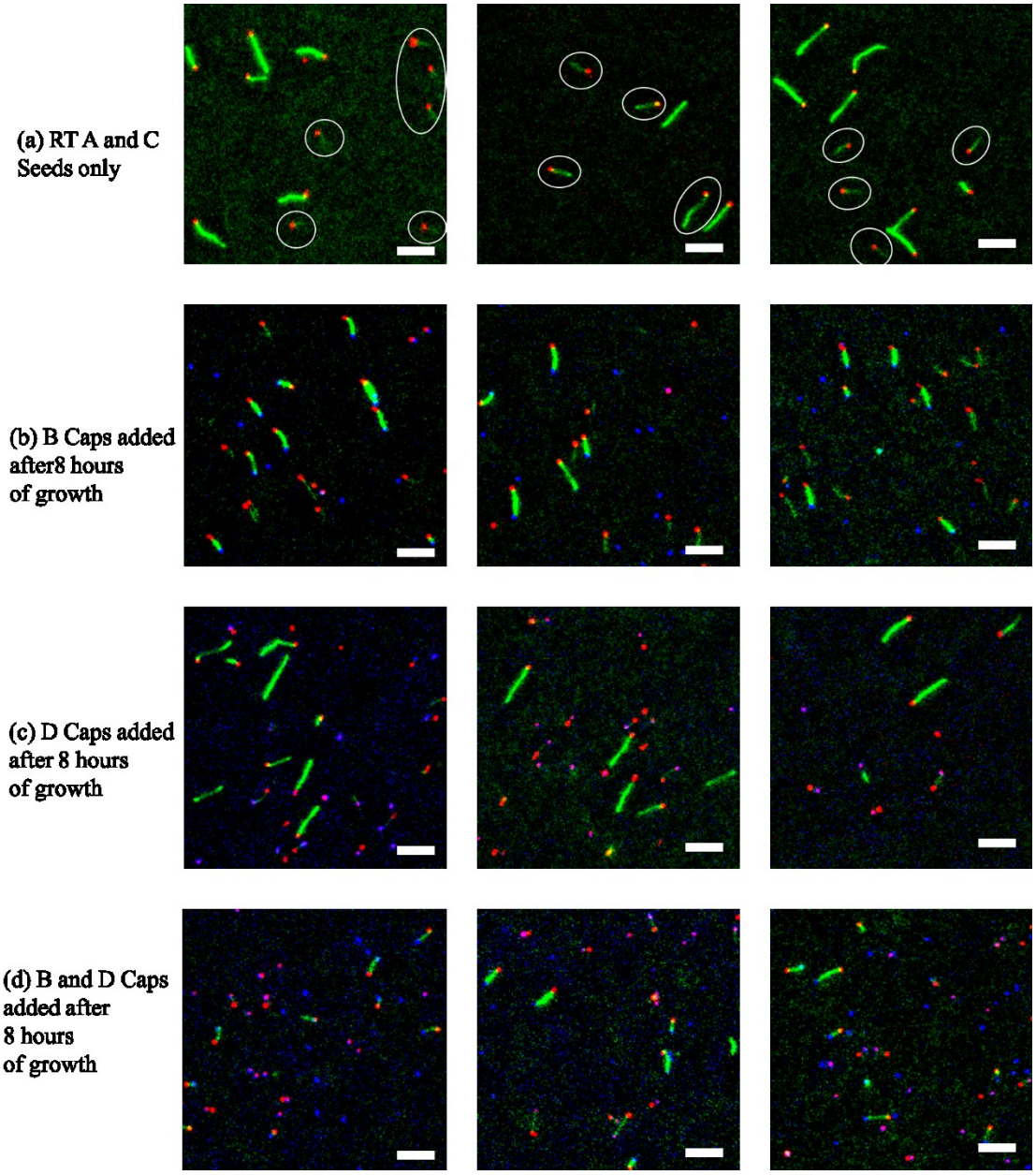

Supplementary Figure S12: **Example fluorescence micrographs showing different types of RS and UV nanotubes that assemble in reactions involving RT A and C seeds and flexible B and D caps.** RS tile nanotubes (Cy3 bright green) grew from RT A seeds labeled with Atto 647N (red) and UV tile nanotubes (Cy3 dim green at 25% incorporation) grew from RT C seeds labeled with Atto 647N (red). Flexible cap B was labeled with Atto 488 (blue) and flexible cap D was labeled with 50% Atto 647N and 50% Atto 488 dyes (purple). Images were taken after 25 hours of growth. (a) Both RT A and C seeded nanotubes grew long when no caps were added. Here, RT C seeded UV nanotubes are highlighted using white markers (b) Only RT A seeded nanotubes stop growing when B caps were added after 8 hours. (c) Only RT C seeded nanotubes stop growing in the presence of D caps. (d) Both

RT A and C seeded nanotubes stop growing in presence of B and D caps. In cases (b-d), caps were added after 8 hours of growth.

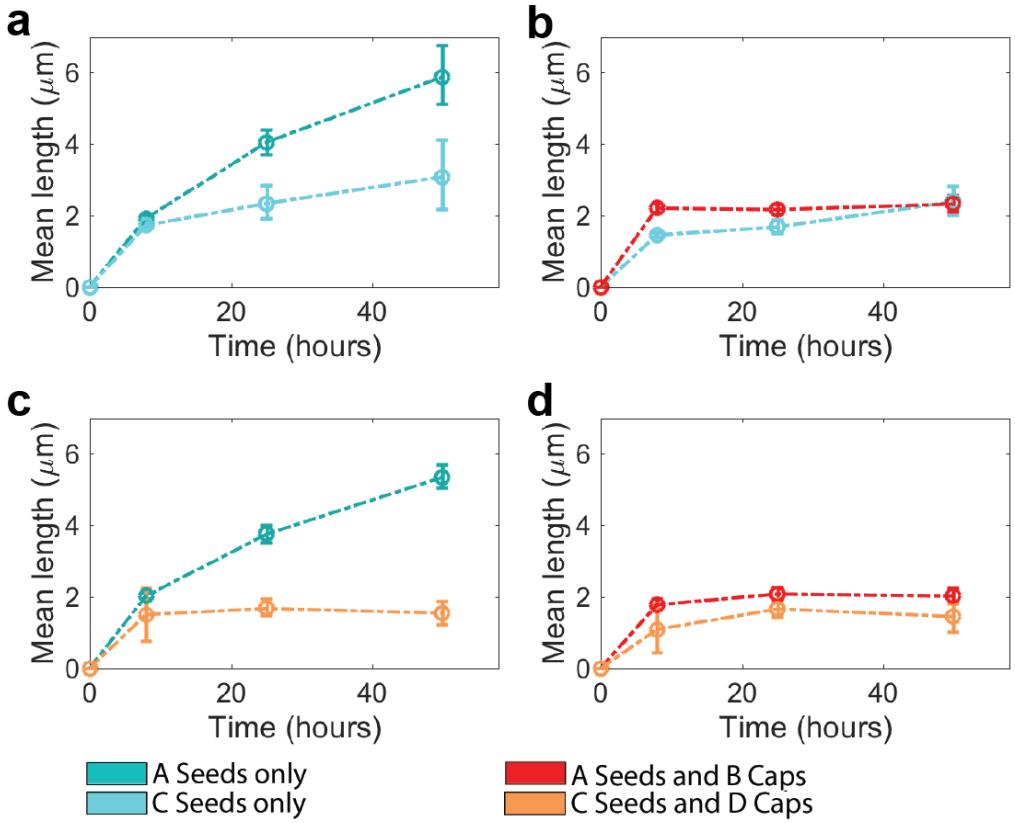

Supplementary Figure S13: **The mean lengths of different types of RS and UV nanotubes that assemble in reactions involving RT A, C seeds and flexible B and D caps. (a)** The mean lengths of RT A and C seeded nanotubes when no caps are added. **(b)** The mean lengths of RT A or C seeded nanotubes when flexible B caps were added at 8 hours. **(c)** The mean lengths of RT A or C seeded nanotubes when flexible D caps were added at 8 hours. **(d)** The mean lengths of RT A and C seeded nanotubes when flexible B and D caps were added at 8 hours.

Supplementary Note S19: Protocol for growing AB DNA nanotube connections.

1. To characterize AB DNA nanotube connections yield, dishes (D29-20-1-N, In Vitro Scientific) were prepared using the dish preparation protocol (see Supp. Note S11).

2. To form nanotube connections, seeds were first annealed using the protocol mentioned in Supp. Table S2.

Supplementary Table S5: Tile recipe for growing AB nanotube connections in glass dishes.

	Final Desired Concentration (nM or fold)	Stock (nM or fold)	To add (μL)
H2O			262.5
RS tiles - ATTO647N	150	400	187.5
10 × TAE Mg^{2+}	1	10	50
Total			500

3. Seeds were then purified in the centrifuge and their concentrations were measured as described [6]. Seed density was adjusted by appropriately diluting the 7.5 μL of seeds solution into 500 μL of the 1 × TAE Mg^{2+} buffer to achieve 150 seeds per field of view. We allowed 10-15 minutes for seeds to attach on the dish glass surface, and then performed washing steps with 1 × TAE Mg^{2+} to remove unattached seeds.

4. After the seeds were attached to the glass surface, 500 μL of the 150 nM of RS tile solution was annealed following the same protocol and then was placed into the dish to allow the nanotube to grow. Then the dish was sealed with Parafilm to prevent solution evaporation.

5. Three time points (12, 48, and 72 hours) were considered for imaging analysis. At 12 hours and all the following time points, tile mixture was removed from the dish and three washing steps were performed with 500 μL of TAE buffer to reduce fluorescence noise. 10 images of Cy3 filter, 10 images of Atto 488 and 10 images of Atto 647N filter were collected using a time-lapse acquisition software ANDOR. 500 μL of the RS tile mixture was annealed and replenished each time and then transferred back into the dish after the image acquisition to allow nanotubes to continue to grow. Dish was then sealed with Parafilm to prevent solution evaporation.

6. We use ImageJ JFilament (http://athena.physics.lehigh.edu/jfilament/) to estimate nanotube connection lengths [5]. 10 images of the same nanotube at each time point (12, 48 and 72 hours) were collected and the longest length determined for each time point was considered to best represent the length of the connection at that time. A connection is deemed successful when the nanotube connection are consistently joined during all the imaging acquisition process.

Supplementary Note S20: Protocol for growing CD nanotube connections.

1. To characterize CD DNA nanotube connections yield, dishes (D29-20-1-N, In Vitro Scientific) were prepared using the dish preparation protocol (see Supp. Note S11).

2. To form nanotube connections, seeds were first annealed using the protocol mentioned in Supp. Table S2.

Supplementary Table S6: Tile recipe for growing CD nanotube connections in glass dishes.

	Final Desired Concentration (nM or fold)	Stock (nM or fold)	To add (μL)
H2O			400
UV tiles - Cy3	40	400	50
10 × TAE Mg^{2+}	1	10	50
Total			500

1. Seeds were then purified in the centrifuge and their concentrations were measured as described [6]. Seed density was adjusted by appropriately diluting the 7.5 μL of seeds solution into 500 μL of the 1 × TAE Mg^{2+} buffer to achieve 150 seeds per field of view. We allowed 10-15 minutes for seeds to attach on the dish glass surface, and then performed washing steps with 1 × TAE Mg^{2+} to remove unattached seeds.

2. After the seeds were attached to the glass surface, 500 μL of the 150 nM of UV tile solution was annealed following the same protocol and then was placed into the dish to allow the nanotube to grow. Then the dish was sealed with Parafilm to prevent solution evaporation.

3. Three time points (12, 48, and 72 hours) were considered for imaging analysis. At 12 hours and all the following time points, tile mixture was removed from the dish and three washing steps were performed with 500 μL of TAE buffer to reduce fluorescence noise. 10 images of Cy3 filter, 10 images of Atto 488 and 10 images of Atto 647N filter were collected using a time-lapse acquisition software ANDOR. 500 μL of the UV tile mixture was annealed and replenished each time and then transferred back into the dish after the image acquisition to allow nanotubes to continue to grow. Dish was then sealed with Parafilm to prevent solution evaporation.

4. We use ImageJ JFilament (http://athena.physics.lehigh.edu/jfilament/) to estimate nanotube connection lengths [5]. 10 images of the same nanotube at each time point (12, 48 and 72 hours) were collected and the longest length determined for each time point was considered to best represent the length of the connection at that time. A connection is deemed successful when the nanotube connection are consistently joined during all the imaging acquisition process.

Supplementary Note S21: Protocol for growing ABCD connections.

1. To characterize AB and CD DNA nanotube connections yield, dishes (D29-20-1-N, In Vitro Scientific) were prepared using the dish preparation protocol (see Supp. Note S11).

2. To form nanotube connections, seeds were first annealed using the protocol mentioned in Supp. Table S2.

Supplementary Table S7: Tile recipe for growing AB and CD nanotube connections simultaneously in glass dishes.

	Final Desired Concentration (nM or fold)	Stock (nM or fold)	To add (μL)
H2O			175
UV tiles - Cy3	80	400	50
10 × TAE Mg^{2+}	1	10	25
Total			250
	Final Desired Concentration (nM or fold)	Stock (nM or fold)	To add (μL)
H2O			37.5
RS tiles – ATTO647N	300	400	187.5
10 × TAE Mg^{2+}	1	10	25
Total			250

1. Seeds were then purified in the centrifuge and their concentrations were measured as described [6]. Seed density was adjusted by appropriately diluting the 7.5 μL of seeds solution into 500 μL of the 1 × TAE Mg^{2+} buffer to achieve 150 seeds per field of view. We allowed 10-15 minutes for seeds to attach on the dish glass surface, and then performed washing steps with 1 × TAE Mg^{2+} to remove unattached seeds.

2. After the seeds were attached to the glass surface, 500 μL of the 150 nM of RS tile solution and 40 nM of UV tile solution was annealed following the same protocol and then was placed into the dish to allow the nanotube to grow. Then the dish was sealed with Parafilm to prevent solution evaporation.

3. Three time points (12, 48, and 72 hours) were considered for imaging analysis. At 12 hours and all the following time points, tile mixture was removed from the dish and three washing steps were performed with 500 μL of TAE buffer to reduce fluorescence noise. 10 images of Cy3 filter, 10 images of Atto 488 and 10 images of

Atto 647N filter were collected using a time-lapse acquisition software ANDOR. 500 μL of the RS and UV tile mixture was annealed and replenished each time and then transferred back into the dish after the image acquisition to allow nanotubes to continue to grow. Dish was then sealed with Parafilm to prevent solution evaporation.

4. We use ImageJ JFilament (http://athena.physics.lehigh.edu/jfilament/) to estimate nanotube connection lengths [5]. 10 images of the same nanotube at each time point (12, 48 and 72 hours) were collected and the longest length determined for each time point was considered to best represent the length of the connection at that time. A connection is deemed successful when the nanotube connection are consistently joined during all the imaging acquisition process.

Supplementary Note S22: Method for determining four types of seeds.

We use MATLAB to detect fluorecence signal in each channel. Images were thresholded and then calculated by MATLAB to return x,y coordinates. In order to use MATLAB, each fluorecence image is thresholded via Image J. Cy3 was thresholded 99.97% of the maximum thresholding, ATTO 488 and ATTO 647 were thresholded 99.37% of the maximum thresholding (Fig. 2). After thresholding, each image is input in MATLAB and corresponding x and y coordinates were returned. If the dots from different fluorcent images were returned the same coordinates, then the seeds were dual labeled.

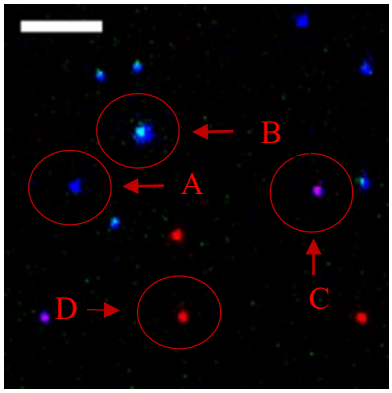

Figure 14. Composite of all types of seeds. Scale bar: 5μm.

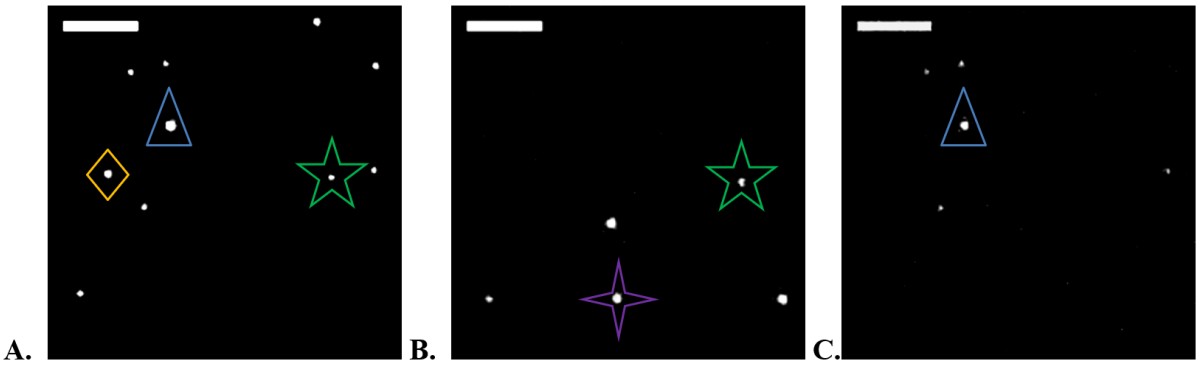

Figure 15. Raw image of each fluorescence channel after thresholding. Scale bar: 5μm.

From Figure 2, A is ATTO488 fluorescence channel, B is ATTO647N fluorescence channel, and C is Cy3 fluorescence channel. Blue triangle indicates Atto488 and Cy3 channel overlap and confirmed B seed. Yellow diamond only contains Atto488 channel and is thus A seed. Green star has Atto488 and Atto647 channel overlap and is C seed, and then purple 4 Point Star has atto647 channel and is D seed.

Supplementary Note S23: Method for determining isolated pair.

The same methodology was adopted to calculated nanotube connection yield. A nanotube connection pair is deemed isolated if no other seeded nanotube is found with the 1.5x connection distance between the two seeds[4]. The circled connections are counted as isolated pair because no other seeded nanotubes are found with the range. The figure below shows AB nanotube connection and CD nanotube connection.

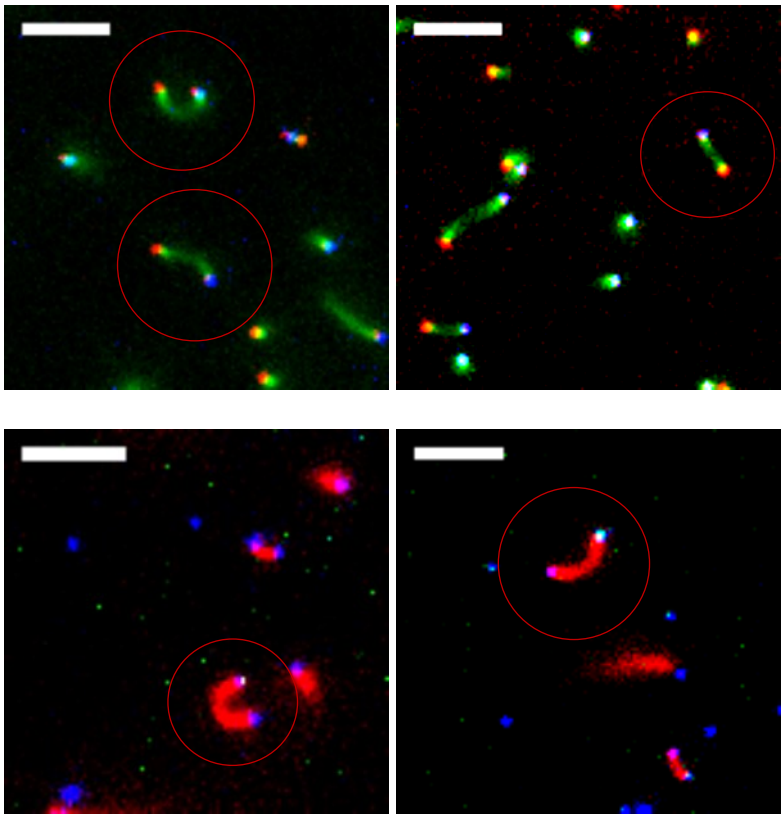

Figure 16. Nanotube Connection Isolated Pair Determination. Scale bar: 5μm.

Supplementary Note S24: Additional AB Connections

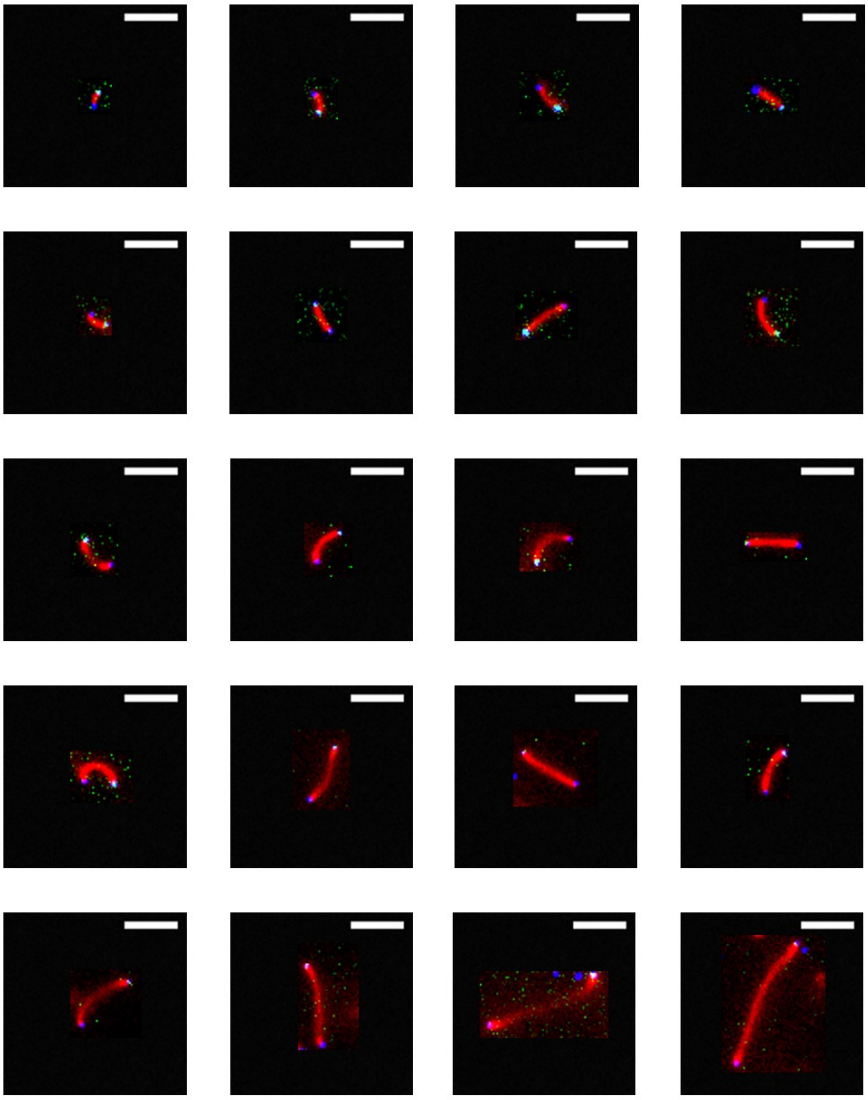

Figure 17. AB Nanotube Connection Isolated Pair. Scale bar: 5μm.

Supplementary Note S25: Additional CD Connections.

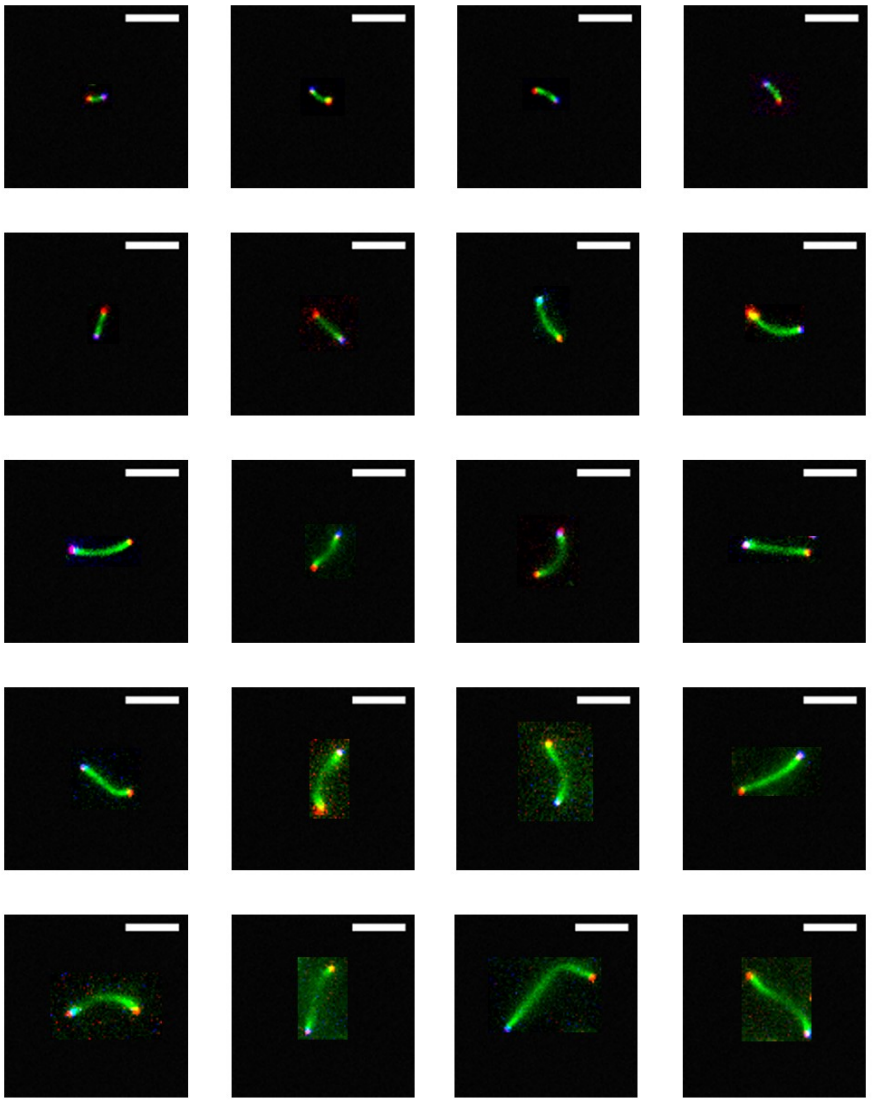

Figure 18. CD Nanotube Connection Isolated Pair. Scale bar: 5μm.

Supplementary Note S26: Additional ABCD Connections.

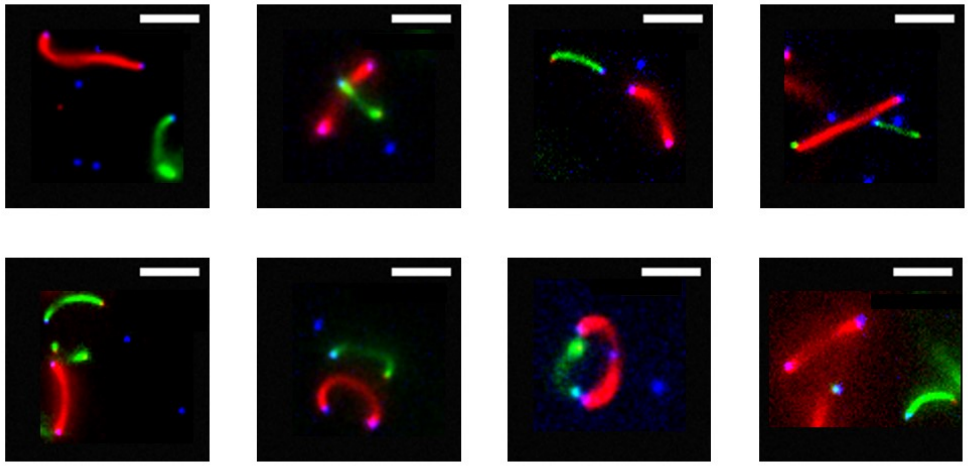

Figure 19. AB and CD Nanotube Connections existing simultaneously. Scale bar: 5μm.

References:

1. Rothemund, P. W.; Ekani-Nkodo, A.; Papadakis, N.; Kumar, A.; Fygenson, D. K.; Winfree, E., Design and Characterization of Programmable DNA Nanotubes. *J. Am. Chem. Soc.* **2004,** *126*, 16344-16352.

2. Mohammed, A. M.; Schulman, R., Directing Self-Assembly of DNA Nanotubes Using Programmable Seeds. *Nano Lett.* **2013,** *13*, 4006-4013.

3. Mohammed, A.; Velazquez, L.; Chisenhall, A.; Schiffels, D.; Fygenson, D.; Schulman, R., Self-Assembly of Precisely Defined DNA Nanotube Superstructures Using DNA Origami Seeds. *Nanoscale* **2017,** *9*, 522-526.

4. Mohammed, A. M.; Šulc, P.; Zenk, J.; Schulman, R., Self-Assembling DNA Nanotubes to Connect Molecular Landmarks. *Nat. Nanotechnol.* **2017,** *12*, 312-316.

5. Smith, M. B.; Li, H.; Shen, T.; Huang, X.; Yusuf, E.; Vavylonis, D., Segmentation and tracking of cytoskeletal filaments using open active contours. *Cytoskeleton* **2010,** *67*, 693-705.

6. Agrawal, D. K.; Jiang, R.; Reinhart, S; Mohammed, A. M.; Jorgenson, T. D.; Schulman, R., Terminating DNA Tile Assembly with Nanostructured Caps. *ACS Nano* 2017

Please note that some of the material is reprinted in:
Agrawal, D. K.; Jiang, R.; Reinhart, S; Mohammed, A. M.; Jorgenson, T. D.; Schulman, R., Terminating DNA Tile Assembly with Nanostructured Caps. *ACS Nano* 2017

Curriculum Vitae

Ruoyu (Roy) Jiang

Position:	Ph.D. candidate	Address:
	Biomedical Engineering	Irvine, CA 92697, USA
Institution:	University of California, Irvine	
Email:	rjiang230@gmail.com	
Phone:	404-834-4866	

EDUCATION

09/2018 – Present
Ph.D. Candidate in the Department of Biomedical Engineering, University of California, Irvine, CA.

08/2016 – 05/2018
M.S., Chemical and Biomolecular Engineering, The Johns Hopkins University, Baltimore, MD.
Thesis: Dynamic Control of DNA Nanotube Self-Assembly Processes
Advisor: Dr. Rebecca Schulman
Graduate Student and Postdoctoral Fellow Research and Education Award (2018)

08/2012 – 05/2016
B.S., Chemical and Biomolecular Engineering, Georgia Institute of Technology, Atlanta, GA.
Graduated with honors.
Dean's List recipient: 2012, 2013, 2014, 2015.

RESEARCH EXPERIENCE

08/2016 – present

Graduate Researcher for Dr. Rebecca Schulman's DNA Nanotechnology Lab at Johns Hopkins University, Baltimore, MD. Developed DNA assembly rules, designed DNA-origami structures and fluorescence imaging technique. First author paper in preparation and second author paper published under *ACS Nano*.

08/2013 – 05/2016
Undergraduate Researcher for Dr. Elsa Reichmanis, Atlanta, GA. Research on polymer BTTT and P3HT and analyzed surface roughness and electron mobility. Developed semiconductor blend approach using Atomic Force Microscopy.
Received PURA funding for independent research project.

LEADERSHIP EXPERIENCE

09/2015 – present

Hope Worldwide Global Volunteer, Philanthropy committee. Dedicated to serve homeless people, help children from age of five to seven with reading and writing. Provided training, grant management, and evaluation services to poor communities.

TEACHING EXPERIENCE

01/2016 – 05/2016

Teaching assistant for Current Topic on DNA Nanotechnology. Engaged with undergraduate students and teach wet lab skills. Coordinated regular experiments and laboratory facilities.

09/2014 – 05/2015

Teaching Assistant for Introduction to Physics at Georgia Institute of Technology, Atlanta, GA. Class taught by Dr. Edwin Greco. Taught weekly section classes, mentoring students in understanding Python and Quantum Mechanics. Teaching effectiveness: 4.8/5.0

PUBLICATIONS

FIRST AUTHORED PUBLICATIONS

Jiang, R.; Schulman, R., "Self-Assembling Multi-Component DNA Nanotube Connections." In preparation for submission to *Nano Letters*. (Manuscript available upon request)

CO-AUTHORED, PEER-REVIEWED PUBLICATIONS

Agrawal, D. K.; **Jiang, R.**; Reinhart, S; Mohammed, A. M.; Jorgenson, T. D.; Schulman, R., Terminating DNA Tile Assembly with Nanostructured Caps. *ACS Nano* **2017**

HONOR

President's Undergraduate Research Award.	(2015)
Graduated with Honors from Georgia Institute of Technology.	(2016)
Dean's List.	(2012, 2013, 2014, 2015)
The Cum Laude Society.	(2012)
Franklin Physics Award.	(2012)
Graduate Student and Postdoctoral Fellow Research and Education Award	(2018)

SKILLS

SOFTWARE ENGINEERING

Programming Languages — PyMol, Python, Pyrosetta, MATLAB®.

LABORATORY SKILLS

Proficient in general laboratory skills, AFM, PCR and microscopy
Limited training in gel electrophoresis and qPCR.

LANGUAGES

Chinese (native), English (professional), French(conversational)